A STUDY ON UNCERTAINTIES IN VIBRATION BASED DAMAGE DETECTION FOR REINFORCED CONCRETE BRIDGE

LAPORAN AKHIR PROJEK PENYELIDIKAN
FRGS VOT: 78416

NORHISHAM BAKHARY
AZLAN ABDUL RAHMAN
BADERUL HISHAM AHMAD
MOHD ZAMRI RAMLI

FAKULTI KEJURUTERAAN AWAM
UNIVERSITI TEKNOLOGI MALAYSIA

2011

UTM UNIVERSITI TEKNOLOGI MALAYSIA	**PUSAT PENGURUSAN PENYELIDIKAN (RMC)**	**UTM/RMC/F/0024 (1998)** **Pindaan: 0**

BORANG PENGESAHAN

LAPORAN AKHIR PENYELIDIKAN

TAJUK PROJEK : A STUDY ON UNCERTAINTIES IN VIBRATION BASED DAMAGE DETECTION FOR REINFORCED CONCRETE BRIDGE

Saya NORHISHAM BAKHARY

(HURUF BESAR)

Mengaku membenarkan **Laporan Akhir Penyelidikan** ini disimpan di Perpustakaan Universiti Teknologi Malaysia dengan syarat-syarat kegunaan seperti berikut :

1. Laporan Akhir Penyelidikan ini adalah hakmilik Universiti Teknologi Malaysia.
2. Perpustakaan Universiti Teknologi Malaysia dibenarkan membuat salinan untuk tujuan rujukan sahaja.
3. Perpustakaan dibenarkan membuat penjualan salinan Laporan Akhir Penyelidikan ini bagi kategori TIDAK TERHAD.
4. * Sila tandakan (/)

☐	SULIT	(Mengandungi maklumat yang berdarjah keselamatan atau Kepentingan Malaysia seperti yang termaktub di dalam AKTA RAHSIA RASMI 1972).
☐	TERHAD	(Mengandungi maklumat TERHAD yang telah ditentukan oleh Organisasi/badan di mana penyelidikan dijalankan).
☑	TIDAK TERHAD	

_____

TANDATANGAN KETUA PENYELIDIK

_____

Nama & Cop Ketua Penyelidik

Tarikh : _____

CATATAN : ***** *Jika Laporan Akhir Penyelidikan ini SULIT atau TERHAD, sila lampirkan surat daripada pihak berkuasa/organisasi berkenaan dengan menyatakan sekali sebab dan tempoh laporan ini perlu dikelaskan sebagai SULIT dan TERHAD.*

ABSTRACT

Many methods have been developed and studied to detect damage through the change of dynamic response of a structure. Due to its capability to recognize pattern and to correlate non-linear and non-unique problem, Artificial Neural Networks (ANN) have received increasing attention for use in detecting damage in structures based on vibration modal parameters. Most successful works reported in the application of ANN for damage detection are limited to numerical examples and small controlled experimental examples only. This is because of the two main constraints for its practical application in detecting damage in real structures. They are: 1) the inevitable existence of uncertainties in vibration measurement data and finite element modeling of the structure, which may lead to erroneous prediction of structural conditions; and 2) enormous computational effort required to reliably train an ANN model when it involves structures with many degrees of freedom. Therefore, most applications of ANN in damage detection are limited to structure systems with a small number of degrees of freedom and quite significant damage levels.

In this thesis, a probabilistic ANN model is proposed to include into consideration the uncertainties in finite element model and measured data. Rossenblueth's point estimate method is used to reduce the calculations in training and testing the probabilistic ANN model. The accuracy of the probabilistic model is verified by Monte Carlo simulations. Using the probabilistic ANN model, the statistics of the stiffness parameters can be predicted which are used to calculate the probability of damage existence (PDE) in each structural member. The reliability and efficiency of this method is demonstrated using both numerical and experimental examples. In addition, a parametric study is carried out to investigate the sensitivity of the proposed method to different damage levels and to different uncertainty levels.

As an ANN model requires enormous computational effort in training the ANN model when the number of degrees of freedom is relatively large, a substructuring approach employing multi-stage ANN is proposed to tackle the problem. Through this method, a structure is divided to several substructures and each substructure is assessed seperately with independently trained ANN model for the substructure. Once the damaged substructures are identified, second-stage ANN models are trained for these substructures to identify the damage locations and severities of the structural element in the substructures. Both the numerical and experimental examples are used to demonstrate the probabilistic multi-stage ANN methods. It is found that this substructuring ANN approach greatly reduces the computational effort while increasing the damage detectability because fine element mesh can be used. It is also found that the probabilistic model gives better damage identification than the deterministic approach. A sensitivity analysis is also conducted to investigate the effect of substructure size, support condition and different uncertainty levels on the damage detectability of the proposed method. The results demonstrated that the detectibility level of the proposed method is independent of the structure type, but dependent on the boundary condition, substructure size and uncertainty level.

TABLE OF CONTENT

LIST OF TABLES

LIST OF FIGURES

LIST OF SYMBOLS

$\{\ \}$	Vector
$[\ ]$	Matrix
$\{\ \}^T, [\ ]^T$	Transposed vector or matrix
j	Imaginary unit ($\sqrt{-1}$)
[M]	Global mass matrix
[C]	Global viscous damping matrix
[K]	Global stiffness matrix
$\ddot{x}$	Vectors of displacement
$\dot{x}$	Vectors of velocity
$\ddot{x}$	Vectors of acceleration
$\{\phi\}$	Mode shape vector
ω_i, f_i	i_{th} modal frequency (*rad/s, Hz*)
λ_i	ith modal eigenvalue
E	Young's modulus (Pa, N/m^2)
E'	Young's modulus at the damage level of interest (Pa, N/m^2)
ρ	Density of material (kg/m^3)
ν	Poisson ratio
$\lambda_i, \hat{\lambda}_i$	*i*th frequencies for training and testing
$\phi_i, \hat{\phi}_i$	*i*th mode shapes for training and testing
X	Noise vector in modal data and structural parameters
α_j	Stiffness parameter of j^{th} segment
$E(F), u_F$	Mean value of statistical variable F

F_{+-},F_{-+}	Upper limit of variables F
F_{--},F_{+-}	Lower limit of variables F
$\sigma(F)$, σ_F	Standard deviation of statistical variable F
L_H	Lower bound of interval H
P_d	Probability of damage existence
P, $prob$	Probability
$fn(\cdot)$	Function
FCI_j	Frequency changes index of j^{th} substructure
F_j', F_j	Frequencies of the damaged and undamaged of j^{th} substructure
f_{ji}', f_{ji}	Normalized i^{th} undamaged and damaged modal frequency of the j^{th} substructure and is the mode number.
$f_{ji_{min}}$, $f_{ji_{max}}$	Maximum and minimum ith modal frequency of the jth substructure that used to train the ANN model.
μ	Confidence level
l_{el}	Damaged element size
L_{sub}	Substructure size
n-p-m	Number of neurons in input, hidden and output layer
p_i	i^{th} column input vector
$w_{p,n}$	Element of weight matrix connecting the n^{th} hidden neuron to the p^{th} output neuron
$f(\ )$	Transfer function
b	Bias
n	Net input
O_t , O_p	Target and predicted ANN outputs
p	Row of the input/output matrix
p_n	Normalized input and output parameters.
N	Number of input neurons
m	Meter
mm	millimetre

Abbreviation

ANN	Artificial Neural Network
AAN	Auto-associative Network
CDF	Cumulative Distribution Function
COMAC	Coordinate Modal Assurance Criteria
C.O.V.	Coefficient of Variation
DFWNN	Dynamic Time-Delay Fuzzy Wavelet Neural Network
DSD	Dynamic Learning Rate Steepest Decent
DSM	Damage Signature Matching
FABP	Fuzzy Adaptive Backpropagation Algorithm
FRF	Frequency Response Function
FCI	Frequency Changes Index
GA	Genetic Algorithm
ICA	Independent component analysis
K-S test	Kolmorogov-Smirnov goodness of fit test
MAC	Modal Assurance Criteria
MSE	Mean Squared Error
MDLAC	Multiple Damage Location Assurance Criteria
NIL	Noise Injection Learning
PDE	Probability of Damage Existence
PDF	Probability Density Function
SRF	Stiffness Reduction Factor
TSD	Tunable Steepest Descent
WNN	Wavelet Neural Network
UFN	Unsupervised Fuzzy Neural networks

CHAPTER 1

INTRODUCTION

1.1 Introduction

Aging civil structures including bridges and buildings around the world are still in service nowadays. Without careful monitoring and maintenance, these structures may suffer severe damage or even collapse that may result in loss of human life and large economic impact. Based on a study by Stidger (2006), in the United States, 24.5% of bridges are classified as substandard and need rehabilitation. In Japan, the number of aged bridges is expected to constitute half of all road bridges in year 2020 (Fujino and Abe 2001). In Europe most of the bridges were built in 1960s, which now reach their critical age and need rehabilitation. Engineers Australia also reported that the overall quality of the national highway system is rated between averages to poor condition (Engineers Australia 2005). There are many factors that can lead to structure failure such as the usual weakening of material properties, the load increments and unexpected event like extreme weather, earthquakes and vehicle impact. In civil structures, damage can be denoted as cracking in the structure, corrosion, deterioration of material properties or loss of prestressing. Many of these defects are not visual and are not easy to identify in most cases.

There have been several disastrous incidents involving structural failures due to loss of structural integrity such as the collapse of Mianus River Bridge in Connecticut in 1983 due to suspected corrosion of steel support members and fatigue loading, the loss of entire fuselage section of Aloha Airlines Boeing 737 in 1988 due to fatigue cracking. More recent incidents include the collapse of Kaoshiung-Pingtung bridge in Taiwan in year 2000 injuring 20 people, the fell of a steel girder from an overpass on Interstate 70 west of Denver in year 2004, crushing one car and killing three people; and most recently in year 2007 in Minneapolis, an eight-lane highway bridge collapsed into the Mississippi River. The incidents above indicate that structural damage has become a crucial problem worldwide; therefore, more reliable and effective damage identification methods are required.

Current damage detection methods are categorized as: (1) local damage detection method and (2) global damage identification method. Non-destructive testing (NDT) methods have been used in local damage detection method, ranging from visual inspection to more advanced methods such as X-rays, acoustic emission, ultrasonic emission, eddy current and other wave propagation methods. However, the efficiency of these approaches highly depends upon accessibility of the structural location and individual expertise. Moreover, these methods require the area of the damage to be known in advance and are very time consuming because they are only sensitive to a small area as compared to the dimension of a civil structure. Therefore practitioner and researchers demand for a global damage detection method that can determine the damage existence, location and damage severity without relying on prior information on the vicinity of the damage.

The majority of work to date in global damage identification methods has been focused on the use of vibration properties to determine the damage existence, location and severities. The theoretical basis for vibration based damage detection is that the occurrence of damages or loss of integrity in a structural system causes changes in the global vibration properties of the structure (e.g. natural frequencies, mode shapes, damping, etc). Consequently, examination of structural response characteristics provides useful information regarding the damage existence, location and severity without prior knowledge of the damage states.

Vibration-based damage detection can be classified into model-based and non-model based methods (James et al. 1997). Model-based damage detection methods locate and quantify damage by correlating an analytical model with test data of the damaged structure. Hence, it can provide quantitative information of damage as well as damage location. These methods require finite element model and intensive computation. Non-model based methods are very simple and straightforward, the damaged structures are assessed by comparing the measurements of the damaged structures and undamaged structures. However, the non-model based methods cannot provide quantitative information of the structures, only location of the damage can be determined.

While there are many approaches that have been investigated and are still being developed to identify damage from vibration properties, the approaches that do not require detailed knowledge of the vulnerable parts or the failure modes of the structure have an advantage to handle unexpected failure patterns. Moreover, the less time consuming methods that provide less hurdles in design and implementation also gain attentions. The Artificial Neural Network (ANN) method is one technique that has been intensively studied.

Artificial Neural Networks (ANN) is a computational model inspired by the structure and the information process capabilities of human brain. It is an assembly of large number of highly interconnected simple processing unit (neurons). The ANN stores knowledge in the form of connection strengths. These strengths are represented by numerical values called weights which can be determined through a series of training process.

ANN has been introduced to structural engineering since late 1980s. The development of simple error backpropagation algorithm by Rumelhart (1986) has boosted the research activities on its application in many areas including in structural engineering. Since then, many papers have been published on its application to structural engineering concentrating in structural analysis, design automation, structural control and finite element mesh generation (Adeli 2001). In damage detection, the ANN can be applied to identify the location and damage extent from the measured dynamic responses. The early works in application of ANN in damage detection began in 1990s and many studies concluded that the ANN model is a promising tool for detecting damage in structures based on dynamic properties. However, the majority of research in this area is limited to computer simulations and small-scale laboratory tests. The practical application of these technologies to civil engineering structures is still under research due to several reasons discussed below.

i) Civil structures have complicated geometry and consist of variety of materials such as concrete, steel; rubber and asphalt, the inaccuracy in estimation of strength and stiffness of materials and structure contribute to uncertainties in modeling. Hence, producing an accurate finite element model is very difficult. This may results in the vibration parameters

generated from such a finite element model not exactly representing the relationship between the modal parameters and the damage parameters of the real structure. In other word, the ANN model may not be reliably trained owing to finite element error. On the other hand, the existence of measurement error in the measured data that is normally used as testing data in an ANN model to detect damage is also unavoidable. Since the reliability of an ANN prediction relies on the accuracy of the both components, the existence of these uncertainties may result in false and inaccurate ANN predictions.

ii) The effect of uncontrolled factors such as temperature, traffic loading and humidity may induce significant amount of uncertainties in the captured data and material properties, thus, will affect the reliability of damage identification. For example an experimental study by Xia et al. (2006) demonstrated that the changes of temperature and humidity cause changes in natural frequencies of the structure. They also concluded that temperature increase results in a reduction in the modulus of elasticity of concrete significantly. Therefore, for reliable damage detection, the effect of uncertainties should be considered for damage identification.

iii) ANN usually requires enormous computational effort especially when structures with many degrees of freedom are involved. Due to this reason, most applications of ANN for damage detection are limited to small structures with limited number of degrees of freedom.

iv) The application of forced vibration test which is normally used for damage identification is difficult for structures in service since it causes service interruption. Application of ambient techniques are more suitable, however this method usually is unable to reliably give higher modes, which is more sensitive to small damage. Therefore, most of the damage detection process in civil engineering would suffer from lack of data since only a small number of measurement points and a few fundamental modes are available.

The aforementioned problems that would arise for damage detection for civil structures provide the motivation of this study, which is intended to find solutions for some of those problems.

1.2 Research objectives

The objectives of this study are:

i) To develop and demonstrate the applicability of damage detection using ANN.

ii) To develop an ANN based probabilistic approach for damage detection with consideration of the finite element modeling error and measurement noise and to analyse the effect of these uncertainties on damage identification result.

iii) To develop and demonstrate a substructure technique based ANN model for damage detection of many degrees of freedom structures.

CHAPTER 2

LITERATURE REVIEW

2.1 Introduction

During 1970s, engineers and researchers in offshore oil industries have made a considerable effort to develop vibration based damage detection technique. The objectives included the detection of near-failing drilling equipment and the prevention of expensive oil pumps from becoming inoperable (Carden and Fanning 2004). The research in aerospace industry in vibration damage detection started in the late 1970s and early 1980s. According to a review by Farrar et al.(2001), the civil engineering community has studied vibration based damage detection since 1980s, vibration properties such as frequency, mode shape and its derivatives have been used for damage assessment focusing on bridge structures.

The vibration based damage detection is based on the equation of motion

$$[M]\{\ddot{x}\} + [C]\{\dot{x}\} + [K]\{x\} = \{0\} \tag{2-1}$$

where $[M]$ is the mass matrix, $[C]$ is the viscous damping matrix, $[K]$ is the stiffness matrix. $\{x\}$, $\{\dot{x}\}$ and $\{\ddot{x}\}$ are vectors of displacement, velocity and acceleration; respectively.

The associated eigenvalue problem is

$$(-\omega_i^2[M] + j\omega_i[C] + [K])\{\phi_i\} = \{0\} \tag{2-2}$$

where ω_i and $\{\phi_i\}$ are the i^{th} modal circular frequency and mode shape respectively. j is the imaginary unit

If damage exists in a structure system, such as changes in the mass, stiffness or damping or combination of them, the vibration characteristics such as natural frequencies and mode shapes will change accordingly. Thus, damage can be detected from changes of vibration properties which can be extracted from the measured response data.

There are three basic types of data used in the vibration based damage detection. They are time domain, frequency domain and modal domain. Time domain data is the time history response of the structure that can be measured by sensors (e.g. displacement, acceleration). This time series data can be converted to the frequency domain using Fourier transform to form a frequency response function (FRF). Further analysis of the frequency domain data is often undertaken to extract the modal domain parameters such as vibration frequency, mode shape and damping.

While all the above data reflect the condition of a structure, damage identification can be done based on data in the time, frequency or modal domain. However, there are arguments about the suitability of data for damage detection since in each stage the processing involves data compression process which results in a reduction in the volume of the data. For example Banks et al. (1996) questioned the suitability of modal data for damage detection arguing that modal data is a global system properties while damage is a local phenomenon. In contrast, according to Friswell and Penny (1997), the FRF and modal data essentially contain the same information unless the modes are out of range. Lee and Shin (2002) pointed out that the modal domain data can be contaminated by modal extraction error not present in the FRF data. They suggest that FRF can provide more information as the modal data is extracted from a very limited range around resonance. Doeblíng and co-workers (1996) concluded in their report that there are disagreements among researchers about the suitable parameters for damage identification. Research in all the three domains are likely to continue because no constructive method has been found yet to identify every type of damage in every type of structure. Nevertheless, most applications of vibration based damage detection focused on the methods that are based on the modal domain. This may be due to the fact that modal properties are

easy to obtain and to interpret as compared to the more abstract features in the frequency domain and the time domain.

Damage can be classified into linear or nonlinear. A linear damage is when the initially linear-elastic structure remains linear-elastic after damage. The changes in the modal characteristics are a result of changes in the geometry, boundary condition or material properties of the structure. The structural response can still be modeled using linear equations of motion. Nonlinear damage is defined as the case when the initially linear-elastic structure behaves in nonlinear manner after the damage has been introduced. One example of nonlinear damage is the formation of a crack that subsequently opens and closes under the normal operating vibration environment. The majority of the studies reported in the technical literature addresses only the problem of linear damage detection (Farrar and Doebling 1997).

Rytter (1993) classified damage identification into four levels:

Level 1: Determination that damage is present in the structure

Level 2: Determination of the geometric location of the damage

Level 3: Quantification of the severity of the damage

Level 4: Prediction of remaining service life of the structure

Doebling et al. (1998) presented an extensive review on the damage detection methods based on modal parameters and Carden and Fanning (2004) provides the updated version. These literature reviews concentrated primarily on Level 1 to 3 only. Level 4 is generally associated with the fields of fracture mechanics, fatigue life analysis, or structural design assessment which is rarely addressed by researchers.

This section reviews various methods for damage detection based on vibration data, emphasizing on structural engineering applications. Due to a vast amount of publications in this area, the literature review in this section mainly focuses on the technical papers published after 1990; however some earlier publications that are considered to be important are also included. The damage identification methods

reviewed below are categorised based on vibration parameters and analysis techniques.

2.2 Artificial neural network methods

Most of the proposed methods in the literature above are a direct process involving constructions of mathematical models, which are then used to develop a relationship between damage conditions and changes in structural response. Since the damage identification is an inverse process, where causes must be discerned from effects, a search for the causes of the structural responses is quite complicated and computationally expensive. A unique solution often does not exist for an inverse problem, especially when insufficient data is available. Thus, it is very difficult to evaluate an existing structure that has suffered some unknown type of damage using traditional damage detection methods based on a priori knowledge of damage scenarios. The model updating techniques which include iterative method and optimization method also results in a huge amount of calculation and is time consuming. Although many algorithms have been developed to improve the updating process, it still remains computationally complex.

As ANNs are known for its capability to model nonlinear and complex relationship, the inverse relationship between structural responses to structural characteristics can be modeled.

The application of ANN to civil engineering began in 1989. The first journal article on civil/structural engineering was published by Adeli and Yeh (1989) to solve a problem in engineering design. Adeli (2001) has conducted a comprehensive review in the application of ANN in civil engineering. In damage detection, Wu et al.(1992) published the first journal article to detect damage from dynamic parameters by employing ANN.

The basic strategy in applying ANN model for damage detection is to train the ANN model to recognize the changes of structural characteristics based on measured response. This is due to the reason that the rules governing the cause and effect

relationships must be established explicitly and methodology for using these relationships must be developed in priori (Wu et al. 1992). Through a training process, ANN is able to extract the relationship between inputs and outputs and then store within the connection strengths.

There are two main steps in building an ANN model, i) training stage; and ii) testing stage. In training, a network is trained by data of various damage cases using an appropriate training algorithm. In the testing stage, the trained ANN is fed with input data that has not been used in the training. To generate a set of data that can be used in training process, the data must contain the information regarding cause and effect relationships. In any typical application of ANN, an appropriate ANN architecture must be determined in the first place followed by selection of training algorithm to train the network. In most cases ANN architecture is expressed as *n-p-m*, where *n,p,m* are the number of neurons in input, hidden and output layer respectively.

In previous studies, many types of parameters corresponding to measured response were applied as the inputs. For damage detection, measured response parameters (time domain or frequency domain or modal domain data) are normally used as the inputs, while for the outputs, the non-parametric and parametric parameters were normally used to represent the condition of the structure. Non-parametric parameter refers to any form of variable used to classify the structure condition, such as binary number, while parametric parameters quantify the damage extent, such as reduction of stiffness value (Xu et al. 2004). The application of ANN for damage detection is the major concern in this study.

As the research in the application of ANN for damage detection progressing, in this subsection, the related studies are reviewed in three major categories: i) Input and output parameter; ii) process mapping and algorithm; and iii) application.

2.2.1 Input and output parameter

As mentioned earlier, the relationships between cause and effect are obtained from training data through an appropriate training scheme. Most researchers in the early

stage focused on determining the appropriate combination of input and output variables.

The first journal article by Wu et al. (1992) applied FRF of acceleration data as the input vector. The FRF between 0 and 20Hz was discretized at the interval of 0.1Hz resulting in 200 spectral values. Binary number, 1 and 0 were used as the output to represent the undamaged and damaged condition of each member in a simulated three-storey building. Povich and Lim (1994) verified the application of FRF as the input parameters to detect damage condition in a 20-bay planar truss composed of 60 struts. 394 input nodes were used, corresponding to spectral values between 0 and 50 Hz. The same binary code was applied as the outputs to represent the condition of each strut. Both studies demonstrated that ANN is capable of learning the behaviour of damaged and undamaged structures and to identify the damaged member from patterns in the FRF of the structure.

Kudva et al. (1992) examined the viability of measured strain values at discrete locations as the inputs to deduce the damage size and locations on a numerically modeled plate stiffened by 4 x 4 array bays. ANN was used to relate the inputs with the damage size and location of the damaged bays. Two output nodes were used; to represent damage location and damage size. The results show that the training performance is good which indicate that ANN is able to provide good correlation between strain values and damage location and size. However, some false predictions are experienced in testing, due to the reason that strain values is unable to provide unique representation of damage location and severities. Furthermore, the output nodes setting used in this study only allow ANN to detect single damage only. Worden et al. (1993) applied the same approach to classify the damaged and undamaged member of an experimental framework structure in terms of binary number. The study suggested that ANN should be trained using noise-corrupted data to produce better classification results if experimental data is employed.

Elkordy et al. (1992) used the percent changes in vibrational signatures obtained from experimental study of a five-story frame as input to backpropagation ANN. They demonstrated that using the percent changes in vibrational signatures rather

than absolute values effectively distinguishes between the patterns corresponding to different damage states. Pandey and Barai (1995) applied vertical displacements at selected nodes as the input parameter to identify damage in a numerically modeled 21-bar bridge truss structure. The outputs are cross sectional area of every member. The damage scenarios considered were formed by reducing the cross section of the corresponding truss members. The ANN models used in this study were able to predict the cross sectional area of the simulated damages with a minimum error percentage.

A more detailed study related to the number of measurement nodes of vibration signature was conducted in Barai and Pandey (1995). The vibration signature of a bridge truss structure under moving load was used as the ANN's input. The prediction performance of ANN models employing single-node; three-node and five-node of measurement were compared. The authors concluded that the vibration signature obtained from single-node provides better performance compared to multiple measurement nodes. However, the authors did not address the issue regarding selection of time interval and length of vibration signature.

Masri et al.(1996) carried out a study regarding the effect of different lengths of vibration signature to ANN performance. A backpropagation ANN model was trained to detect the abnormality in a linear and nonlinear single-degree-of freedom system based on vibration signature. The inputs of the network are the relative displacement and relative velocity, and the output is the restoring force. The results show that better training and prediction performances are obtained when longer vibration signature is used as the input. This is aligned with the ANN learning theory that more information provides the better prediction results. However, there was no specific guideline provided on selecting the appropriate length of the vibration signature. The application of this method to actual data was demonstrated in Nakamura et al. (1998), while Masri et al.(2000) applied the proposed approach to experimental nonlinear multi-degree of freedom system.

The use of time series data such as FRF and vibration signature required a small sampling rate, in turn, a tremendous amount of training data is needed and a large

training time may involve. In order to address this issue, researchers proposed several alternatives.

In Spillman et al. (1993), instead of using spectral values, the authors applied the amplitudes and frequencies of the first two modal peaks of Fourier transformed acceleration time history signal together with impact intensity and location of the sensor as inputs to ANN model. A 4.5m steel bridge element was used as an example. Damage was introduced by cutting and bolting a plate reinforcement over top of the cut. With the plate attached, the element was considered undamaged. With the bolts loosened, the element was considered to be partially damaged. The impact intensity and location were also used as inputs. An ANN model with 14 inputs, 20 hidden nodes and 3 outputs were used, one for each of the possible damage. The results show that the proportion of correct diagnosis was around 60%. The authors justified this number by citing the small size of the training data.

Islam and Craig (1994) applied natural frequency as the input parameters of ANN in determining the location and size of delamination in a cantilever delaminated composite beams. Numerical and experimental examples were used to verify the proposed method. The ANN architecture consisted of three layers with five nodes in the input layer corresponding to the first five modal frequencies. Three and two nodes were used in hidden and output layers respectively. The nodes at the output layer corresponding to delamination size and location. The ANN was trained with 14000 training patterns. Their results showed a good agreement between natural frequency and damage location and size. The simulated and experimental damages were successfully detected. Ceravolo and De Stefano (1995) also applied natural frequency as the input to ANN model to predict the (x,y) coordinates corresponding to the damage location. A truss structure simulated by finite element model was used as the example. The damage was imposed by removing truss elements. A backpropagation ANN model with 10 input corresponding to 10 modal frequencies, 10 hidden nodes and two output nodes corresponding to the x and y position was used. Only single-damage cases were considered. The network was trained with 18 samples consisting of various single-damage cases. The ANN located the damages well.

Similar input parameters were applied by Ferregut et al.(1995) to detect damage in numerically modeled aluminium cantilever beam. A backpropagation with 6 input nodes, 17 hidden nodes and 11 output nodes was applied. The first output node in output layer was for damage magnitude, while the other 10 were for damage location. The ANN was trained with 240 pairs of input and output data. The damages were simulated by reducing the width and depth of the corresponding element from 1% to 30%. The results show that only severe damages were identified. This may be due to the reason that the natural frequency alone is not sensitive to small damage. A similar outcome was experienced by Kirkegaard and Rytter (1994), when similar input parameter was applied to identify damage in a 20-m steel lattice mast subject to wind excitation. Damage was simulated by replacing lower diagonal with bolted joints of diminished thickness. The ANN model was used to identify the mapping from the first five modes of frequencies to the percentage of damages in member stiffness. One output was used for each element of interest. The network was trained with 21 examples generated from a finite element model. The results show that at 100% damage, the ANN was able to locate and quantify damage. At 50% damage the ANN was able to predict the existence of damage but not the magnitude. The damage less than 50% was not detected.

From the studies above, it is observed that natural frequencies alone are not effective to identify damage in structures. Good results only limited to the cantilever structure and single-damage only. As mentioned earlier, it is not capable in differentiating damage in a symmetrical structure. Moreover, the frequency shift due to a small damage is not significant, thus the frequency is not sensitive to small damages.

Elkordy et al. (1993) applied mode shapes as the inputs to ANN model to identify damage in a five story building. The ANN model was trained using data generated from finite element model and tested with numerical and experimental data. Two types of ANN models were used. The two ANN models were trained using 11 and 9 training data respectively. The first model was used to classify the structure members into damaged or undamaged, while the second was used to determine the percent change in member stiffness. The output of the first and the second ANN model were good when tested with numerical data but inaccurate results were observed when the

experimental data was used. According to the authors, this may be because of the inevitable measurement error in the measured data.

More comprehensive study regarding input parameter was conducted by Tsou and Shen (1994). In their study, the detectability of two ANN model with different input variables are compared. The first ANN model was trained using changes in eigenvalues as the input parameters and the second ANN model was trained using a combination of frequencies and mode shapes as the input vector. Those ANN were tested with single and multiple damages. Instead of applying the conventional classification method, a new ANN architecture was also proposed to deal with parametric output parameter of multiple damages. Each node in the output layer was used to represent the stiffness loses of each member. Finite element model of a three degree of freedom and an eight degree of freedom spring system was used as the examples. The authors concluded that the ANN with changes in eigenvalues as the inputs was able to detect single and multiple damages in a simple system. However, for more complicated problems, the information from mode shape is required to provide more precise identification. The authors also claimed that by using modal data as input parameters the length of the input vector was significantly reduced as compared to FRF. Levin and Lieven (1998) verified the use of natural frequency and mode shape as the input parameters to ANN model to update the finite element model based on experiment modal data. A radial basis neural network was applied to map the relationship between the vector and the structure properties. A simple ten-element cantilever beam was used as an example. The successful applications of natural frequency and mode shape as input parameter were also reported in other studies.(Ko et al. 2002; Mehrjoo et al. 2007; Yun and Bahng 2000; Zapico et al. 2001).

A comparative study between static displacement and modal data as diagnostic parameters for damage detection using ANN was conducted by Zhao et al. (1998). A counterpropagation ANN was used to predict Young's modulus of each structure member. For static displacement, a numerical plane frame was used as an example. Single and multiple damages were used for testing. The ANN was used to identify the relationship between static displacement and Young's modulus of each member. The results show that ANN was not successful to detect multiple damages based on

static displacement. For modal parameters, four different input parameters were considered. i) natural frequencies; ii) mode shapes; iii) slope array; and iv) state arrays. A three-span continuous beam was used as an example. The results show that natural frequencies and slope arrays provide better results compared to mode shapes and state arrays. The author concluded that the dynamics parameters are good diagnostic parameters for damage detection, while static displacement is not suitable to detect multiple damages as similar displacements can be obtained with different combination of damage and loading.

Zang and Imregun (2001a) proposed a different method to reduce the size of FRF as input variables. The authors employed a principal component analysis to reduce the size of FRF before it can be used as the input variables. The output of the ANN model is the condition of structure (healthy or damaged). The original FRF data of railways wheels with 4096 data points in x, y and z direction was reduced to 7, 9 and 13 for x,y and z direction respectively. The reduced data sets were used as input vectors to three different ANN models. 80 samples were used for training and 20 cases for testing. The results show that all the damage cases were correctly classified. Zang and Imregun (2001b) quantified the above approach for slight damage detection. Kim and Kapania (2006) enhanced the above method by applying principal component together with orthogonal array method to reduce the number of training data. According to Zang and Imregun (2001b) the application of FRF to detect damage location and severities is still very difficult since a fine spatial resolution of FRF is needed for damage location and the quality of raw FRF data remains a major consideration.

Instead of using measured response parameters directly as the input variables to ANN model, several researchers proposed proxy variables as the input parameters to overcome the shortcomings of the existing method. Rhim and Lee (1995) highlighted an issue regarding a large number of sensors needed if dynamic parameters are used directly as the inputs. In their study, transfer functions of auto-regressive model with exogenous input (ARX) served as the input patterns for damage classification using backpropagation ANN. A Transfer functions was used as the system feature by combining the information on a dynamic system from a given input-output data pair.

The ANN was used to identify the map from characteristic polynomial to an empirical damage scale. Each of the four outputs represented a different level of damage, where 0 indicated no damage and 1 for total damage. The damage cases were modeled as delamination in finite element model of a composite cantilever beam. The authors chose ANN with 13 input nodes, 30 hidden nodes and 4 outputs and trained with 10 training patterns. The ANN model was tested with three examples and correctly identified the damage in those cases.

The development of wavelet-based approach for vibration data processing, which is claimed to be more accurate, has enhanced the research in damage detection. Only one paper found on the use of wavelet variables as the input parameters to ANN for damage detection. Yam et al. (2003) applied structural damage feature proxy vectors as the input to ANN to increase the sensitivity of the existing method to small and incipient structural damage. Location and severity of the damage are used as the output variables. The vectors were constructed based on energy variation of structural vibration response. The vibration responses are decomposed into wavelet sub-signals to extract structural damage information using wavelet packet analysis method (WPA). By using a specified formula, the sub-signals are composed to form a non-dimensional damage feature proxy vector. Numerical and experimental PVC sandwich plates were used to verify the method. In numerical example, a damage scenario with 12 cracks was modeled in the finite element model. A Backpropagation ANN (32-16-4) was applied. 108 sets of training data were used for training. The results show that the ANN was able to predict the crack location for all the 12 crack cases. In experimental example, 6 crack cases with different length were considered. Some errors in the results were observed in determining the crack length. This is again because of the measurement error and modeling error.

Lam et al. (2006) proposed to use the changes of Ritz vectors as the features to characterize the damage pattern defined by the corresponding locations and severities. This approach is based on the reason that Ritz vectors possess higher sensitivity to structural damage than natural frequency and mode shape. Ritz vectors were extracted from frequencies and mode shapes using flexibility matrix. A Radial basis function neural network was employed to identify the map between changes of

Ritz vector and *E* values of any possible damage location. A numerically modeled two-bay truss structure with 11 members was used to illustrate the proposed method. ANN with 9 input neurons, 41 hidden nodes and 11 output nodes was used. Three damage types were simulated for testing, ranging from single-damage to triple-damage. The locations and damage severities for all cases were successfully identified. The author concluded that the ANN trained with Ritz vector changes provides more reliable results.

From the reviews above, the input parameters that used to identify damage with an ANN model ranging from direct application of time domain data (e.g. vibration signature), frequency domain (FRF) to modal domain data (frequency and mode shape). Several attempts in using proxy parameters derived from dynamic data are also reviewed. Despite of the fact that each vibration parameter has its own pros and cons in damage identification as mentioned earlier, the application of time series data (vibration signature and FRF) as the input parameter has another issue. In ANN model, the values at each time interval are represented by an input node, thus for time series data, a large number of nodes at the ANN's input layer are needed. This leads to a phenomenon known as '*curse of dimensionality* ' as discussed by Bishop (1995) which significantly jeopardizes the efficiency and accuracy of ANN training process. The modal frequency has the advantage of ease and accuracy of measurement, since it is a global properties and not spatially specific, extra information, such as mode shape can be used together to identify damage. Since these parameters are not a time-based parameter, the number of ANN input node depends on the number of modes and measurement points only, hence the length of the input variables can be substantially reduced.

Application of wavelet data as the input variables provides an alternative for damage detection, nevertheless there are many types of wavelets and there is no systematic method to choose the most appropriate wavelet transform data for damage detection (Marwala 2000).

It is important that the output of ANN is able to provide as much information as possible about the damage status. In the early stage, most researchers applied non-

parametric parameter as the outputs. This type of output parameter classified the structure conditions to damaged and undamaged condition, thus the results are limited to level 1 in Rytter's terminology. Attempts to use parametric parameters as the outputs are subjected to small structure system only. This may be due to computational power that limits the training of large dimension ANN model, because certain training algorithms require high computer memory to train the ANN model. For example, Levenberg-Marquardt algorithm requires high computational power, but in many cases it converges while the other algorithms such as conjugate gradient and variable learning rate algorithm may not converge (Hagan and Menhaj 1994). As a result, in most studies, only minimum number of output node is used at the ANN output layer. This leads the researchers to use the coding system such as binary code as the output to represent different structural location and condition. This limitation also induces the difficulty in detecting multiple damages. As technology grows, more studies used parametric parameters, involving structural parameters (e.g. damage location and severity) as the outputs, thus qualitative way of damage detection have taken place, and better information can be obtained.

2.2.2 Process mapping and training algorithm

Among various types of ANN models, multi-layer neural networks with backpropagation algorithm are most commonly used in damage detection (Elkordy et al. 1993; Elkordy et al. 1994; Povich and Lim 1994; Spillman et al. 1993; Wu et al. 1992). Although this ANN model has been proven to be an effective tool in damage detection, it still suffers several drawbacks such as slow convergence and the possibility to be trapped into local minima especially when it involves time series input parameters. In this subsection, studies pertaining to various methods in improving the conventional ANN model for damage identification are reviewed. This includes the improvement of ANN performance in terms of mapping topology, training algorithm and ANN integrated approach.

Szewczyk and Hajela (1994) introduced a new algorithm called Feature-sensitive Neural Network to overcome the problem in variation of static displacements under different load conditions. According to the authors, the feature-sensitive neural

network is a modified version of counterpropagation neural network, which features increased processing power over standard ANN while preserving its general characteristics. This was done by implementing a clustering device as the hidden layer to classify the input pattern on the basis of minimum disturbance principle. As a result, only the weight vector of one neuron (the closest to a current input) is modified. At the output layer, a nonlinear interpolation scheme was introduced to increase the prediction accuracy. This new algorithm was applied on three numerical structures of increasing complexity: a 2-dimensional six-bar truss, 2-dimensional 18-degree of freedom portal frame and 3-dimensional 12-degree of freedom system. The networks were trained with 200, 3600 and 3000 examples respectively. Quite satisfactory results were exhibited for simple structure, but poor results were observed for complex structures.

Ceravolo et al. (1995) extended the standard process mapping by applying hierarchical ANN to detect the presence of structural faults. The network consists of two levels of ANN model. The first level was used to determine the damaged area, and the second level identified the damaged element in the area. Acceleration cross-correlation values recorded over 1 second, with sampling period 0.005 second were used as the inputs to backpropagation ANN model at both levels. Both networks were trained with 54 and 18 training samples. A 5m numerically modeled beam was served as the example. Although all the 12 simulated single-damage cases were successfully detected, this approach is limited to single-damage cases only.

Worden (1997) applied novelty detection method using Auto-associative network (AAN) in simple 3-degree of freedom simulated lumped-parameter mechanical system. The purpose of the approach is to identify any changes in the system. The AAN was forced to reproduce the patterns which were presented at the input layer. The novelty index, which was defined as Euclidean distance between undamaged and damaged pattern was used as the indicator of abnormality. The input and output of the AAN was 50 spaced points of FRF between 0 to 50Hz. The effect of measurement error was also considered by applying normally distributed noise in the inputs. 50%, 10% and 1% fault cases were simulated by reducing the stiffness of one of the spring in the system. The results showed that the AAN was able to detect the

abnormality for 50% and 10% cases, but had difficulties to detect abnormality in 1% damaged case. The author also demonstrated that the reliability of the proposed approach also decreased as the noise increased. This method was only limited to damage detection of level 1 in Rytters terminology.

Hung and Kao (2002) upgraded the novel detection method proposed by Worden (1997) to comply with level 2 detection in Rytter's terminology. Another ANN model was introduced in the second stage to determine the location and severity. The novel ANN model in the first stage was used to identify the undamaged and damaged states of a structural system. The relative displacement, velocity and acceleration were used as the input and output for the ANN in this stage. The partial derivatives of the outputs of ANN in the first stage were used as the input for the ANN in the second stage to determine the damage locations and severities. Examples of a single degree-of freedom system and a multiple degrees-of freedom system were used to demonstrate the approach. Simulated cases for both systems were satisfactorily diagnosed. Kao and Hung (2003) further demonstrated the above approach using free vibration responses.

Xu et al. (2004) proposed a new strategy of novel detection method to identify damage directly from the vibration time-domain responses. The authors also claimed that the proposed method is feasible to identify stiffness and damping without the parameters of an undamaged structure to be known as a priori. Two ANN models were applied. The first ANN model was used to model the time-domain behaviour of a reference structure and the second was to identify the parameter of the structure. Velocity and displacement and excitation force at the k time step were used as the inputs and the outputs were velocity and displacement at the $k+1$ time step. The deviation of the outputs from reference values indicates damage existence. The error between the reference and the output values was then applied as the input for the second ANN model to predict the parameters of the structure. A numerical five-story frame was used as an example. The results showed that the stiffness parameters were predicted with less than 7% error.

In Marwala and Hunt (1999), a new mapping topology called committee neural network to combine the information from FRF and modal data were proposed. Two backpropagation ANN models were used to predict the *fault identity* based on FRF and modal data respectively. Frequency energy calculated from FRF was used as the input for the first ANN model and modal properties for the second. The predicted fault identity values were combined to represent the condition of the structure. In this study, a simulated 1.0m cantilever beam was used to illustrate the method. The beam was divided into 5 segments, and the committee ANN was used to identify the damage existence in each segment. An ANN architecture of 50-25-5 was selected for the first ANN model and for the second one 55-25-5 was applied. 243 data were used for training both networks. The results showed that those ANN was trainable with low mean errors but no testing has been demonstrated. Marwala (2000) enhanced the above study by applying wavelet transform data together with FRF and modal properties. An experimental data of ten steel seam-welded cylindrical shells was used for verification. The author claimed that the performance of the proposed approach is not influenced by error and the effectiveness of the method is enhanced when experimental data are applied.

Chang et al.(2000) proposed a modified backpropagation ANN algorithm known as iterative artificial neural network to increase the ANN prediction accuracy in damage detection based on modal data. The outputs of the trained ANN are fed to finite element model to calculate the dynamic characteristics. If the calculated characteristics deviate from the measured ones, the ANN model would go through a retraining process. Natural frequencies and changes of mode shape curvatures were used as the inputs, while structural stiffness was used as the outputs. A numerical model and an experimental clamped-clamped reinforced concrete T beam were used as the example. The results showed that all four simulated damage cases were successfully detected; however, some slight errors were observed when experimental data was used. According to the authors, this may be due to uncertainties related to material properties or material in homogeneity.

Attempts to improve the performance of conventional backpropagation ANN algorithm demonstrated in several studies above have shown promising results,

however the computational efficiency is still an issue. Luo and Hanagud (1997) proposed a dynamic learning rate steepest decent (DSD) algorithm to speed up the training time. The DSD was used to train a neural network for direct identification of composite structural damage through structural dynamic responses. Through numerical experiments, the proposed method was shown to have much better learning ability than the standard constant learning rate steepest descent method and the accelerated steepest descendent method. The same approach was further demonstrated by Zhu et al. (2002).

Xu et al. (2000) improved the above algorithm by introducing the concept of dynamically adjusted learning rate and additional jump factor to speed up the convergence of multilayer neural network. According to the authors the proposed algorithm is able to alleviate the oscillation and stagnation in backpropagation algorithm, thus speed up the convergence of the ANN model. In that study, the ANN model was used to identify the correlation between the displacement response and the location/size of the cracks. A numerically modeled anisotropic laminated plate was used as the example. The authors claimed that the proposed algorithm can speed up the convergence of neural network.

Liang and Feng (2001) argued the efficiency of dynamically adjusted learning rate algorithms since this method heavily depends on selection of control parameters such as error rate controller and learning rate controller that are typically determined based on trial and error. Thus, the authors proposed a fuzzy adaptive backpropagation (FABP) algorithm by integrating fuzzy logic concept with the characteristics of ANN to identify the restoring forces in a nonlinear vibration system. By applying fuzzy concept, error function and the changes of learning rate are defined fuzzily based on human expertise. The authors concluded that FABP is able to increase the training speed of the network. Nevertheless, this method has its own limitation. The design of fuzzy logic approach still requires a rule based formulation which is very difficult to implement and also time consuming. To tackle this problem, Fang et al.(2005) developed a tunable steepest descent (TSD) algorithm which is based on DSD algorithm incorporated with heuristics approach to improve the ANN training process. According to the authors, a heuristic rule in which the

learning rate is kept as large as possible to the extent that the network can learn without increasing the error is used to determine the step size. This algorithm was used to train ANN to establish relationship between FRF and damage location/severity of a 20-elements cantilever beam. Key spectral points around the resonant frequencies in FRF data together with 78 points of stiffness loss were chosen as the input. The outputs were the stiffness loss of five specified locations of the beam. The results show that ANN trained with TSD algorithm was able to detect single and multiple damages. A comparison of training performance of the proposed method with DSD and FABP was also performed. The authors concluded that TSD algorithm outperforms DSD and FABP in training effectiveness without increasing the algorithm complexity.

Another strategy to improve the performance of the conventional backpropagation ANN for damage detection was proposed by Hung et al.(2003). The authors applied Wavelet Neural Network (WNN) as a non-parametric system identification based on a study by Zhang and Benveniste (1992). The wavelet decomposition method was combined with ANN structure to enhance the convergence accuracy and to overcome the problem of local minima in a conventional ANN. The feasibility of WNN was examined using a five story 1/2-scaled steel frame excited under Kobe earthquake. During the training, the story acceleration responses were used as input and outputs. The authors found that the WNN performed equally well as a conventional ANN, however, the training time needed for a WNN is much less than a conventional ANN.

However, according to Adeli (2006), the WNN method suffers three major drawbacks: i) lack of an efficient constructive model; ii) the need to find the model parameters such as the input vector dimension by trial and error; and iii) low identification accuracy. Thus, the author proposed a new multiparadigm dynamic time-delay fuzzy WNN (DFWNN) model to tackle the above problems. The method is based on the integration of four different computing concepts: dynamic time delay ANN, wavelet, fuzzy logic and the reconstructed state space concept from chaos theory. The same input and output parameters were used and the same example was applied. The performance of the DFWNN and WNN was compared. The results

show that the proposed method provides more accurate output as compared to WNN. Jiang and Adeli (2005) demonstrated the application of DFWNN for nonlinear highrise buildings. Wen et al. (2007) proposed a parametric version of this method namely Unsupervised Fuzzy Neural networks (UFN). The authors investigated the feasibility of unsupervised ANN incorporated fuzzy logic to determine damage location and severity. The performance of UFN and conventional backpropagation ANN were compared. Additionally, the effect of measured noise and the use of incomplete modal data were investigated. A finite element model of the same structure was applied for verification. This study concluded that both backpropagation ANN and UFN are capable of locating the damage. The use of fuzzy relationship in UFN increased detection robustness and flexibility of ANN model to noise. Nonetheless, the traditional shortcomings of fuzzy logic in determining the fuzzy rule are still an issue.

Suh et al. (2000) demonstrated another hybrid technique by combining ANN with genetic algorithm to identify the location and depth of cracks in a structure with frequency information only. Multilayer ANN trained by backpropagation algorithm was used to learn the input (the location and depth of a crack) and output (the structural eigenfrequencies) relation of structural system. With the trained ANN, genetic algorithm was applied to identify the crack location and depth minimizing the difference from the measured frequencies. Finite element model of a clamped-free beam and a clamped-clamped plane frame were used to confirm the effectiveness of the proposed method.

The issue regarding the complexity of ANN design was addressed in Yuen and Lam (2006). They developed a mathematically rigorous method to select the optimal class of ANN models based on Bayesian probabilistic method. The damage detection method presented in their study consisted of two phases. The first was to identify the damage location using vibration signature and the second was to estimate the damage severity based on modal parameter. A numerical model of a five-story shear building was used to quantify the method. The authors only focused on selecting the best number of nodes in hidden layer. The efficiency of this method were compared with

the rule of thumb to calculate the number of hidden nodes suggested by Kermanshahi (1999). No comparison in terms of ANN performance has been made.

Sahoo and Maity (2007) followed up the above study to consider the problem in selection of the network parameters such as learning and momentum rate, convergence criteria, training algorithm. The authors applied neuro-genetic algorithm to determine the damage location and severity based on modal parameter and strain value. Genetic algorithm was applied to select the suitable values of the network parameters by treating them as variables and backpropagation ANN for damage detection. The efficiency of the algorithm was tested with two structures, a beam and a plane frame.

Although algorithm/mapping topology proposed in some studies has been claimed feasible to improve the conventional multilayer backpropagation ANN, there were no specific guideline on their applications, moreover, the mechanism has not been well explained and quantified. Most of them are context dependant and certain algorithms are difficult to apply. It must also be noted that the accuracy of ANN prediction is also influenced by the characteristic of training data. In most of the studies, there were no detailed explanations on how the training data were prepared. Through a literature search, no article that investigates the influence of training data characteristic to ANN performance for the purpose of damage detection is found.

2.2.3 Application

Although great progress has been made in application of ANN for damage detection, most of the presented works only demonstrated their feasibility through numerical simulations. A few successful verification works using experimental data are limited to simple laboratory tests under controlled conditions, such as beam-like structure (Islam and Craig 1994; Levin and Lieven 1998; Sahin and Shenoi 2003) and cylindrical shell (Marwala 2000; Yu et al. 2007). There are also several studies involving experiments in uncontrolled conditions and most of them reported the ANN model less successful (Chang et al. 2000; Feng and Bahng 1999; Worden et al. 1993; Zapico et al. 2001), probably because of the inevitable modeling and

measurement error. Those studies recommended that noise should be considered in training. But only a few studies are found addressing this problem.

Ortiz et al. (1997) investigated the application of noise corrupted training data based on a study by Matsouka (1992). The corrupted analytical data was used to train the ANN model to reduce the effect of error in measurement data. The method was illustrated using a numerically modeled cantilever beam. This method is known as noise injection learning method (NIL).The author concluded that the network trained with data containing noise had a tendency to provide better results when tested with noisy experimental data. Lee et al. (2002b) further investigated the method using experimental data of a bridge structure model under traffic loading, and provided the same conclusion. This approach was then applied in several other studies (Lee and Yun 2006; Shahin et al. 2003; Yeung and Smith 2005).

For modeling error, Lee et al. (2005) applied the difference of mode shape before and after damage as inputs to ANN model. Two numerical models, laboratory and field test data were used to verify the proposed method. The authors concluded that the mode shape differences or the ratios of mode shapes before and after damage is less sensitive to modeling error in the baseline finite element model. Ni et al. (2002) suggested a method using differences in the estimated element-level stiffness before and after damages as the output variables to deal with modeling error.

Most of the studies in applications of ANN for damage detection have been limited to example structures with small number of degrees of freedom and the damage levels have been usually assumed quite significant. This is because the computational time needed and the computer memory required to train and test an ANN model increase exponentially with the number of freedom in a structure model. To improve the computational efficiency, Yun and Bahng (2000) proposed an approach employing the substructural method and submatrix scaling factor to tackle this problem. A numerical modeled truss structure with 55 elements was used to demonstrate the approach. The damage scenarios considered were formed by reducing the stiffness of one or a few truss members. The strategy was to divide the structure to several substructures and the identification process is carried out on a

substructure at a time. Frequencies and mode shapes were used as the inputs and submatrix scaling factors were used as the output. This study also demonstrated the efficiency of the proposed method with the effect of measurement noise by employing NIL.

Qu et al.(2004) further investigated this approach using FRF as the inputs. The spectral lines used were from 0Hz to 200Hz with an interval of 0.2Hz. Independent component analysis (ICA) was used to reduce the length of input data. The study employed the same truss structure as Yun and Bahng (2000) for verification. Damage scenarios were simulated by reducing the stiffness of two of the truss member. The authors claimed that the method improved the ability and computational efficiency to identify damages in large structures.

However, in the above method, early and sometimes subjective judgement using conventional technique such as visual inspection is required to select the probable damage areas. To improve this method Ko et al. (2002) has developed a three-stage identification technique. A novelty technique utilizing auto associative neural network is suggested in the first stage to identify the damage existence in the structure, followed by a combination of modal curvature index and modal flexibility index to identify the damage area in the second stage. Once a probable damage area is identified an ANN model is used to determine the damage location and severity in the third stage. The method was demonstrated using numerical model of Kap Shui Mun Bridge in Hong Kong. The method has some shortcomings: i) the novel detection approach used in the first stage may not be sensitive enough to trigger the alarm for damage existence, as shown in two of the twelve cases analysed in the study; ii) modal curvature index and modal flexibility index are sometimes unable to provide accurate identification especially when damage is near the support area, as demonstrated in the study; iii) if the damage occurs in multiple areas, expensive computation is still required in the third stage to train the ANN model as the number of areas that contain damages increases.

2.3 Summary

This chapter presents a review of the vibration based damage detection methods. The review demonstrates that the ANN based methods provide several advantages over the traditional mathematical methods

i) ANN is able to detect damage correctly, even when trained with incomplete data, without using data expansion or finite element reduction methods.
ii) Once properly trained, the ANN calculation is relatively fast. The need for construction of mathematical models can be avoided.
iii) There is no prior limit on the type of vibration parameters to be used as the diagnostic parameter. The inputs and outputs can be selected with certain flexibility without increasing the complexity of the training process.

Although many studies demonstrated that ANN is a feasible tool for damage detection based on vibration data, several problems still remain to be resolved before this approach becomes a truly viable method for structural health monitoring and damage identification.

The impact of uncertainties on the reliability of ANN models for structural damage detection needs to be analysed. In practice uncertainties in the finite element model parameters and modeling errors are inevitable. The existence of modeling error in a finite element model due to the inaccuracy of physical parameters, non-ideal boundary conditions, finite element discretization and nonlinear structural properties may result in the vibration parameters generated from such a finite element model not exactly representing the relationship between the modal parameters and the damage parameters of the real structure. On the other hand, the existence of measurement noise in the measured data that is normally used as the testing data for damage identification is unavoidable. Since the reliability of an ANN prediction relies on the accuracy of both components, the existence of these uncertainties may result in false and inaccurate ANN predictions.

Another problem is the difficulty to apply ANN to detect local and small damage especially in complex structures. This is because it needs a fine finite element mesh to detect small local damages in a structure, which will results in a large number of elements in the finite element model of a structure, hence, a high dimension network in the ANN model. It then requires excessive computational time and computer memory to train the ANN model. The computational time and computer memory needed to train an ANN model increase dramatically with the number of the structural degrees of freedom. Therefore, in most examples published in the literature that use ANN to detect damage, rather large finite elements are used in structure model to reduce the degrees of freedom. Since a large element is insensitive to a small damage and severe damage scenarios are usually assumed to demonstrate the ANN model.

CHAPTER 3

DETERMINISTIC DAMAGE DETECTION USING ARTIFICIAL NEURAL NETWORK

3.1 Introduction

ANN can handle problems involving imprecise data and that are highly nonlinear and complex. They are ideally suited for pattern recognition and do not require a prior fundamental understanding of the process or phenomena being modeled (Bhagat 1990). As damage detection is an inverse process involving the comparison of the changes in structural response, it appears to be within the scope of pattern recognition capabilities of ANN.

This chapter demonstrates the ability of a deterministic ANN model to identify damage in structures. '*Deterministic*' method implies that the ANN model is trained using data from finite element model and the uncertainties in finite element model and measured data are not considered. Numerical models of a reinforced concrete slab and a single span steel frame are used to demonstrate the method. Experimental data of the reinforced concrete slab is applied for verification. To evaluate the effect of different input parameters on ANN performance, a sensitivity study is performed by using different combinations of input parameters to train the ANN model, such as using different numbers of natural frequencies or a combination of natural frequencies and mode shapes.

Modal data (frequencies and mode shapes) are used as the input parameters to predict the elemental stiffness parameter of the structure in this study. Modal data has been selected based on the following considerations:

i) Modal data is easy to obtain from measurements of the structural behaviour.

ii) Frequency represents global behaviours, while the mode vector represents local characteristics.

iii) Modal data is not subjected to time constraint; hence, the length of the input pattern can be selected based on the number of modes and degree of freedom.

3.2 ANN model

ANN involves processing elements or neurons and interconnection weights between the neurons. These interconnection weights determine the nature and the strength of the connections between neurons. Figure 4-1 shows a neuron with an input vector of R variables.

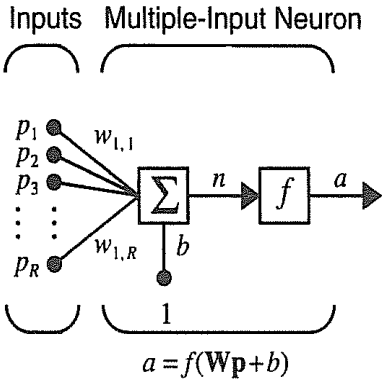

Figure 3-1: A neuron with an input vector of R variables (Hagan et al. 1995)

The inputs p_1, p_2 ,..., p_R are multiplied by weights $w_{1,1}$, $w_{1,2}$, ...,$w_{1,R}$ and the weighted values are summed together with a bias b to produce the net input n:

$$n = w_{1,1}p_1 + w_{1,2}p_2 + \cdots + w_{1,R}p_R + b \tag{3-1}$$

The expression in matrix form:

$$n = Wp + b \tag{3-2}$$

The neuron output can be written as:

$$a = f(Wp + b) \tag{3-3}$$

where $f(\cdot)$ is the transfer function.

Examples of transfer functions are: hard limit, linear, log-sigmoid and sigmoid. Hagan et al.(1995) provides detail explanation regarding the transfer functions. For normal applications, the neurons are combined and arranged in layers and it is known as *multilayer perceptron*. The layer which receives the inputs is called an input layer while the layer which provides output is known as output layer. The middle layers are called hidden layers. Figure 4-2 exhibits an ANN model with two hidden layers.

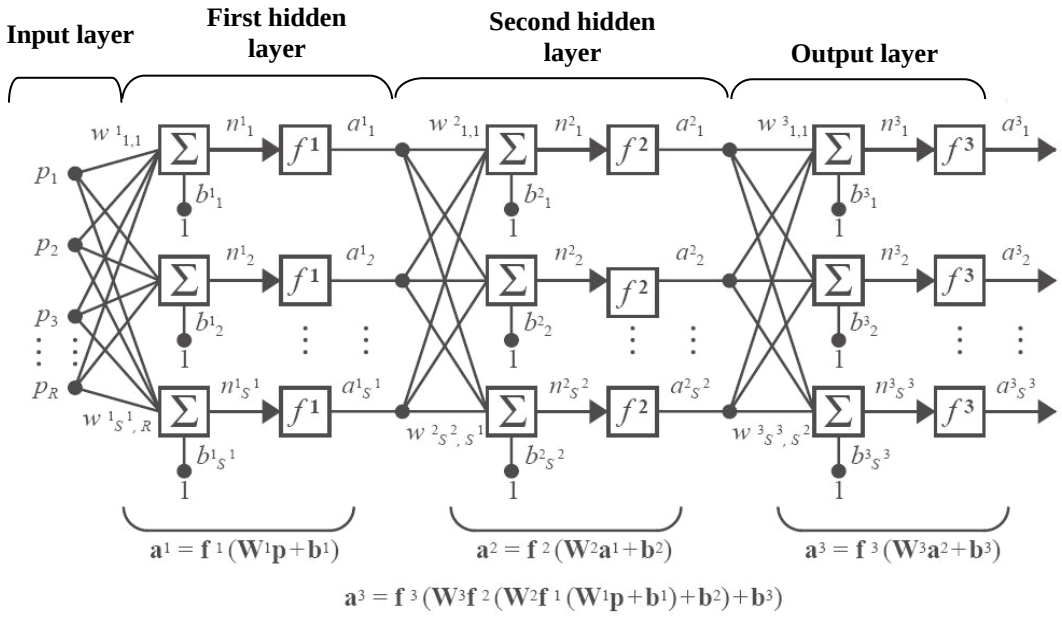

Figure 3-2: ANN model with two hidden layers (Hagan et al. 1995)

As shown in the figure, there are *R* inputs, S^1neurons in the first hidden layer, S^2 in the second hidden layer and S^3 neurons in the output layer. The outputs of the first hidden layer are the inputs tofor the second hidden layer and the output of the second hidden layer are the inputs to the output layer. Typically, there are two main stages in building an ANN model: i) selection of an ANN architecture; ii) training the ANN model. Details of both stages are explained in the following subsections.

3.2.1 Selection of an ANN architecture

Many types of ANN have been developed, such as Hopfield neural network, Radial Basis neural network and Kohonen neural network. In this study, multilayer perceptron ANN model is used. The reason is that multilayer perceptron networks have been applied successfully to many different problems (Rumelhart and McCleland 1986) and it has been proven to be an universal approximator, which means that it can approximate any continuous multivariate function to any degree of accuracy (Funahashi 1989; Hornik et al. 1989)

A multilayer perceptron consists of an input layer, one or more hidden layer and an output layer. The number of neurons in input and output layer depends on the length of input and output vectors. However, there are no standard rules available for determining the appropriate number of hidden layers and hidden neurons per layer. General rules of thumb have been proposed by a number of researchers. For example, Shih (1994) proposed the pyramidical topology, which can be used to approximate numbers of hidden layers and hidden neurons. In the Kalmorogov and Lippmann's approach (Maren et al. 1990), the number of hidden neurons is calculated as $2N+1$, where N is the number of input neurons. Gately (1996) suggested the number of hidden nodes to be equal to the total of the number of inputs and outputs. Azroff (1994) concludes that the optimum number of hidden neurons and hidden layers is highly problem dependant. Ash (1989) and Kaastra and Boyd (1996) suggest a trial and error method to determine the number of hidden neuron. The trial and error method has been widely applied by researchers in many areas including damage detection (Sahin and Shenoi 2003; Spillman et al. 1993; Szewczyk and Hajela 1992; Yun and Bahng 2000). In this study, an ANN architecture with one hidden layer is used and the number of hidden neurons is determined using the trial and error method.

Another component in an ANN model that needs to be specified is the transfer function. The transfer function is chosen by the designer to meet certain requirements of the problem to be solved by ANN. This transfer function may be a linear or a nonlinear function of n (refer to Figure 4-1). In this study, a hyperbolic tangent sigmoid function (*tansig*) is chosen for hidden and output layer since the input and

output vectors are normalized between -1 to 1. This transfer function is also known as sigmoid function. The hyperbolic tangent sigmoid function is shown in Figure 4-3. The input and output normalization process will be described in the following subsection.

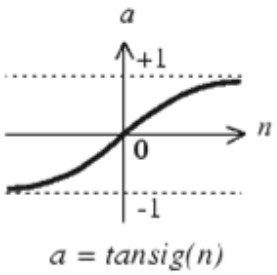

Figure 3-3: Hyperbolic tangent sigmoid function (Hagan et al. 1995)

This transfer function takes the input and squashes the output into the range of -1 to 1, according to the expression:

$$a = \frac{e^{n} - e^{-n}}{e^{n} + e^{-n}} \tag{3-4}$$

where *a* is the output and *n* is the input

Neural network toolbox which runs on MATLAB platform is used to model the ANN model in this study.

3.2.2 Training an ANN model

Once the ANN architecture has been configured, the weights must be set to minimize the prediction error. This process is known as training. The training process is performed by introducing a set of input and output data to the ANN model. The network then processes the inputs and compares its resulting outputs against the desired outputs. This type of training process is known as supervised learning. The learning process is performed by a learning algorithm. The well-known example is backpropagation algorithm (Fausett 1994; Haykin 1994). Through backpropagation

algorithm, the process is repeated until the error between the desired output and the predicted output met the specific stopping criteria. The differences between desired output and the predicted output are combined and denoted by an error function.

3.2.2.1 Learning algorithm

Backpropagation algorithms are categorized into traditional and modern second order algorithm. According to Bishop (1995) and Shepherd (1997), modern second-order algorithms such as Conjugate gradient and Levenberg-Marquardt are substantially more efficient for many problems. A comparison study between Leverberg Maquardt algorithm and Conjugate gradient algorithm was carried out by Hagan and Menhaj (1994), and the authors found that Leverberg Maquardt outperformed Conjugate gradient algorithm in terms of convergence performance. As a result, this study employs Leverberg Maquardt algorithm to train the network. This algorithm is a variation of Newton's method that was designed for minimizing functions that are sums of squares of other nonlinear functions. Detail derivation of Leverberg Maquardt algorithm can be found in Bishop (1995) and Hagan et al. (1995). In this study, mean squared error (MSE) is used as the error function.

$$MSE = \frac{1}{n}\sum_{j=1}^{n}(O_t - O_p)^2 \tag{3-5}$$

where O_t and O_p are the target and predicted outputs and n is the number of data.

MSE indicates the difference between the ANN output value and the desired value. The relationship between input and output variables is considered established when the MSE value is close to 0.

3.2.2.2 Stopping criteria

A multilayer perceptron ANN model is prone to an overfitting problem (Geman et al. 1992). Under the overfitting situation, the training performance still increases while the performance on unseen data becomes worse. Several methods have been

proposed by researchers to overcome overfitting, such as pruning (Hassibi and Stork 1993) , regularization methods (Krogh and Hertz 1995) and early stopping method (Prechelt 1995). According to Finnoff et al. (1993), early stopping method is widely applied because it is simple to understand and has been reported superior than the regularization method. In this study early stopping method is applied as the stopping criteria.

This study applies four basic steps of early stopping method.

i) Split the training data into a training set and a validation set
ii) Train only on the training set and evaluate the per-example error on the validation set once in a while. In this study the error is assessed in every fifth training cycle (epoch).
iii) Stop training as soon as the error on the validation set is higher than the last time it was checked.
iv) Use the weights the network had in that previous step as the result of the training run.

3.2.2.3 Training data

The training data to train the ANN model is generated using the finite element model of the desired structure. It is very important that the training data represents the largest possible range of input data. In this study, there is no prior assumption of the damage area, thus the data is generated randomly over all possible damage areas. Latin hypercube sampling method (Helton and Davis 2003) is employed to guarantee that the training data is generated uniformly over each area within the specified range of damage severities.

As mentioned earlier, the input variables for the ANN model in this study comprises of frequency and mode shape. Both parameters vary in different range of magnitude, and thus it is easy to see that rows of the input matrix with large magnitude variation dominate the value of the distance, making inputs with small magnitude differences irrelevant to the estimation process. To overcome this problem, the input and output data are normalized within the prescribed bounds. In this study, input and output data

are normalized between the interval of [-1, 1]. The normalized inputs and outputs are calculated by:

$$p_n = \frac{2(p - \min(p))}{(\max(p) - \min(p))} - 1 \tag{3-6}$$

where p is a row of the input/output matrix and p_n is the normalized input and output parameters.

Testing steps took place after the training process. A new set of data is applied to the trained model for damage detection. The testing data are normalized using precalculated minimum and maximum values of training data. In this study, numerically simulated damage data is used to train the ANN model. For testing, both numerical and experimental data are applied.

3.3 Numerical examples

This section demonstrates the ability of ANN in detecting damage from noise-free data. Two different structures are used as the examples which are; i) a two-span reinforced concrete slab and ii) a single-span steel portal frame. Both structures are modeled using finite element model through *Structural Dynamics Toolbox* (Balmes 1996), which runs on MATLAB platform. Several damage cases involving single and multiple damages are simulated to assess the ANN model. The damages are imposed by reducing the E values of each corresponding segment.

3.3.1 Numerical example 1 – Concrete slab

To demonstrate the ability of ANN in damage detection, a numerical example of the concrete slab presented in Chapter 3 is utilized. The slab is modeled with 52 shell elements and 81 nodes and the supports are idealized as simply supported. The slab is divided into seven segments and every element within the same segment is assumed to have the same material properties. The material properties used are: Young's modulus (E) = 3.3 $\times$ 10^{10} N/mm^2, mass density (ρ) = $\times 10^3$ kg/m^3 and Poisson's ratio (υ) = 0.2. Figure 4-4(a)-(b) show the slab mesh together with node

number and the slab segmentation. Modal analysis is conducted using finite element to generate the input and output data to train the ANN model. Four damage scenarios are simulated to assess the ANN ability in damage detection. Scenarios 1 to 3 consist of a single damage in segment 2 with different severities. Multiple damages are simulated in scenario 4 involving segment 2, 4 and 6. Table 4-1 show the *E* values of the damage scenarios.

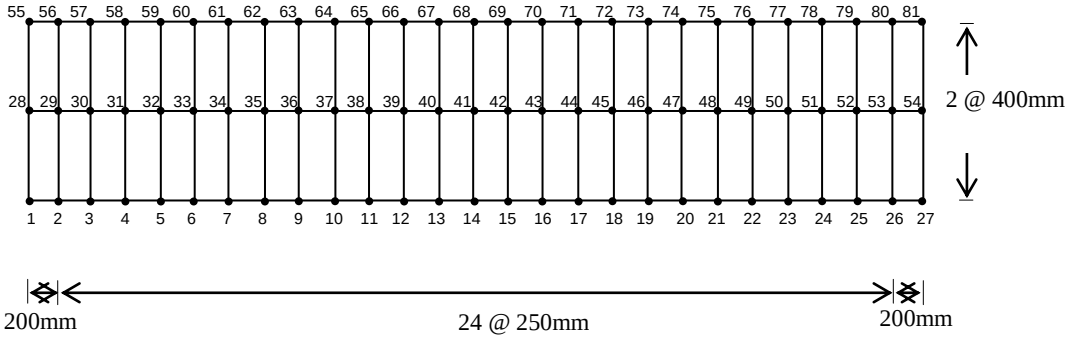

(a) Finite element mesh

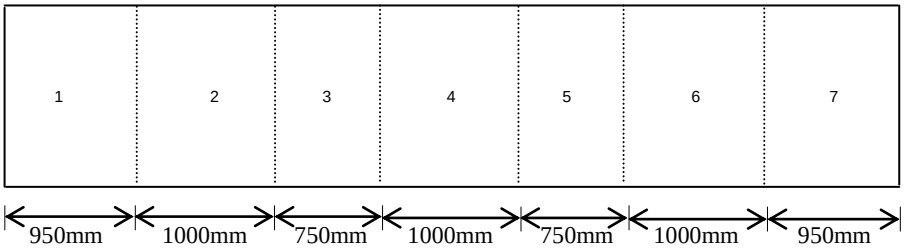

(b) 7 segments of the slab

Figure 3-4: Slab model

Table 3-1: *E* values for Scenario1 to Scenario 4

Segment	1	2	3	4	5	6	7
Scenario 1	$1.0\times E$	$\mathbf{0.95}\times \boldsymbol{E}$	$1.0\times E$	$1.0\times E$	$1.0\times E$	$1.0\times E$	$1.0\times E$
Scenario 2	$1.0\times E$	$\mathbf{0.90}\times \boldsymbol{E}$	$1.0\times E$	$1.0\times E$	$1.0\times E$	$1.0\times E$	$1.0\times E$
Scenario 3	$1.0\times E$	$\mathbf{0.85}\times \boldsymbol{E}$	$1.0\times E$	$1.0\times E$	$1.0\times E$	$1.0\times E$	$1.0\times E$
Scenario 4	$1.0\times E$	$\mathbf{0.85}\times \boldsymbol{E}$	$1.0\times E$	$\mathbf{0.85}\times \boldsymbol{E}$	$1.0\times E$	$\mathbf{0.85}\times \boldsymbol{E}$	$1.0\times E$

The frequencies of the first four modes generated from the finite element analysis are shown in Table 4-2. The values in the parenthesis are the percentage of frequency change as compared to the undamaged state. The average percentage of the frequency change decreases from -0.48% (scenario 1) to -2.79% (scenario 4) as the damage severities increase. Figure 4.5(a)-(d) illustrate the first four mode shapes of the slab in different damage states. It is assumed that the mode shapes are measured at every node on the centreline along the span length. It is observed that the mode shape differences are more obvious when severer damage occurs. Only frequencies and mode shapes of the first four modes are selected as the inputs to train the ANN model. All mode shape values at the points on the centreline are considered except the points at the supports as they provide 0 values in every mode. The outputs are *E* values of each segment. Thus, there are 112 input nodes and 7 output nodes used in the ANN model. Figure 4-6 shows the ANN architecture.

Table 3-2: Frequencies of the slab in different damage states (Hz)

	Undamaged	**Scenario 1**	**Scenario 2**	**Scenario 3**	**Scenario 4**
1st mode	18.222	18.086 (-0.72)	17.933 (-0.84)	17.776 (-0.88)	17.334 (-2.48)
2nd mode	28.576	27.910 (-0.59)	27.731 (-0.64)	27.558 (-0.63)	26.3119 (-4.52)
3rd mode	72.107	71.872 (-0.33)	71.599 (-0.38)	71.315 (-0.40)	69.997 (-1.85)
4th mode	87.733	87.495 (-0.27)	87.226 (-0.31)	86.958 (-0.31)	84.963 (-2.29)
Average of change (%)		-0.48	-0.54	-0.55	-2.79

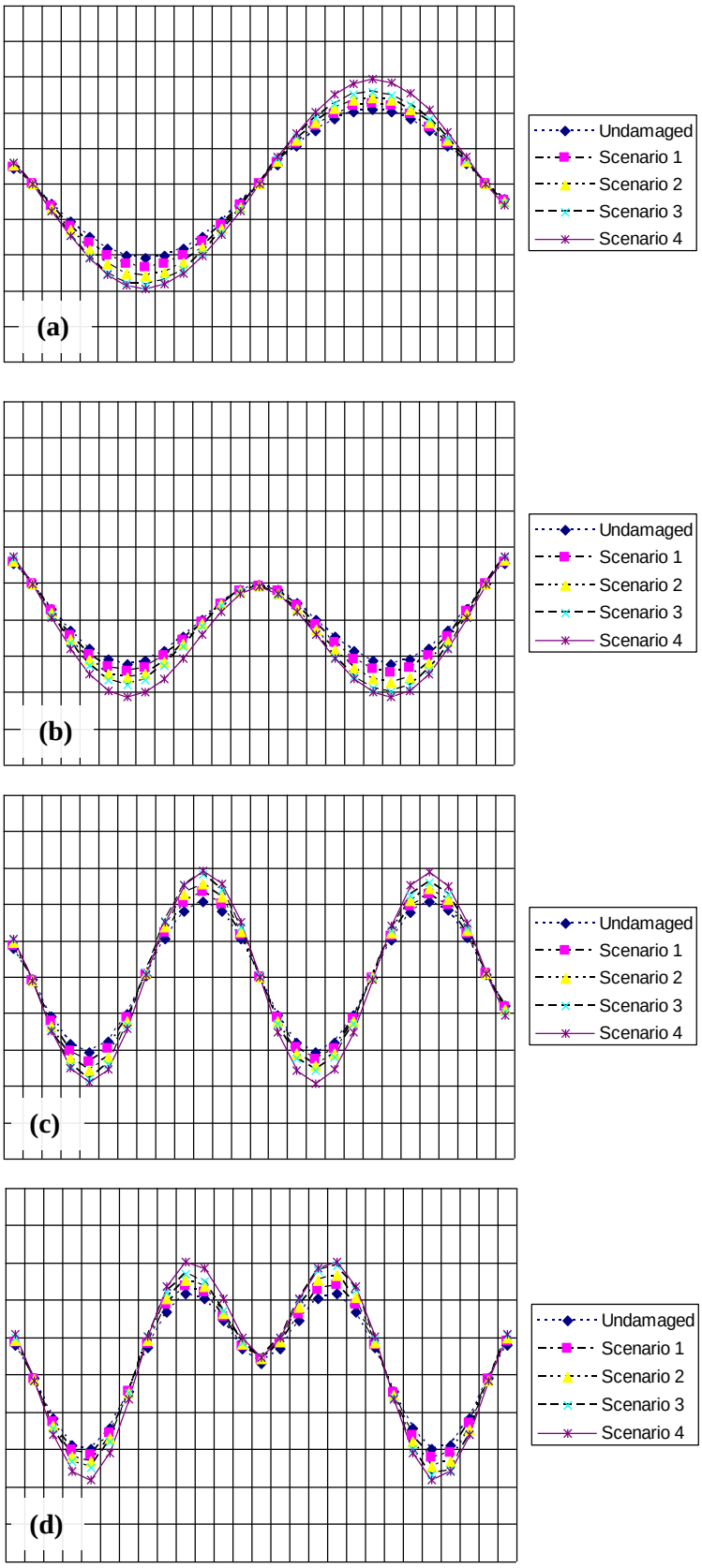

Figure 3-5: The first four mode shapes in different damage states. (a) Mode 1 (b) Mode 2 (c) Mode 3 (d) Mode 4

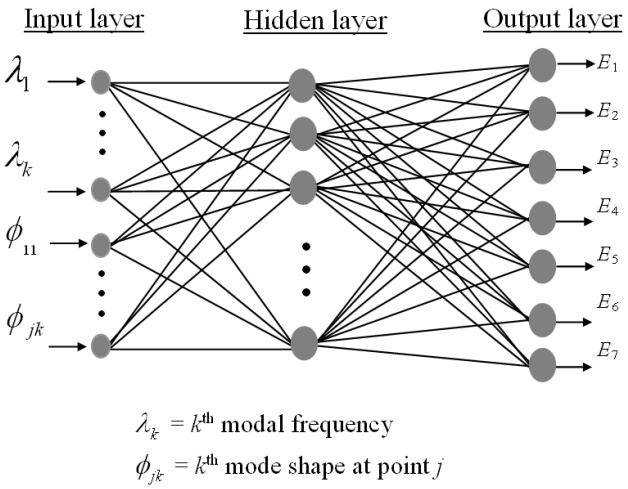

Figure 3-6: ANN architecture

To train the model, 1200 cases are generated, with the elastic modulus values for each member varying from 0.2*E* to 1.5*E*, using the finite element model. To apply the early stopping method, the data are randomly partitioned into training set and validation set in a ratio of 2:1, resulting in 800 data sets for training and 400 data sets for validation. The probability density functions of *E* values of every segment are uniformly distributed as shown in Figure 4-7(a)-(g).

A series of trial and error process are performed to select the best number of hidden neurons. ANN models with different number of hidden neurons are trained and each ANN model is evaluated based on training performance. The number of hidden neurons is varied from 4 to 36 hidden neurons with the increment of two. Figure 4-8 illustrates the ANN training and validation performance at different number of neurons. It is seen that the training MSE values decrease indicating that the performance of ANN improves when the number of hidden neurons are increased to 16 hidden neurons (MSE = 0.0026) and then it remained around the same magnitude up to 22 hidden neurons before went up to 0.0126 at 36 hidden neurons. The same trend is also observed in validation performance, where the minimum error occurred at 16 hidden neurons. Based on this result, the ANN with least error (16 hidden neurons) is selected. Figure 4-9 illustrates the training and validation performance of the selected ANN model with increasing number of epochs. It is shown that the training stopped at 31st epoch with a MSE value of validation 0.035. Generally the training process is satisfactory as both the training and validation performances converged at low MSE values.

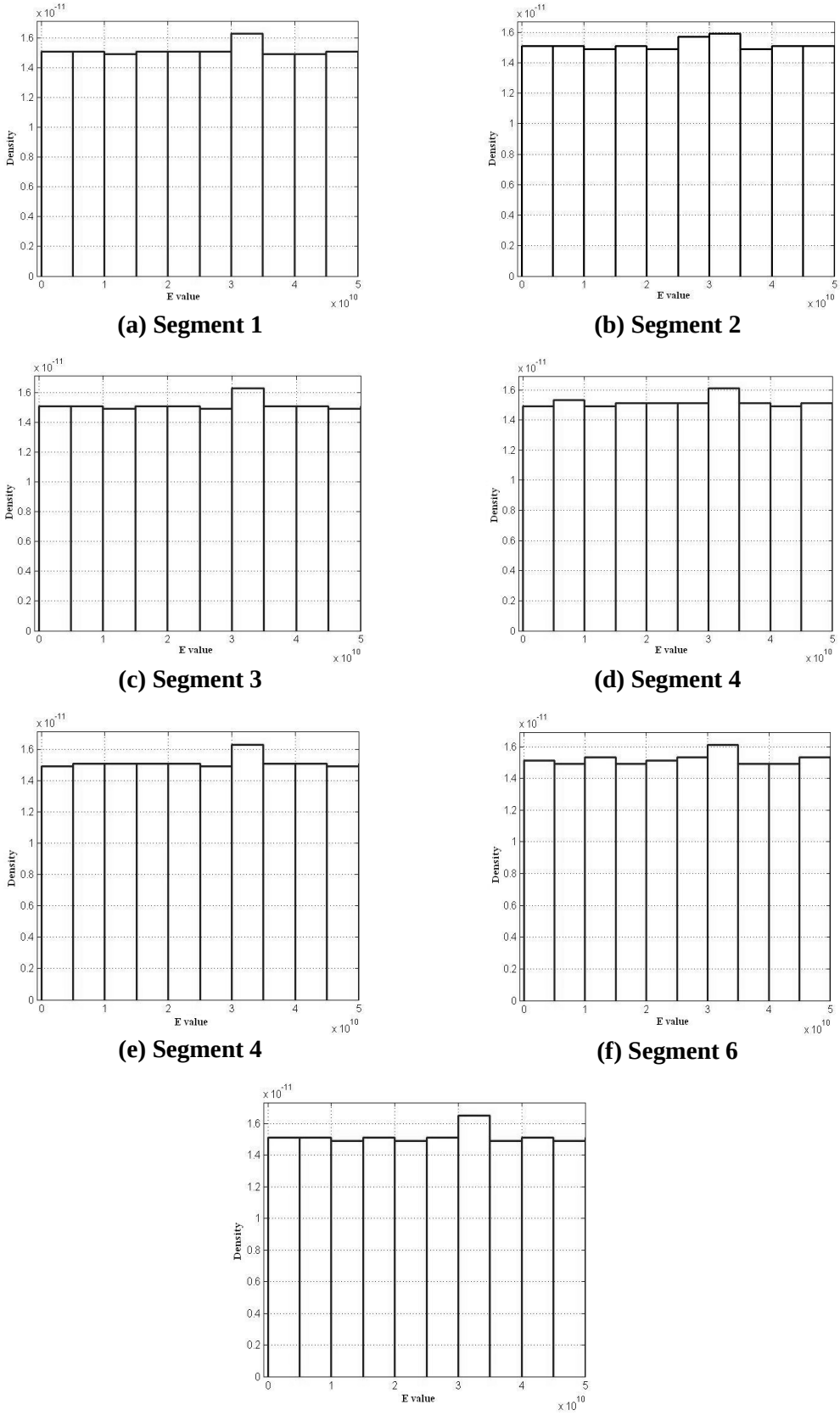

(a) Segment 1

(b) Segment 2

(c) Segment 3

(d) Segment 4

(e) Segment 4

(f) Segment 6

(g) Segment 7

Figure 3-7: Probability density functions of *E* value at different segments.

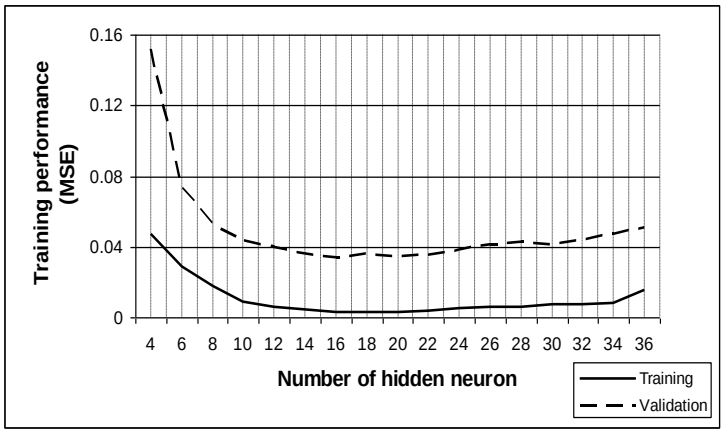

Figure 3-8: ANN performance with different number of neurons

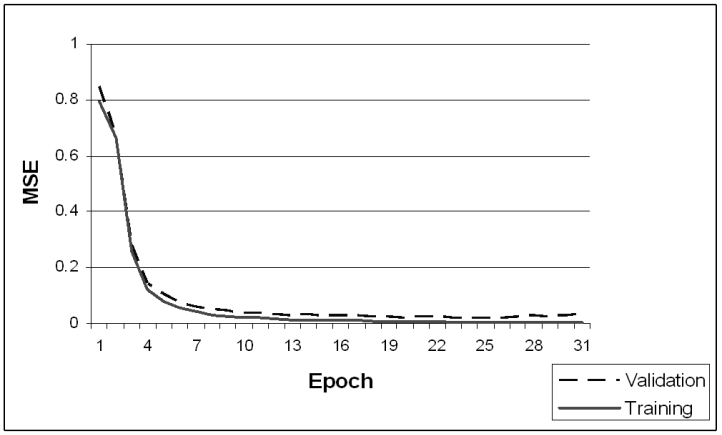

Figure 3-9: ANN performance with increasing number of epochs

Once the appropriate ANN is determined, the testing data are fed to the trained model to predict the location and severity of the simulated damage cases. These testing data are the four simulated damage scenarios in Table 4-1. Figure 4-10(a)-(d) show the predicted results in comparison with the actual values. The changes of the stiffness parameter or the damage severity for each segment are defined by a Stiffness Reduction Ratio (SRF) as:

$$SRF = 1 - \frac{E'}{E} \tag{3-7}$$

where E is the Young's modulus of the undamaged state and E' is that at the damage level of interest.

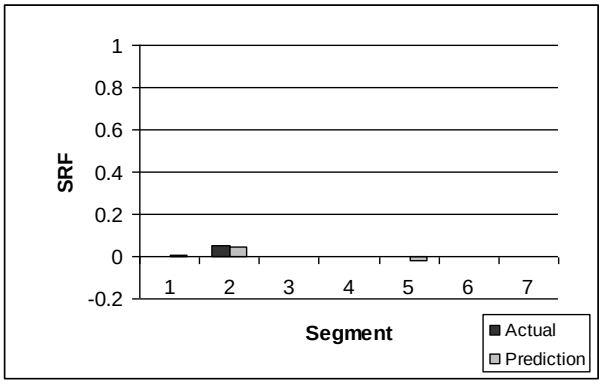

(a) Scenario 1

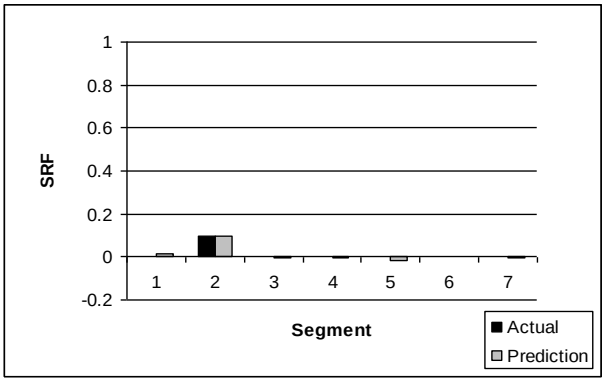

(b) Scenario 2

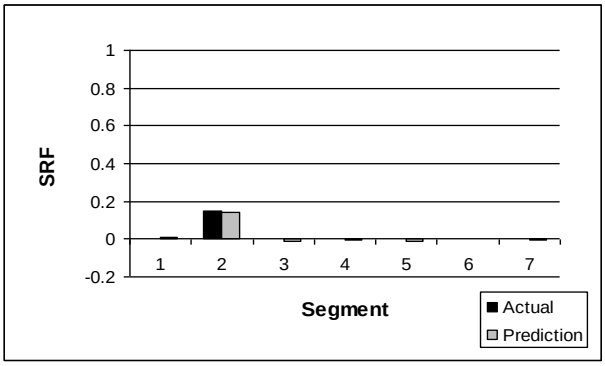

(c) Scenario 3

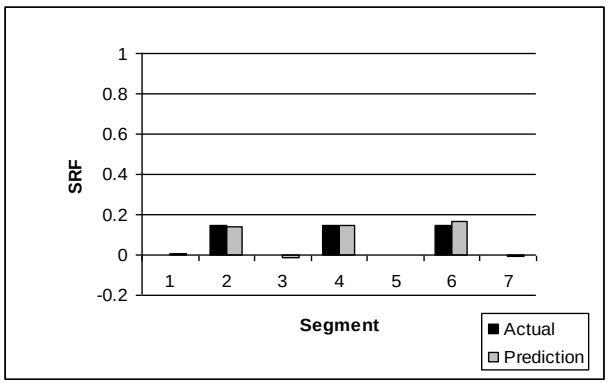

(d) Scenario 4

Figure 3-10: ANN prediction result

The results show that the predicted SRF values are very similar to the actual SRF values, which indicate that the ANN model is able to predict the locations and severities of the damage correctly. Some minor overestimation and underestimation of the SRF values are observed at undamaged segments due to numerical error. This type of error was also experienced by many other researchers. However, as the errors are very small, they are unlikely to lead to false damage identifications.

3.3.2 Numerical example 2 – Steel frame

To further demonstrate the ability of ANN for damage detection, a single span steel portal frame shown in Figure 4-11 is used as an example. The cross section of beam is 40.50 × 6.0 mm^2, and column is 50.50× 6.0mm^2. The span length and height of the frame are both 1000mm. Rigid connections are applied between the beam and the columns, and the supports are assumed as clamped. The material properties used are: $E = 2.1\times10^{11} N/m^2, \rho = 7.67\times10^3, \nu = 0.2$. The frame is modeled with 10 elements in each member. To reduce the computational time and memory requirement, the elements are lumped into 6 segments as shown in the figure. Each segment consists of 5 elements, and the 5 elements in each segment are assumed to have the same stiffness values.

Modal analysis is conducted using the finite element model to estimate the vibration frequencies and mode shapes of the frame structure. These vibration properties are used as input and output data to train and test the ANN model. Two damage scenarios are generated to assess the ANN prediction performance. Scenario 1 consists of damage in two segments (1 & 4) of the frame, and scenario 2 consists of damage in four segments (1, 3, 5 & 6). Table 4-3 shows the *E* values for scenario 1 and scenario 2. The frequencies and mode shapes of the first three modes are shown in Table 4-4 and Figure 4-12.

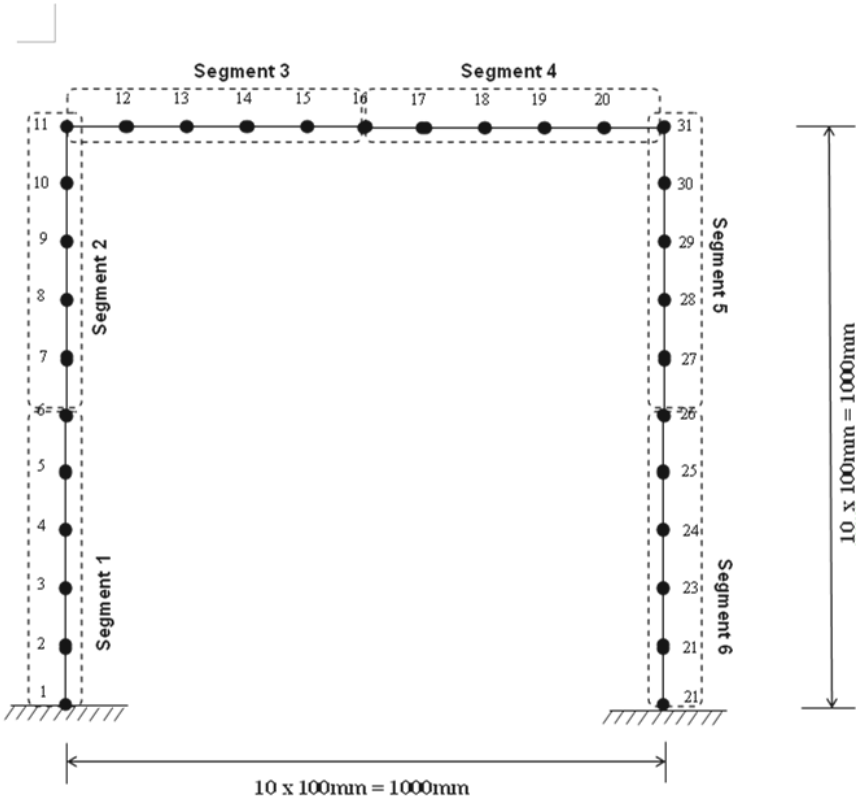

Figure 3-11: Finite element model of the steel portal frame

Table 3-3: *E* values for scenario 1 and 2

Segment	**1**	**2**	**3**	**4**	**5**	**6**
Scenario 1	$0.4\times E$	$1.0\times E$	$1.0\times E$	$0.2\times E$	$1.0\times E$	$1.0\times E$
Scenario 2	$0.4\times E$	$1.0\times E$	$0.3\times E$	$1.0\times E$	$0.4\times E$	$0.3\times E$

Table 3-4: Frequencies of the frame in different damage states

	Undamaged	**Scenario 1**	**Scenario 2**
Mode 1	4.628	3.937	3.530
Mode 2	16.112	12.567	11.269
Mode 3	20.649	16.491	14.891

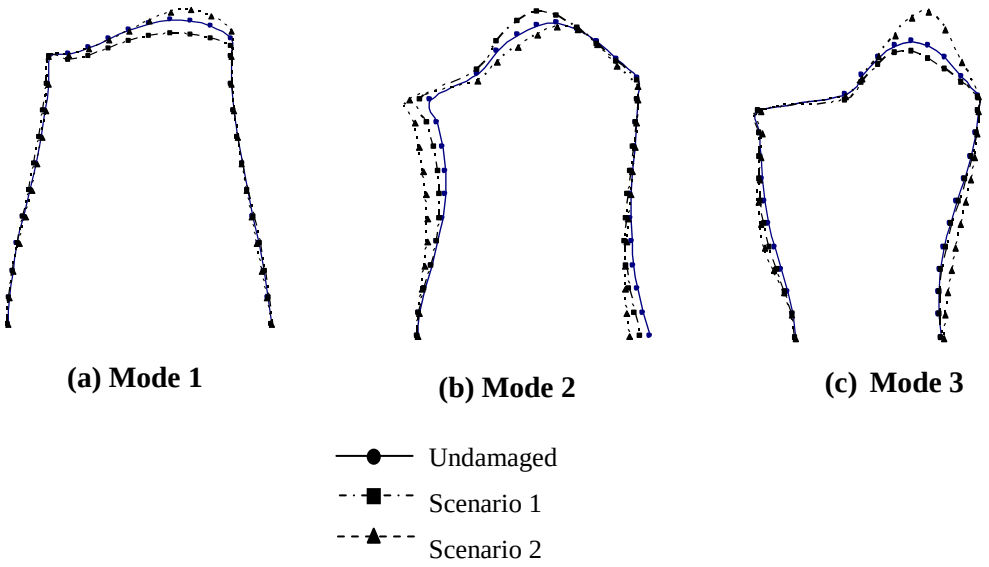

Figure 3-12: First three mode shapes of undamaged, scenario 1 and scenario 2 state

To train the ANN model, 1200 data sets are generated based on the Latin hypercube sampling method. The data are divided into training and validation sets in a ratio of 2:1. A trial and error method is utilized to attain the best ANN topology. Only nine mode shape points and frequencies for the first three modes are used as the input parameters and Young's modulus (*E* values) of all the segments are used as the output. The selected points are 2, 6, 10, 12, 16, 20, 21, 26 and 30. By using the same trial and error process, the best ANN model obtained is with 17 hidden neurons. The trained ANN model is then assessed by introducing the modal parameters of the two damage scenarios mentioned above. Figure 4-13(a)-(b) show the predicted SRF values for every segment in comparison with the actual values.

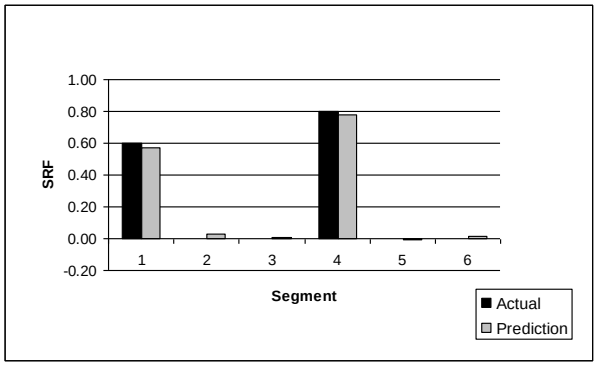

(a) Scenario 1

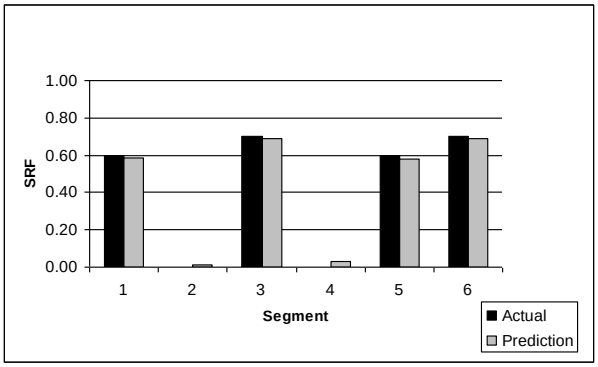

(b) Scenario 2

Figure 3-13: ANN prediction results

The figure shows that the location and severities of the damage are accurately predicted. Some minor numerical errors are also seen in other segments, however these are considered acceptable.

Both examples show that the ANN model is capable of detecting damage location and severity of the damage accurately from frequency and mode shape data. This indicates that ANN model is capable of learning the features of the damage information and provides satisfactory results from noise free data.

3.4 Sensitivity study

In this section more detailed studies are carried out to investigate the sensitivity of the ANN technique to different combination of input parameters. For this purpose, the numerical model of the concrete slab and two of the simulated damage scenarios described above are used for demonstration. Damage scenario 3 and 4 are used to represent a single and a multiple-damages case. To evaluate the effect of different

input parameters on ANN performance, five ANN models with different input combinations are used to detect the simulated damage scenarios. Table 4-5 shows the input combinations for each ANN model. The outputs are *E* values of all the segments. Similar procedure is performed to design the ANN models and the same data sets as in section 4.3.1 are used for training and validation. Table 4-6 shows the ANN architectures and the training and validation performance for every ANN model. The prediction results of the ANN models in comparison with the actual values are shown in Figure 4-14(a)-(b) to 4-18(a)-(b). A typical ANN architecture is expressed as *n-p-m*, where *n,p,m* are the number of neurons in input, hidden and output layer respectively

Table 3-5: ANN model with different combinations of input parameter

Model	Input parameter
1	Frequencies of the first three modes
2	Mode shapes of the first three modes
3	frequency and mode shape of the first mode
4	frequencies and mode shapes of the first two modes
5	frequencies and mode shapes of the first three modes

Table 3-6: Training and validation performance of ANN models

Model	ANN architecture	Training performance (MSE)	Validation performance (MSE)
1	3-12-7	0.2451	0.2801
2	81-16-7	0.0083	0.0493
3	28-14-7	0.0266	0.0737
4	56-18-7	0.0097	0.0572
5	84-18-7	0.0037	0.0434

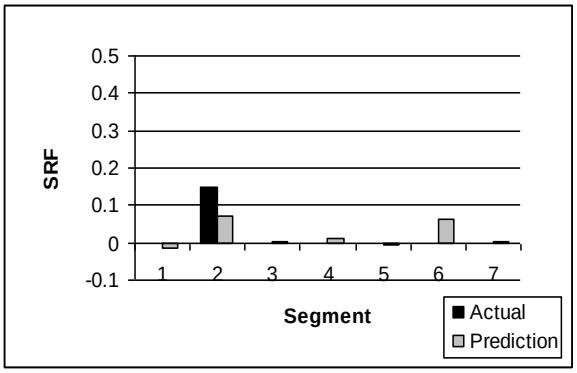

(a) Scenario 3

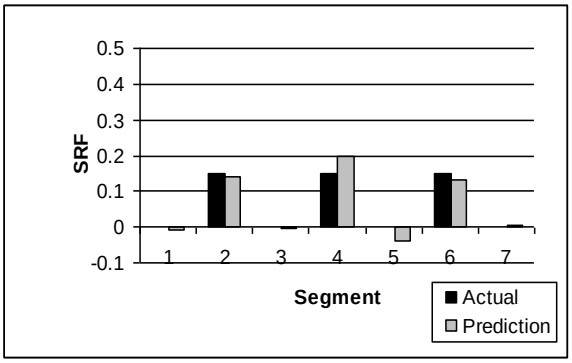

(b) Scenario 4

Figure 3-14: Prediction results of model 1

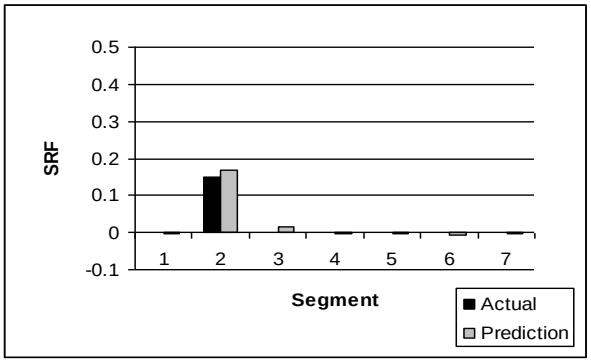

(a) Scenario 3

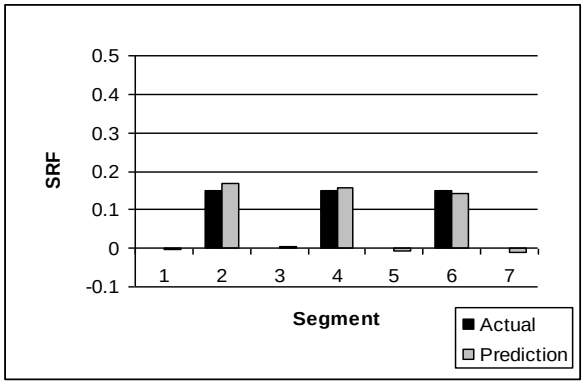

(b) Scenario 4

Figure 3-15: Prediction results of model 2

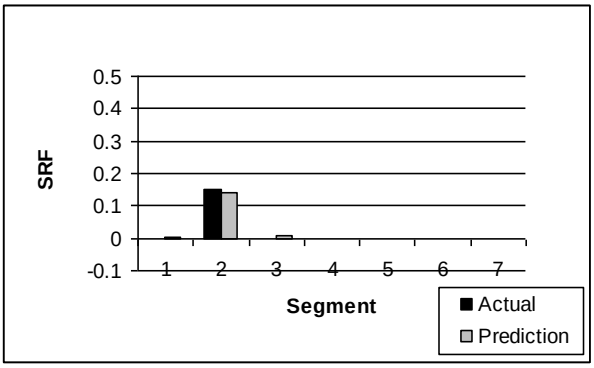

(a) Scenario 3

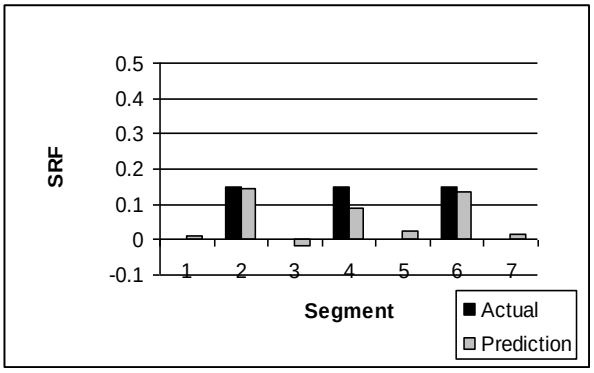

(b) Scenario 4

Figure 3-16: Prediction results of model 3

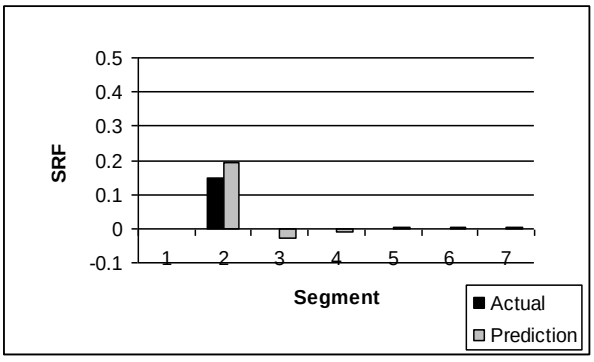

(a) Scenario 3

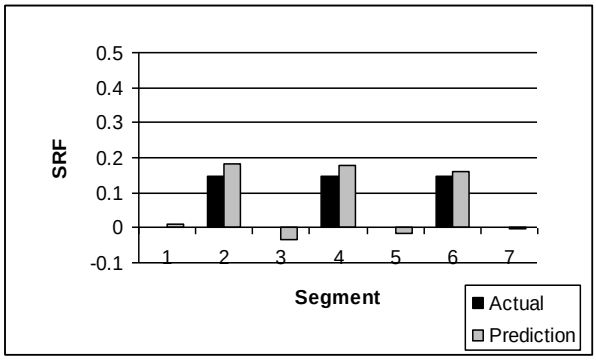

(b) Scenario 4

Figure 3-17: Prediction results of model 4

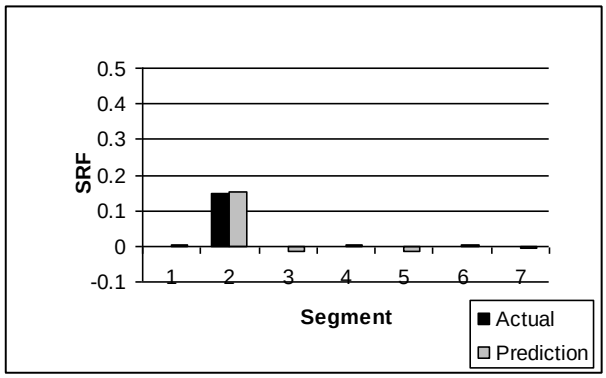

(a) Scenario 3

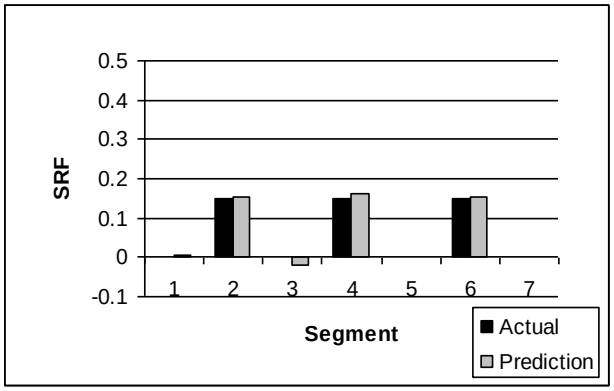

(b) Scenario 4

Figure 3-18: Prediction results of model 5

From Table 4-6, it can be found that the ANN model trained using frequencies only (model 1) provides the lowest training and validation performance with rather high MSE values as compared to other models. As early stopping method is applied in this study, the training process stops when the error on the validation set begins to increase. The error may be due to the reason that the trained ANN model is unable to learn the input and output relationship sufficiently from the training sets given, resulting in a relatively large error in validation. Another possible reason is that the frequencies that are used as the input parameters are not sufficient to provide a unique solution to predict symmetric damages in a symmetric structure, which may result in the network to generalize a single damage as multiple damages or vice versa. This is evidenced in the prediction results shown in Figure 4-14(a)-(b), where the predicted SRF values of element 2 and 6 are similar, which indicates a single damage is predicted as multiple damages, but for symmetric multiple damages all the damage locations and severities are well predicted.

The training and validation performance of ANN model trained with mode shapes as the inputs (model 2) are also shown in the table. Both training and validation error are rather low indicating that the ANN model is able to learn the relationship between mode shapes and damage locations and severities well. The prediction results for single and multiple damages are also good as shown in Figure 4-15(a)-(b) where the damage locations and severities for the both damages cases are accurately predicted. This indicates that mode shape is sensitive to structural damage. However in practice, the measured mode shapes usually have relatively larger errors than the measured frequencies, which may lead to unsatisfactory damage detection results if actual measured mode shapes are used.

A combination of the frequencies and modes shapes with incremental number of modes are used as the input parameters for model 3, model 4 and model 5. As indicated in the table, low MSE values are obtained for training and validation of model 3, model 4 and model 5, indicating that the relationships between input and output are established in all those ANN models. It is also observed that the training and validation performance improve when more numbers of modes are used as the input variable. In terms of the prediction results, both damage scenarios are correctly identified by the ANN models as shown in Figure 4-16(a)-(b) to Figure 4-18(a)-(b). However, model 3 provides less accurate prediction where SRF at segment 4 in scenario 4 is underestimated and some minor false damage estimations are also noticed at segment 5 and 6. The prediction accuracy improves when more numbers of modes are used. For example, for model 5 (Figure 4-18(a)-(b)), the predicted SRF values are almost similar to the actual SRF with less false prediction as compared to model 3 and model 4. These results indicate that ANN provides better prediction when more information is provided. However in practice, high modes are difficult to obtain and higher modes may also introduce more noise, thus does not necessarily give more accurate prediction. The results also indicate that the combination of global and local vibration parameters provides a better outcome than using global parameters only.

3.5 Experimental example

The laboratory tested concrete slab data given in Chapter 3 are used as testing data in this section. A new ANN model is developed to match the arrangement of the measurement point and the measured number of modes of the slab. The first two modal frequencies and mode shapes are used as the input parameters and only six mode shape points are used in training to match the sensor locations of the tested slab. The points are 32, 35, 38, 44, 47, and 50 (refer to Figure 4-4(a)). Points 29, 41, and 53 are not used since they provide 0 values in every mode. Table 4-7 shows the comparison of the frequencies produced by numerical model and the experimental measured frequencies in undamaged state. Figure 4-19(a)-(b) compare the mode shapes.

Table 3-7: Comparison of numerical and experimental frequencies

Mode	Numerical	Experimental	Error
1	18.222	17.818	2.2%
2	28.576	25.472	10.8%
Average of difference (%)			6.5%

From Table 4-7, it is observed that there is a discrepancy between the numerical and experimental frequencies with an average error of 6.5%. The same situation also occurs for mode shapes, where the discrepancy of mode shapes is more obvious in mode 2. This is because of the existence of modeling error in finite element model and measurement error in measured data.

The same procedure is applied to build the ANN model and the same training cases as in section 4.3.1 are used to train the network. The best ANN model obtained is 14-14-7 and the training and validation performance (MSE) are 0.0175 and 0.0602, respectively. The experimental data are then introduced to the trained ANN model. Figure 4-20(a)-(j) show the predicted results from level 1 to level 10 of experimental data.

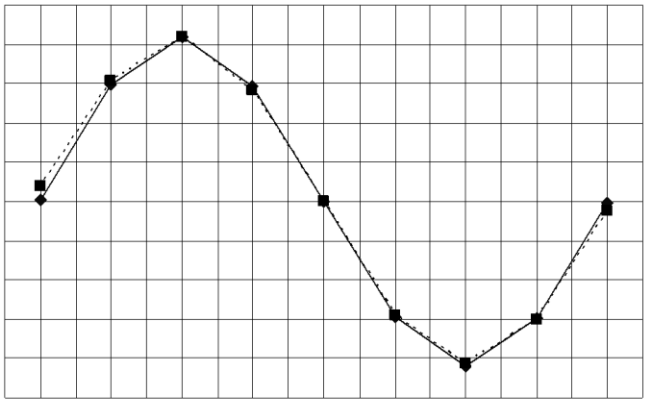

(a) Mode 1

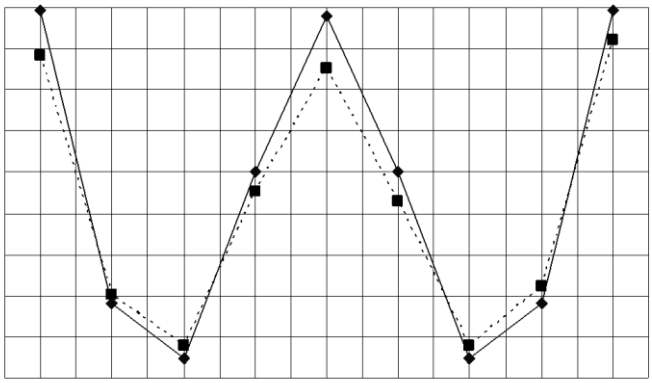

(b) Mode 2

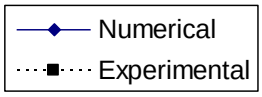

Figure 3-19: Comparison of numerical and experimental mode shapes

The figures show that the general trend of the predicted damage does not match the damage pattern obtained in the experiment. At level 1, severe damage is predicted at segment 3 and 6, while in experiment there was no significant crack observed in both spans. The same situation occurs at level 2 to level 6 where the ANN falsely predicts the crack in the right span (segment 6) and severe damage in the left span (segment 2 and 3). At the same loading level in the experiment, the severe damage in the left span only occured at level 3 to level 6, while in the right span the cracks were obviously seen only at loading level 7. The predicted damage, from level 8 to level 10 also does not match the crack pattern observed in the experiment.

The results indicate that ANN trained with simulated vibration parameters (deterministic ANN) fails to provide reliable structural damage prediction when

tested with noisy experimental data. The reason is that, the existence of modeling error in the finite element model may result in the vibration parameters generated from such a finite element model not exactly representing the relationship between the modal parameters and the damage parameters of the corresponding experimental structure, while the measurement noise also leads to erroneous predictions of the structural vibration properties.

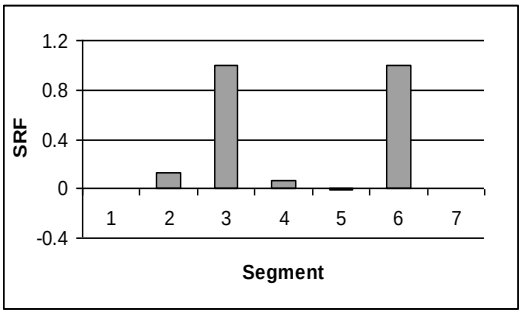

(a) Level 1 (6kN (left)-0kN(right))

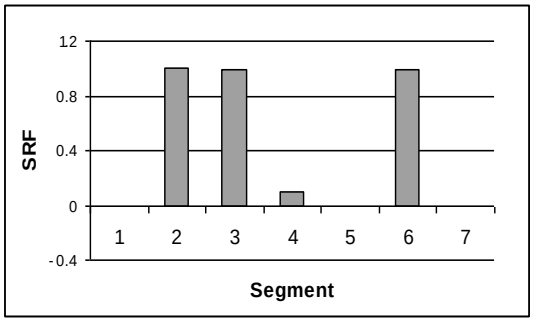

(b) Level 2 (12kN (left)-0kN(right))

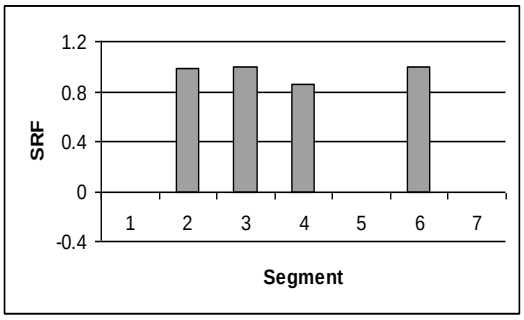

(c) Level 3 (18kN (left)-0kN(right))

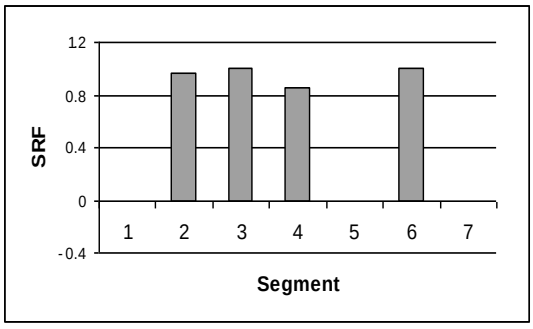

(d) Level 4 (18kN (left)-3kN(right))

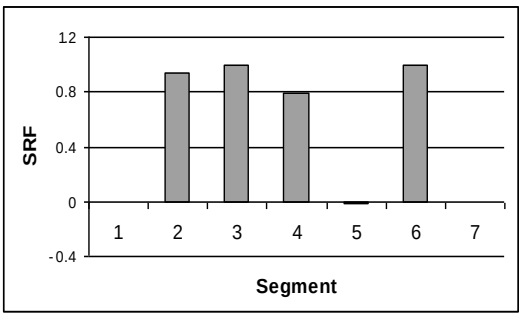

(e) Level 5 (18kN (left)-6kN(right))

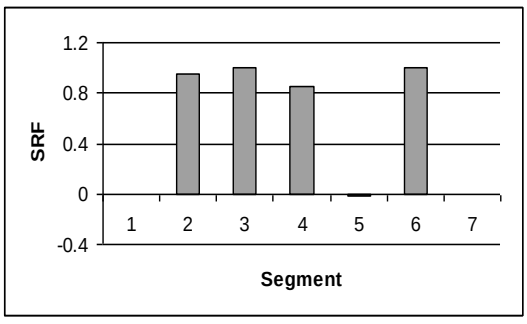

(f) Level 6 (18kN (left)-12kN(right))

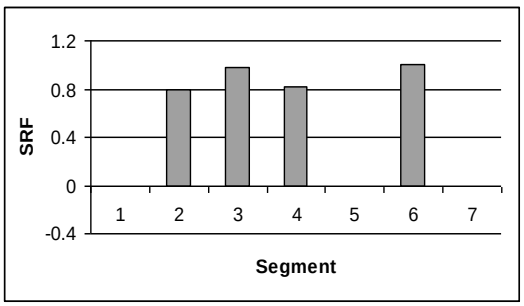

(g) Level 7 (18kN (left)-18kN(right))

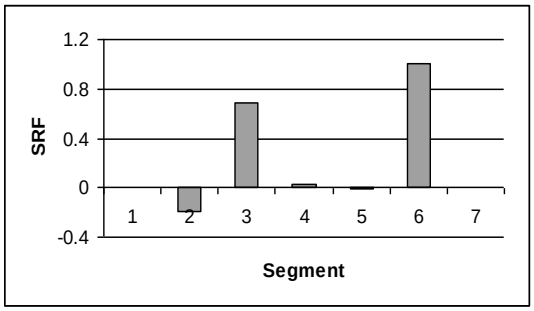

(h) Level 8 (25kN (left)-25kN(right))

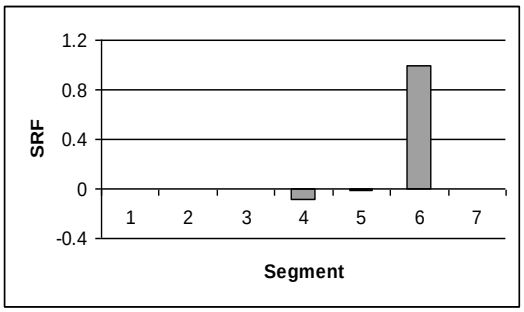

(g) Level 9 (32kN (left)-26kN(right))

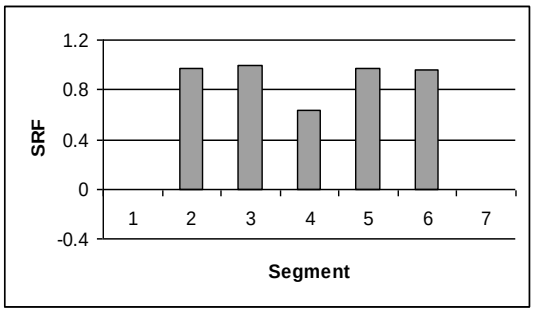

(h) Level 10 (38kN (left)-38kN(right))

Figure 3-20: Prediction results of the tested concrete slab

3.6 Summary

In this chapter, the ANN models are trained using modal data from numerical simulations and then applied to detect damage location and severity for example structures using numerical and experimental data. A sensitivity study has been conducted to investigate the sensitivity of the ANN technique using different combinations of input parameters. The results demonstrate that:

i) A deterministic ANN model is capable of detecting structural damage if the data is noise-free, but unable to provide a good prediction from noisy data. Based on the results, it is evident that ANN models have successfully predicted the simulated damages generated using a finite element model but failed to give reasonable results using experimental data.

ii) An ANN model trained with a combination of global and local parameters (frequency and mode shape) provides more reliable results in detecting damage location and severity.

iii) To apply an ANN model to structural damage detection, it is important to consider the uncertainties in the finite element model and the measured data.

CHAPTER 4

STRUCTURE DAMAGE DETECTION USING ARTIFICIAL NEURAL NETWORK WITH A MULTI-STAGE SUBSTRUCTING TECHNIQUE

4.1 Introduction

Another issue in application of ANN in damage detection is that it requires enormous computational effort and sometimes prohibitive for training an ANN model, especially when structures with many degrees of freedom are involved. Consequently, almost all the previous examples used to demonstrate the ANN model in the literature limited the structural members to a small number of large elements and quite significant damage levels. This makes the structural vibration properties not sensitive to small damage in a large element. As a result, ANN is not a feasible method for detecting small damage in a large structure. For example, Zhao et al.(1998) used ANN to identify damage of a 9m beam with 18 elements. The damage was introduced as a stiffness reduction of 15% to 45% of the original stiffness value of each element. Chang et al. (2000) employed ANN to detect damage in an eight-element RC beam. The damage considered was stiffness reduction of 10% to 25% of design stiffness values in each element. Pandey and Barai (1991) applied ANN to detect damage in a 0.5m long 21-bar truss bridge model. The damage scenarios considered were formed by reducing the cross sectional area of a small number of truss members.

Examples of successful identification of local small damage in structures by ANN are quite limited. This is because a fine finite element mesh is needed to detect small local damage in a structure. This results in a large number of elements in the finite element model of a structure, and hence a high dimension network in the ANN model. It then requires significant computational time and computer memory to train the ANN model. The computational time and computer memory needed to train an ANN model increases dramatically with increasing number of structural degrees of freedom. That is why in most examples; rather large elements are used in structure

model to reduce the degrees of freedom. Since a large element is insensitive to small damage, severe damage scenarios are usually assumed to demonstrate the feasibility of ANN.

Several attempts have also been made to apply ANN to complex structures with large degrees of freedom. In those studies, the structures are divided to a small number of segments. Each segment consists of several elements (Lee et al. 2002a; Ni et al. 2000; Xu and Humar 2006) and all the elements within the same segment are assumed to have the same material properties. This simplification reduces the number of variables and makes training ANN model efficient. However, it also makes the ANN model insensitive to small local damage, and therefore reduces its ability to provide reliable structure damage detection.

Some studies have applied the substructuring technique for structural condition identification. Oreta et al.(1994) and Koh et al. (2003) demonstrated the substructural approach derived from static condensation using a Genetic algorithm and the Extended Kalman Filter to identify the physical properties in a specified damage area of a model frame structure. As static condensation depends on the information from other part of the structure, the derivation of the substructure model is complicated and the computation is also relatively time consuming. Moreover, certain prescribed rules are needed to use those mathematical models. Recently, Yuen and Katafygiotis (2006) presented a probabilistic substructure identification and health determination methodology for linear systems using time history data. In this study, the authors proved that the condition of the substructure can be determined by considering acceleration only from the substructure of interest within a large structure through probability method.

Yun and Bhang (2000) and Mehrjoo et al. (2007) have applied the substructure technique for damage detection using ANN. In their study, they assumed that the damage occurs at the predetermined area and the ANN models were trained using the training cases that were generated with damages of the components in the corresponding area only. Those studies implied that, to identify damage in a substructure, only measurement data on the substructure of interest is required,

instead of the whole structure. However, this method still depends on subjective judgement using conventional techniques such as visual inspection to select the probable damage areas. This chapter presents an approach to detect small structural damage using ANN with a progressive substructuring technique. A multi-stage ANN model is proposed as a basic structure for the damage detection system. A two-span concrete slab and a one-span two-storey frame with various damage scenarios in single and multiple locations are used as the examples in this chapter. The effectiveness of the proposed method as compared to the conventional one-stage ANN method is demonstrated.

4.2 Methodology

A progressive substructuring technique applies the substructure technique together with a multi-stage ANN models to detect the location and extent of the damage. Through this method, a structure is divided to several substructures, and each substructure is assessed independently. Once the damaged substructure is identified, a second stage ANN model is developed to identify the location and severity of small structural damage. Because only the damaged substructure is involved in the second stage ANN model, the number of degrees of freedom in each ANN model is small thus reduce the excessive computational demand.

In this study, the substructure is defined as an independent structure by assuming the fixed interface. The method was introduced by Hurty (1964), and is known as Component Mode Synthesis (CMS). In CMS, the mode shape components are assembled to construct Ritz vectors, which are subsequently used to construct the mode shapes for the whole structure. This idea is adopted in the present study because any change of condition in the structure will change the condition of some or all the substructures. Since frequency alone is not sufficient to detect damage location, the mode shapes of the full structure at points corresponding to the substructure are also used to train and test the ANN model. In each substructure, although the available mode shape points are limited, the components of the mode vectors of the substructure are affected by most of the stiffness parameters of the substructure (Yun and Bahng 2000).

Furthermore, this idea is also based on the ability of the ANN approximation technique to handles non-unique cases by either returning one of the possible solutions or an average taken over all possible solutions (Szewczyk and Hajela 1992). In addition, ANN is also capable of recognizing patterns, where the ANN output is dependant on the likeness of given input data to the population that is used to train the network. Hence, when the testing data is close to the training data, satisfactory output can be obtained.

4.2.1 Multi-stage ANN model

Without losing generality, the multi-stage ANN system used in this study is briefly discussed below. Figure 6-1 depicts the basic structure of the system.

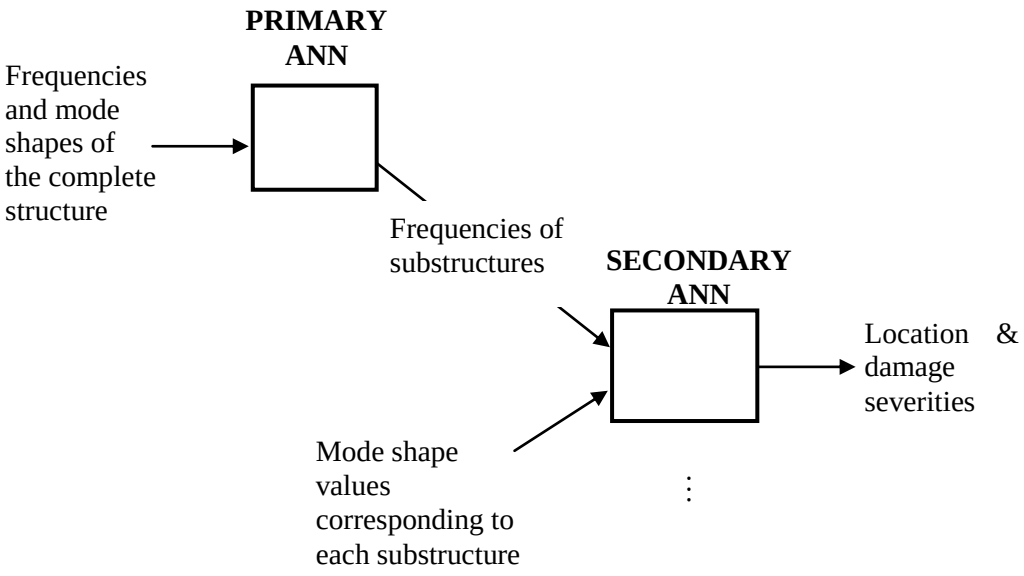

Figure 4-1: Structure of the two-stage ANN

The ANN model in the first stage is referred to as the *primary ANN* and the second stage ANN is referred to as the *secondary ANN*. The primary ANN is used to identify the substructures that have suffered damage while the secondary ANN identifies the damage location and estimate the damage severities. Each primary ANN is trained to relate the frequencies and mode shapes of the full structure and the frequencies of every substructure. Once the relationship is established, the ANN model can be used

to estimate the frequencies of each substructure from modal parameters of the full structure. The substructures that suffer damage can be identified from their frequency changes. In this study, the frequency change index (FCI) is defined as:

$$FCI_j = 1 - \left(\frac{F_j'}{F_j} \right)^2 \tag{4-1}$$

where F_j' and F_j are calculated from the frequencies of the damaged and undamaged j^{th} substructure as:

$$F_j = \frac{1}{k} \sum_{i=1}^{k} f_{ji} \tag{4-2}$$

$$F_j' = \frac{1}{k} \sum_{i=1}^{k} f_{ji}' \tag{4-3}$$

where f_{ji}' and f_{ji} are the normalized damaged and undamaged i^{th} modal frequency of the j^{th} substructure. i is the mode number (i = 1, 2, …k). The normalized frequencies are calculated by:

$$f_{ji} = \frac{\hat{f}_{ji} - f_{ji_{\min}}}{f_{ji_{\max}} - f_{ji_{\max}}} \tag{4-4}$$

$$f_{ji}' = \frac{\hat{f}_{ji}' - f_{ji_{\min}}}{f_{ji_{\max}} - f_{ji_{\max}}} \tag{4-5}$$

where $\hat{f}_{ji}$ and $\hat{f}_{ji}'$ are the predicted damaged and undamaged i^{th} modal frequency of the j^{th} substructure. $f_{ji_{\min}}$ and $f_{ji_{\max}}$ are the maximum and minimum i^{th} modal frequency of the j^{th} substructure that used to train the ANN model.

In the secondary ANN model, each substructure which is identified to have frequency change by the primary ANN model is represented by a new independent ANN model to predict the E values (Young's modulus) of the elements in this substructure. The output of the primary ANN model, together with the mode shape

values of the full structure at nodal points corresponding to the substructure, are used as the input variables. The change of the stiffness parameter or the damage severity for each element is denoted by a SRF (Equation (4-7)).

In both stages, the same ANN model configurations as in the previous chapters are applied.

4.2.2 Design of primary ANN

As mentioned above, the primary ANN is designed to detect the existence of damage in any substructure based on the frequency changes of each substructure. For this purpose, the ANN in this stage is used to predict the frequencies of every substructure from the modal parameters of the full structure. If further resolution in the damaged location is needed, the substructure can be further divided into smaller substructures, and this process can be repeated to any number of desired stages depending on the size of the substructure under consideration and the required accuracy of the identification results. For example, Figure 6-2 shows the two-stage primary ANN model.

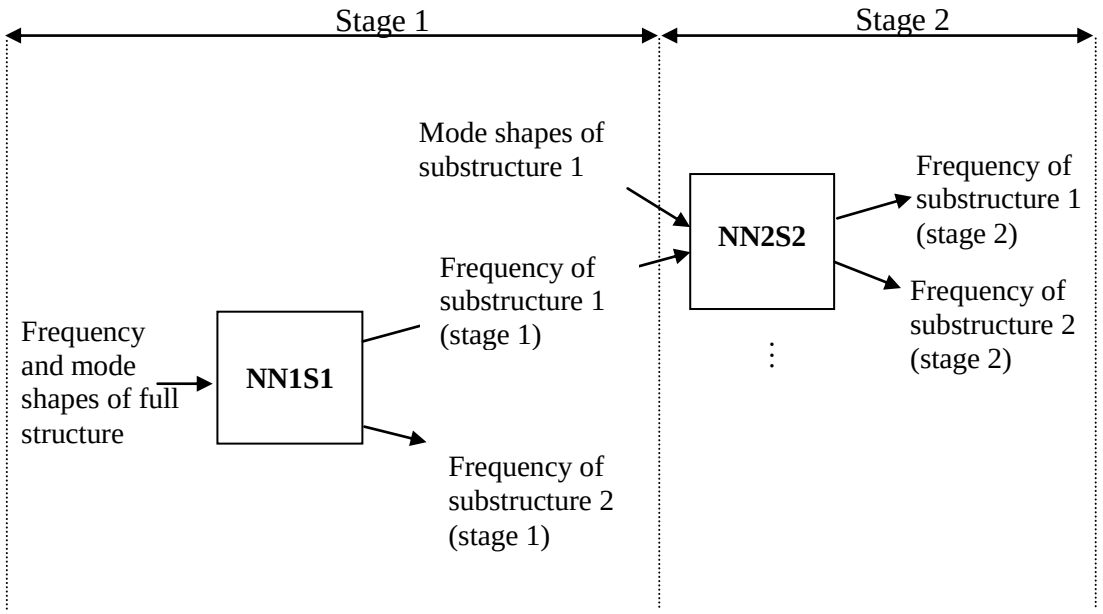

Figure 4-2: Schematic diagram of a two-stage primary ANN

In the figure, a two-stage primary ANN model is shown. In the first stage, the ANN (NN1S1) in used to predict the frequencies of two substructures based on frequencies and mode shapes of the full structure. The outputs of the ANN in the first stage (frequencies) supplemented by mode shapes of the nodal points of the corresponding substructure are used as the inputs to the ANN in the second stage. For this example, the first substructure is further divided into another two substructures and NN2S2 is used to predict their frequencies and allow their conditions to be examined. In other words, if a damaged substructure is identified in the first stage, another ANN model corresponding to the damaged substructure can be built in the second stage to increase the resolution of the damage location. At this stage, if needed, the measurement points can be refined by adding more measurement points focusing on the identified substructure. This process can be further extended to more stages. Since ANN models only need to be built for the damaged substructures, and the number of unknowns in each model can be kept to a minimum in the refinement process, this process will not substantially increase the computational time and the requirement for computer memory.

4.2.3 Design of secondary ANN

After determining the damaged substructures, the specific damage element and the damage severities are identified using the secondary ANN. Only the elements involved in the damaged substructure need to be taken as possible damage components in this network. Therefore, only ANN model for the identified substructure is built and trained using damage cases pertaining to the elements in the damaged substructure.

The secondary ANN receives information from the primary ANN and determines the location and severity of the damage. The frequencies of the substructures from the primary ANN and the mode shapes of the corresponding substructure are used as the inputs to predict the *E* values of each element in the identified substructure.

Figure 6-3 depicts the structure of the secondary ANN for substructure *j*. The input variables for ANN model (NN_j) in the figure are modal frequencies ($\lambda s_1^j ... \lambda s_n^j$) and

mode shapes ($\phi s_1^j ... \phi s_n^j$) of substructure *j* and the output variables are the *E* values of *m* elements in substructure *j* ($E_1^j ... E_m^j$). If more than one substructure is involved, each of them is represented by a different ANN model. Therefore, the ANN models can be designed independently.

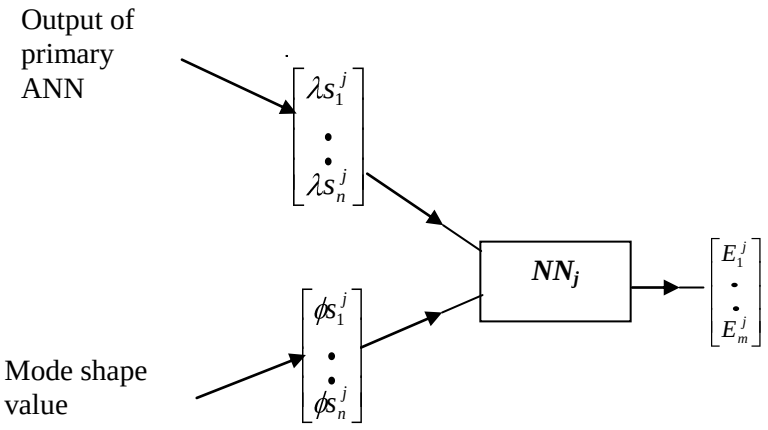

Figure 4-3: Schematic diagram of a secondary ANN

4.2.4 Training data

To ensure that the trained ANN model can accurately represent the behaviour of the system, the training samples should cover all possible combinations and ranges of input and output variation. To obtain the complete combination of damage cases in a large degree of freedom system, a large number of finite element simulations and training data are required. For example if there are *k* degrees of freedom in the system and there are two possible damage cases (damaged and undamaged), the total number of complete combinations of damaged and undamaged cases in each degree of freedom are 2^k. Therefore, if a complete combination cases are considered, a large amount of training samples is inevitably required for a large degree of freedom system.

The application of Latin hypercube sampling alone to generate the training data for a large degree of freedom system may result in the training data not representing the true interaction of damaged and undamaged cases in each degree of freedom. This is

because every element is assumed as damaged with uniformly distributed damage severities. Stein (1987) provides a detailed explanation regarding this phenomenon. As an alternative, the author suggested Orthogonal Array (OA) method to reduce the variation of damage cases while maintaining the effect of every damage case to the structure.

According to Besterfield et al. (1995), OA can provide a systematic way of studying the effects of the individual factor on the outcome as well as how these factors interact. OA also provides a fully balanced experimental arrangement. The notation of OA(N, k, s, t) is used to represent an OA that has N number of experimental runs, k, factors (parameters) with s levels and a strength of t (Hedayat et al. 1999). The strength represents the number of columns where all the possibilities can be seen an equal number of times. In this study, the appropriate OAs are selected from a library of OA (Sloane 2007) and the strength are taken as 3. The efficiency of OA has been proven in many studies (Chang et al. 2000; Chang et al. 2002; Tang 1993). Using OA, only $k(s-1) +1$ or greater number of combinations are required for representing the complete combination of the sample space. If the number of parameter is less than the number of experiment in OA, not assigned experiment can be left empty. Therefore, in this study, the value of N implies the number of combinations considered to generate the training data.

A four-step procedure suggested by Besterfield et al. (1995) to select the appropriate OA is applied. The steps are: (i) define k and s; (ii) determine N; (iii) select OA and (iv) consider any interactions. Latin hypercube sampling is used to make sure that the damage severities in each damaged element are uniformly distributed.

The vibration properties for the full structure and the substructures are computed using finite element analysis. The same material properties are used for the full structure and the corresponding substructures, and hence, any changes of condition in full structure will affect the condition of the corresponding substructure. For training the ANN models the frequencies and the mode shapes are used as the inputs. The training data for the ANN at the first stage are directly obtained from the finite element model, while for the subsequent stages the frequencies are generated from

the ANN model in the previous stage to reduce the effect of duplication error propagation from the earlier stage on ANN prediction. The generated frequencies are then combined with the mode shapes to form a set of input variables for the second stage ANN model. The same procedure applies if more than two stages are needed.

4.3 Numerical example 1 – Concrete slab

A two-span concrete slab with dimension of 6400mm x 800mm x 100mm shown in Figure 6-4 is used as an example. The boundary conditions are idealized as pin supports at the middle span and at 200mm from left and right end of the slab. The material properties are: $E = 3.4 \times 10^{10} N/mm^2, \rho = 2.45 \times 10^3 kg/m^3, v = 0.2$. For damage detection purposes, the slab is divided to 32 segments as shown in Figure 6-4.

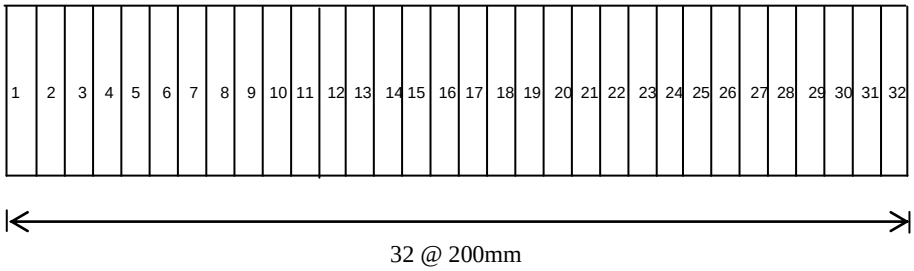

Figure 4-4: Segment of the slab

Four damage scenarios are simulated to assess the ANN performance as listed in Table 6-1. It is assumed that the mode shapes are measured at every 200mm with 33 measurement points on the centreline along the span length. Scenario 1 and 2 consist of damage at the middle of the first span (segment 7 & 8) with increasing damage severity. A severer damage case is simulated in scenario 3, where lower *E* values are applied to segments 5 to 10. In scenario 4, damage is assumed to occur in 16 segments in both spans and at the middle support. The modal analysis is conducted using finite element analysis, and the first three frequencies for these simulated damage scenarios are listed in Table 6-2.

In this example, the ANN is applied to detect the simulated damages and for the purpose of comparison; the predictions of the conventional approach and the proposed technique are compared. The term ‘conventional ANN’ refers to the one-stage ANN technique where the output variables consist of the E values of all the elements.

Table 4-1: Damage scenarios

Scenario	Element number	E value
1	7	$0.95\times E$
	8	$0.95\times E$
2	7	$0.90\times E$
	8	$0.90\times E$
3	5	$0.85\times E$
	6	$0.85\times E$
	7	$0.85\times E$
	8	$0.85\times E$
	9	$0.85\times E$
	10	$0.85\times E$
4	5	$0.90\times E$
	6	$0.90\times E$
	7	$0.85\times E$
	8	$0.85\times E$
	9	$0.90\times E$
	10	$0.90\times E$
	15	$0.90\times E$
	16	$0.90\times E$
	17	$0.90\times E$
	18	$0.90\times E$
	23	$0.95\times E$
	24	$0.95\times E$
	25	$0.90\times E$
	26	$0.90\times E$
	27	$0.95\times E$
	28	$0.95\times E$

Table 4-2: First three frequencies of the undamaged and damaged structure

	Undamaged	Scenario 1	Scenario 2	Scenario 3	Scenario 4
Mode 1	18.540	18.481	18.417	18.028	17.928
Mode 2	28.873	28.788	28.698	28.255	27.623
Mode 3	73.646	73.554	73.454	72.472	72.157

4.3.1 Conventional ANN

First, consider the one-stage ANN model for damage detection. The input variables for the ANN model are the first two modal frequencies and mode shapes of the slab and the outputs are *E* values of every element. An ANN model with one hidden layer is applied. The number of hidden neuron is determined by trial and error. Since there are 32 segments on the slab and two levels of damage (damaged and undamaged), the combination of damaged and undamaged cases over those elements is obtained by using OA33.32.2.3., as shown in Figure 6-5. The levels are indicated by 0 (undamaged) and 1 (damaged). This OA has 33 rows representing the damaged and undamaged combinations and 32 columns for each segment. The severities of each damaged segment are uniformly varied between 0.2*E* and 1.8*E* using Latin hypercube sampling. There are 1650 and 330 damage cases generated for training and validation data respectively.

Here, 62 input nodes are used in the input layer which consist of the first two modal frequencies and mode shapes. Mode shape values at all points are considered except 3 points at the supports since they provided 0 values in every mode.

Table 6-3 shows the training and validation performance of the one-stage ANN model with 4 to 13 hidden neurons. The training is conducted using a personal computer with Pentium 4 3.2GHz processor and 2GB memory. As indicated in the table, the training and validation performance improves when the number of hidden neurons increases, which means that higher numbers of hidden neurons are needed to successfully train this ANN model. However, increase the hidden neurons significantly increases the computational time and memory. When 10 or more neurons are introduced in hidden layer, it caused memory overflow of the computer system used in this study. This indicates that the current operating system memory is not sufficient to be used to train those ANN models. For a smaller number of hidden neurons (4, 6 and 9), the ANN models are trainable. However, the training performances are rather poor with relatively large MSE values. The training time also increases when the dimension of the ANN increases.

00000000000000000000000000000000
01010101010101010101010101010101
00110011001100110011001100110011
01100110011001100110011001100110
00001111000011110000111100001111
01011010010110100101101001011010
00111100001111000011110000111100
01101001011010010110100101101001
00000000111111110000000011111111
01010110101010010101011010101001
00110011110011000011001111001100
01100101100110100110010110011010
00001111111100000000111111110000
01011001101001100101100110100110
00111100110000110011110011000011
01101010100101010110101010010101
00000000000000000111111111111111
01010101010101011010101010101010
00110011001100111100110011001100
01100110011001101001100110011001
00001111000011111111000011110000
01011010010110101010010110100101
00111100001111001100001111000011
01101001011010011001011010010110
00000000111111111111111100000000
01010110101010011010100101010110
00110011110011001100110000110011
01100101100110101001101001100101
00001111111100001111000000001111
01011001101001101010011001011001
00111100110000111100001100111100
01101010100101011001010101101010
11111111111111111111111111111111

Figure 4-5: Orthogonal array (OA33.32.2.3)

Table 4-3: Performance of one-stage ANN model

Model	Training performance (MSE)	Validation performance (MSE)	Elapsed time (Second)
62-4-32	0.748	0.773	511.2
62-6-32	0.671	0.754	671.5
62-9-32	0.295	0.356	910.1
62-10-32	Out of memory	-	-
62-13-32	Out of memory	-	-

Figure 6-6(a)-(d) illustrate the comparison between the actual and the predicted *E* values when the simulated damage scenarios are applied to ANN model (62-9-32). For scenario 1 and 2, the damage at segment 7 and 8 are undetectable. For scenario 3, the damage locations are detected, however their severities are underestimated. There are also some false predictions. For scenario 4, damage at the left span and at the

center support are correctly located but the severity is still poorly estimated. The damage in the right span is not detected and there are also some false damage identification. These results show that the trained ANN model does not reliably predict the simulated damage in the concrete slab. This is because the ANN model is insufficiently trained and the relationship between inputs and outputs is not well established. If the model is trained with more hidden neurons, its reliability in predicting damage will be improved, but the computational time and required computer memory prevent using more than 10 hidden neurons. This example demonstrates that a one-stage ANN model cannot be efficiently applied to estimate large number of parameters, because the large number of outputs will result in a large dimension of weights in the interconnected neurons, and that will lead to the requirement of more computational time and a large amount of computer memory. For this reason, many publications using an ANN model to detect structural damage limit the output parameter to a minimum number as discussed earlier.

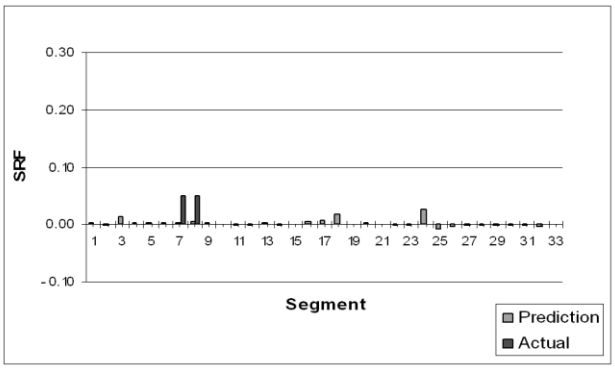

(a) Scenario 1

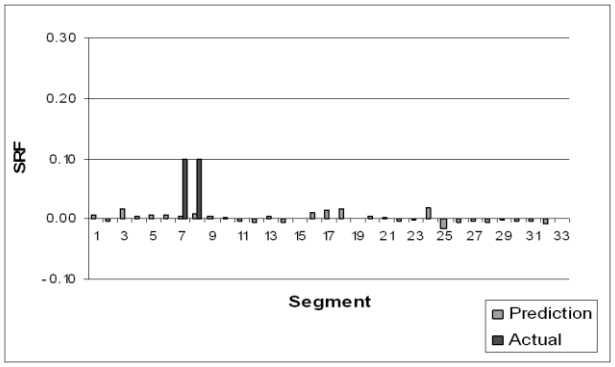

(b) Scenario 2

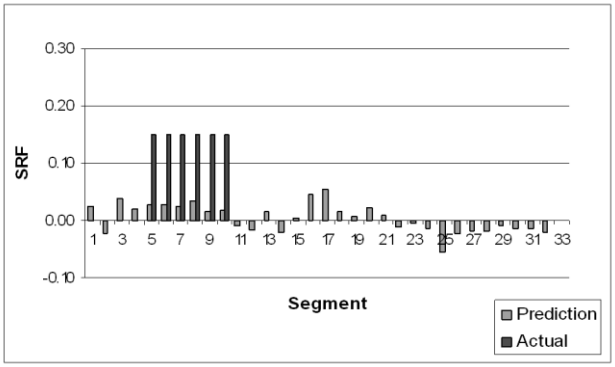

(c) Scenario 3

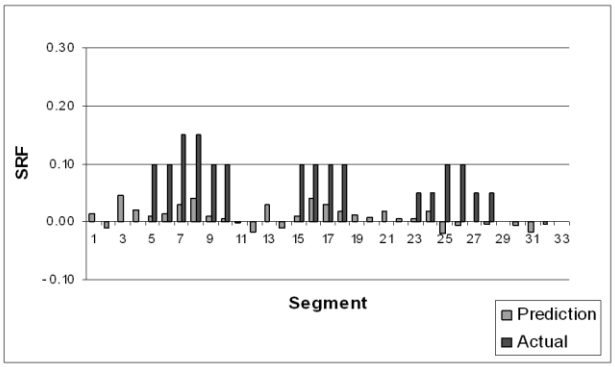

(d) Scenario 4

Figure 4-6: One-stage ANN prediction results

4.3.2 Damage detection using multi-stage substructuring technique

To apply the proposed approach, the slab is divided to 4 substructures. Each is 1.6m in length and consists of 8 elements, as illustrated in Figure 6-7. Two-stage ANN models are applied at the primary level to assess the condition of substructures. Then a secondary level ANN model is applied to substructures with detected condition changes in the primary level to predict the location and severity of damage in the substructure. Figure 6-8 shows the ANN architecture. All the simulated four damage scenarios are used as the testing data in this example.

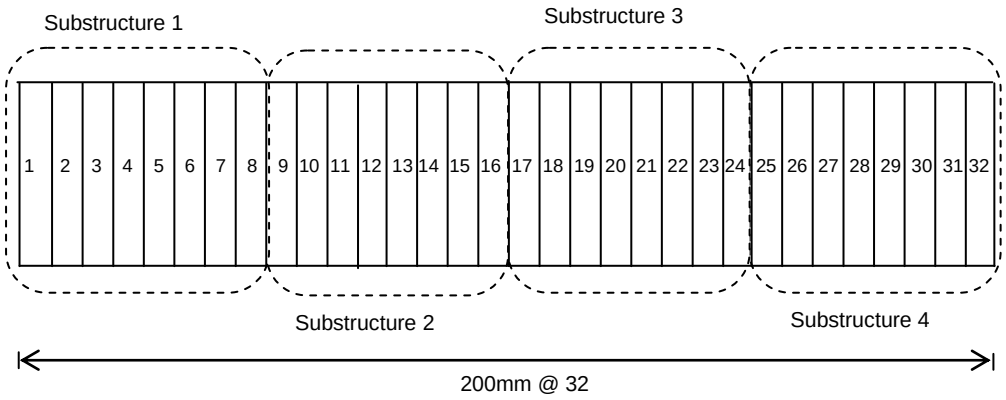

Figure 4-7: Substructures of the slab

There are three ANN models in the primary level. NNP1 is used as an intermediate model to generate the frequencies for the ANN models in the second stage. The slab is firstly divided into two substructures, each of which is 3.2m in length. NNP1 is trained to predict the frequencies of these two substructures. The inputs of NNP1 are the first two modal frequencies ($f_{full}^{1}, f_{full}^{2}$) and mode shape values ($\phi_{full}^{1}, \phi_{full}^{2}$) of full structure. The outputs of NNP1 are the first three frequencies of the two substructures ($f_{S1sub1}^{1} \cdots f_{S1sub1}^{3}, f_{S1sub2}^{1} \cdots f_{S1sub2}^{3}$). The superscripts indicate the mode number. The subscripts indicate the stage number together with substructure number. At the second stage, the two substructures are further subdivided into four substructures. As shown in the figure, NNP2 and NNP3 are the ANN models at this stage. NNP2 is used to predict the frequencies of substructure 1 and 2 at the second stage ($f_{S2sub1}^{1} \cdots f_{S2sub1}^{3}, f_{S2sub2}^{1} \cdots f_{S2sub2}^{3}$), while NNP3 predicts the frequencies of substructure 3 and 4 ($f_{S2sub3}^{1} \cdots f_{S2sub3}^{3}, f_{S2sub4}^{1} \cdots f_{S2sub4}^{3}$). The inputs for the ANN

models at this stage are the frequencies predicted from the first stage ANN model (NNP1) and the mode shapes of the corresponding substructures. The mode shape values applied to NNP2 and NNP3 are the actual measured mode shape values of the corresponding substructures $(\phi_{S1sub1}{}^{1}...\phi_{S1sub1}{}^{3}, \phi_{S1sub2}{}^{1}...\phi_{S1sub2}{}^{3})$. The outputs of the ANN model in this stage are the three modal frequencies of the four substructures. The conditions of those substructures are examined at this stage. For substructures with identified condition change, the secondary ANN model is built independently for each of those substructures to predict the location and severity of damage. In this example, the ANN models (NNS1…NNS4) in the secondary level are used to predict the simulated damage scenarios. The process used in the previous stage is applied again to form the input variables for the corresponding ANN model at this level. The outputs are the *E* values of each element $(E1...E32)$.

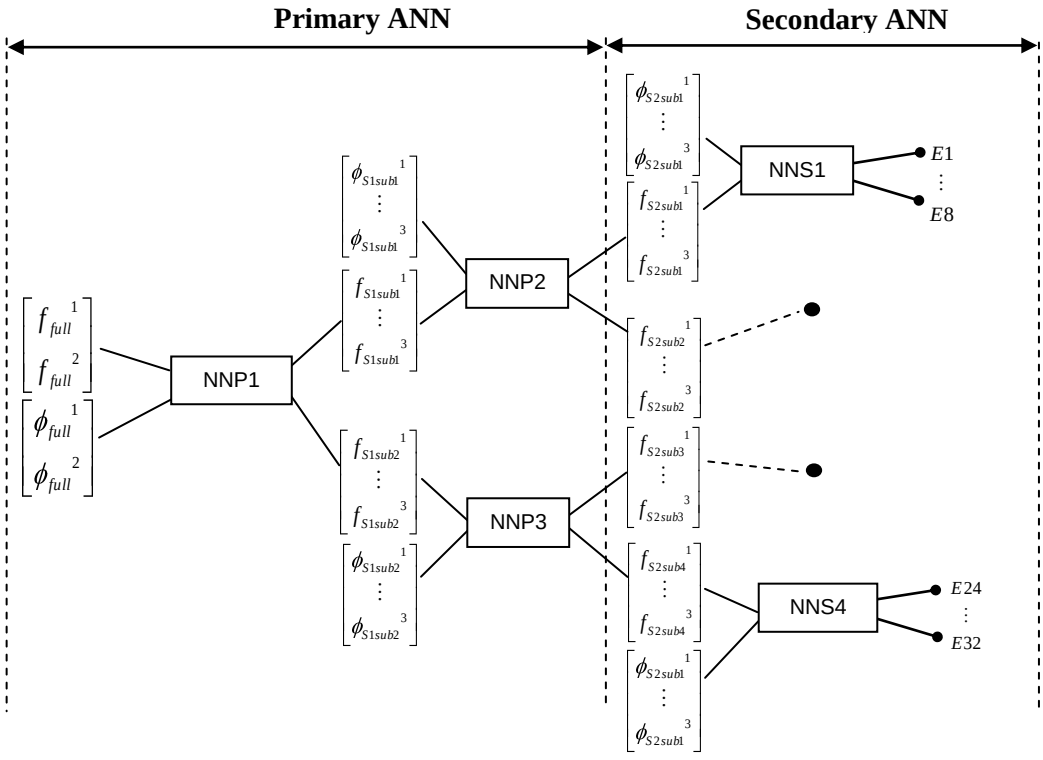

Figure 4-8 : ANN architecture

The ANN models in the primary stage are trained using the same training patterns as in the conventional ANN model. Table 6-4 lists the ANN models used in the primary stage together with their performances and elapsed time. It is observed that the MSE values for training and validation are low for all ANN models indicating that the relationship between inputs and outputs are established. Figure 6-9 shows the

calculated FCI values of substructures obtained from the primary ANN. The FCI values indicate condition changes in each substructure, and are used to select the substructures for which it is necessary to build the secondary level ANN models.

Table 4-4: Performance of the primary ANN

Model	Training performance (MSE)	Validation performance (MSE)	Elapsed time (Second)
NNP1 (62-20-6)	0.0047	0.0067	327.7
NNP2 (48-15-6)	0.0035	0.0047	235.3
NNP3 (48-17-6)	0.0045	0.0053	296.2

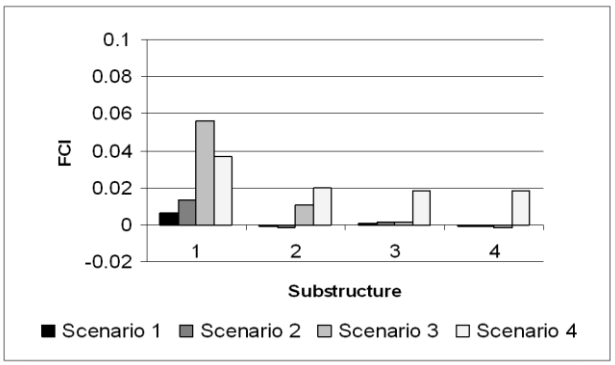

Figure 4-9: Output of primary ANN

As shown in Figure 6-9, relatively high FCI values occur only at substructure 1 for damage scenario 1 and 2, while for scenario 3 the high FCI values are observed at both substructure 1 and 2. For scenario 4, the high FCI values occur at every substructure. These results indicate that the substructures that contain damage are correctly identified in the primary ANN stage.

In the secondary stage, the ANN models are built corresponding to the damaged substructure identified in the primary stage. For scenario 1 and 2, only one ANN model involved (NNS1) in the secondary stage, since only substructure 1 is identified as damaged. For scenario 3, two ANN models are involved (NNS1 and NNS2), while for scenario 4, four ANN models are involved (NNS1 to NNS4) in the secondary stage. Since only 8 elements are involved in substructure 1, OA9.8.2.3 is used to generate the training cases for NNS1 in scenario 1 and 2. 900 and 270 cases

are used for training and validation. For scenario 3, 1360 and 510 cases are used for training and validation of NNS1 and NNS2. OA17.16.2.3 is used to generate the training cases for the 16 elements in substructure 1 and 2 for scenario 3. For scenario 4, the same training and validation cases as in the primary stage are applied since all the four substructures are identified as damaged.

Table 6.5(a)-(c) lists the performance of the ANN models in the secondary stage for all cases. The table shows that the relationships between inputs and outputs for ANN model in all cases are established with low MSE values in training and validation process. It is also observed that the time required for training the ANN models in primary and secondary level is less than those given in Table 6-3 for the one-stage ANN model due to the smaller ANN dimension used.

Table 4-5 : Performance of the secondary ANN

(a) Case 1 and Case 2

Model	**Training performance (MSE)**	**Validation performance (MSE)**	**Elapsed time (Second)**
NNS1 (27-21-8)	0.085	0.095	197.3

(b) Case 3

Model	**Training performance (MSE)**	**Validation performance (MSE)**	**Elapsed time (Second)**
NNS1 (27-18-8)	0.081	0.097	172.7
NNS2 (27-16-8)	0.091	0.099	171.2

(c) **Case 4**

Model	**Training performance (MSE)**	**Validation performance (MSE)**	**Elapsed time (Second)**
NNS1 (27-18-8)	0.0745	0.0833	164.3
NNS2 (27-17-8)	0.0832	0.0921	135.3
NNS3 (27-20-8)	0.0623	0.0685	217.2
NNS4 (27-19-8)	0.0914	0.0957	198.7

The comparisons between the actual and predicted SRF values for all the four cases are illustrated in Figure 6-10.

From the results in Figure 6-10(a)-(d), it is seen that for Scenario 1 and 2 the damage locations are correctly identified with slightly underestimated SRF values and minor positive and negative false identification in other elements. Those errors may be due to the fact that the duplication errors are unavoidable because the errors in the output layer of each ANN model (frequencies) are added when the input values propagate to the upper level ANN model, so the final outputs have duplicated errors.

For Scenario 3 and Scenario 4, where the damage occurred in multiple substructures, all the damaged elements are also correctly identified. However, it is also observed that the negative false identifications in the left and right elements and the underestimations of SRF are more obvious. The reason is that, besides the effect of duplicated errors in frequencies, another possible factor that adds to this occurrence especially when the damages occur in multiple substructures is the existence of uncertainty in mode shapes due to the damage in other substructures These uncertainties lead to a larger range of modal parameter variation in the training and testing data of each ANN. As a result, the ANN models are more likely to extrapolate the output instead of interpolate. The testing cases outside the range of the training data or inside large ‘holes’ of the training data may require extrapolation which result in a larger ANN prediction error as compared to interpolation (Bhagat 1990). Another possible factor that contributes to the errors is the numerical errors associated with nonlinearity caused by relatively large damage levels of structural elements, which may result in false identification, as mentioned by Xia et al. (2003).

In comparison with the conventional technique, this approach provides better result in terms of damage location and severities. Moreover, by comparing the time required for training the ANN model and predicting the damage with the conventional one-stage ANN model, as given in Table 6-3, the presented multi-stage method significantly reduces the computational time.

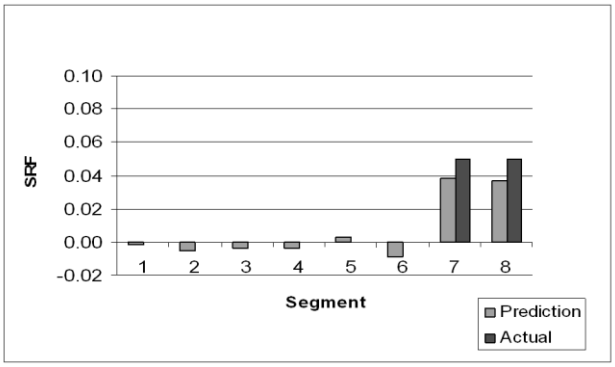

(a) Scenario 1

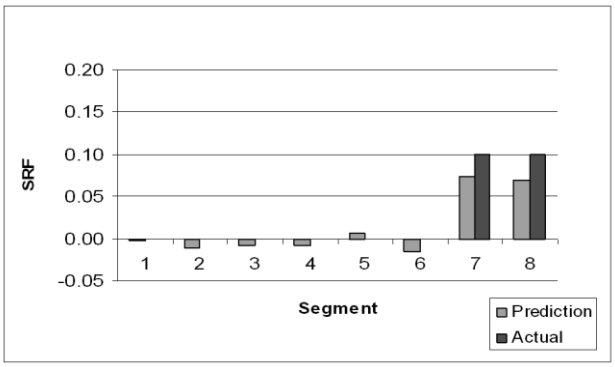

(b) Scenario 2

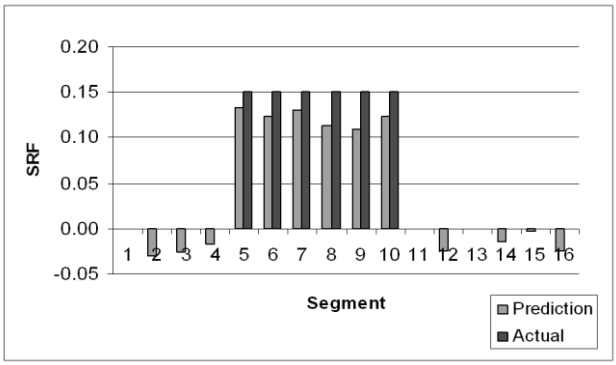

(c) Scenario 3

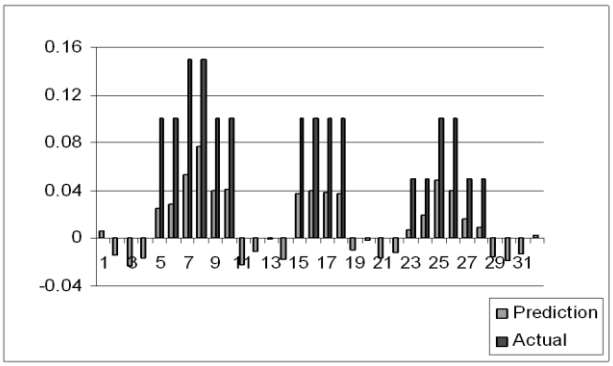

(d) Scenario 4

Figure 4-10: Output of secondary ANN

4.4 Numerical example 2 – Two-storey frame

To further demonstrate the efficiency of the purposed approach, a single span two-storey frame as shown in Figure 6-11 is considered. The modulus of elasticity is taken as 2.8×10^{10} N/mm^2 and the mass density as 2450 kg/m^3. The cross section of the beams and columns are shown in the figure. Rigid connections between the beams and the columns are assumed, and the supports are assumed to be fixed. The frame is modeled with 24 elements and 23 nodes. Each element is 1500mm in length. Modal analysis is conducted using finite element analysis. Two damage cases are generated to demonstrate the proposed approach. Case 1 consists of damage at a second floor beam while for Case 2 the damage is at Joint 1 and 2. The damage severities together with the elements and substructures involved for each case are listed in Table 6-6. The first three frequencies for the undamaged and damaged cases are given in Table 6-7. To apply the proposed approach, the frame is divided into three substructures. Each substructure representing one floor consists of 8 elements.

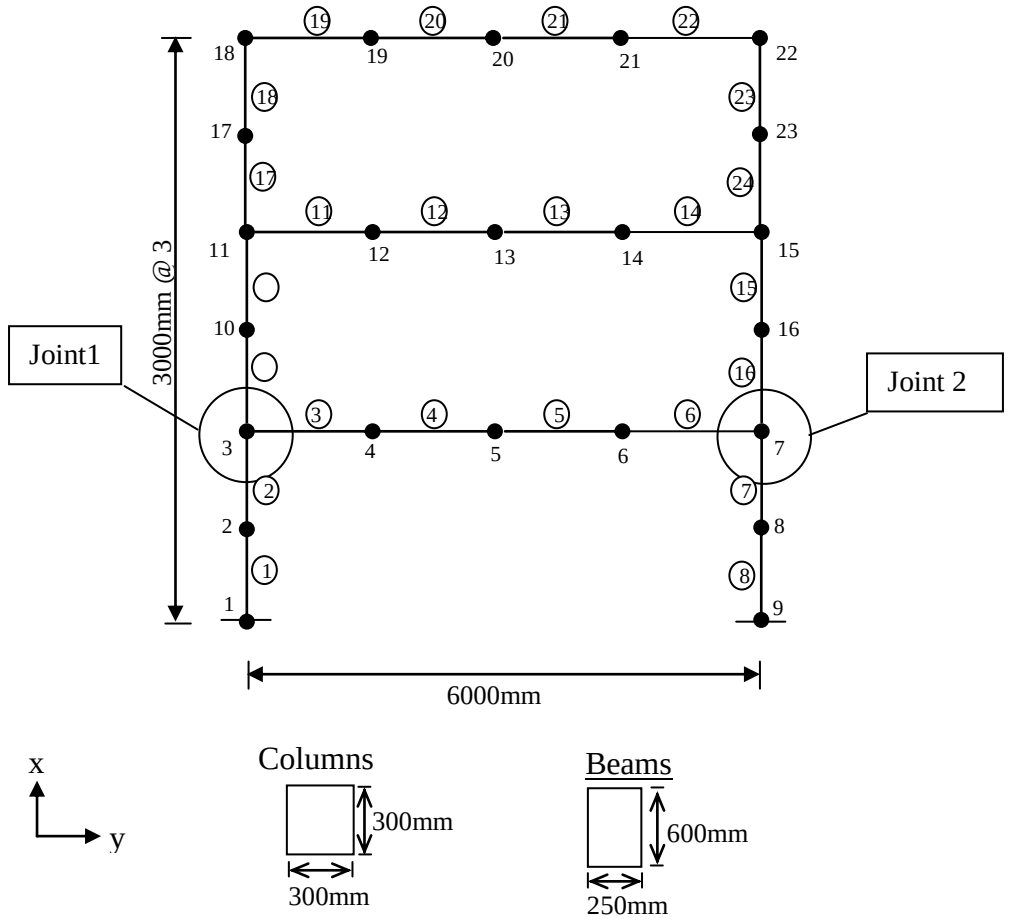

Figure 4-11: Finite element model of the frame

Only one ANN model is developed for primary ANN (NNP1) as shown in Figure 6-12. The first three modal frequencies ($f_{full}^{1} \cdots f_{full}^{3}$) and mode shapes ($\phi_{full}^{1} \cdots \phi_{full}^{3}$) are used as the inputs, and the outputs are the first three modal frequencies of each substructure ($f_{S1sub1}^{1} \cdots f_{S1sub1}^{3}, f_{S1sub2}^{1} \cdots f_{S1sub2}^{3}, f_{S1sub3}^{1} \cdots f_{S1sub3}^{3}$). The mode shapes used are specified by the x-translations of the columns and the y-translation of the beams. For training the primary ANN, training cases are generated based on orthogonal array OA25.24.2.3. For each damage case 42 different severities are generated using Latin hypercube sampling, resulting in 1050 training cases. For validation purposes, 240 damage cases are generated using the same method. Figure 6-13(a)-(b) show the FCI values predicted from the primary ANN model for case 1 and case 2. The higher FCI value occurred at the substructure that contains the damage, indicating the damaged substructures for both cases are correctly identified.

Table 4-6: Damage cases for frame

Case	Structure	Element	E value	Substructure
1	Beam	11	$0.90 \times E$	
		12	$0.90 \times E$	2
		13	$0.90 \times E$	
		14	$0.90 \times E$	
2		2	$0.85 \times E$	
	Joint 1	3	$0.85 \times E$	
		9	$0.85 \times E$	1,2
		6	$0.85 \times E$	
	Joint 2	7	$0.85 \times E$	
		16	$0.85 \times E$	

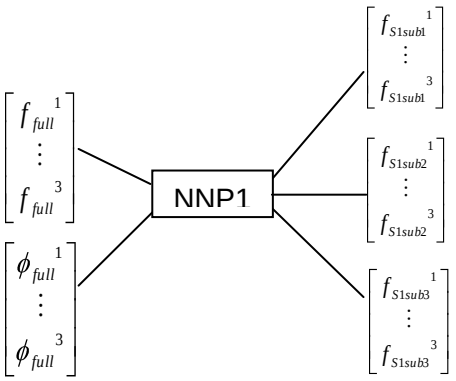

Figure 4-12: Primary ANN for example 2

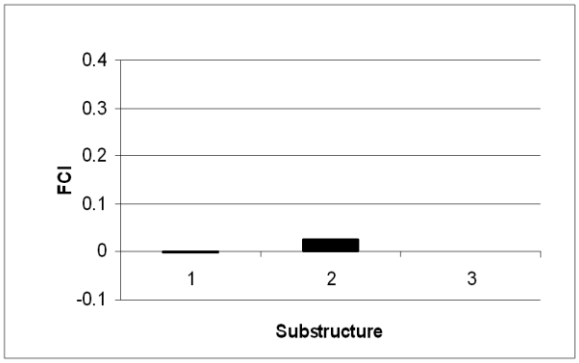

(a)Case 1

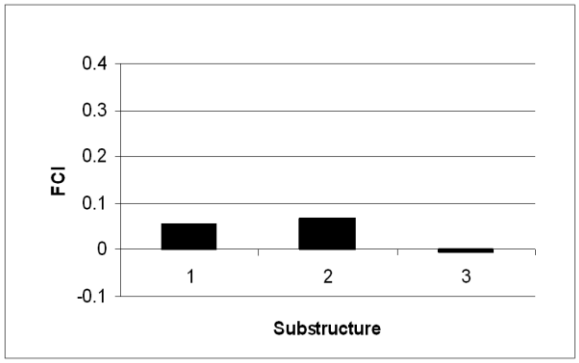

(b) Case 2

Figure 4-13: Output of the primary stage

For case 1, only one secondary ANN model (NNS1) is developed for substructure 2 to determine the damage, whereas for case 2, two secondary ANN models are developed for substructures 1 and 2 (NNS1 and NNS2). By using the method described earlier, ANN models for corresponding substructures are then trained and tested. The details of ANN models are shown in Table 6-7 and Table 6-8(a)-(b). Figure 6-14(a)-(b) show the identification results. From the figure, it is observed that the damaged elements for both cases are all correctly identified. However, the damage severities for both cases are underestimated and some minor positive and negative false identifications occur due to the reasons mentioned earlier.

Table 4-7: Performance of the primary ANN

Model	Training performance (MSE)	Validation performance (MSE)	Elapsed time (Second)
NNP1 (66-17-9)	0.0432	0.0882	211.1

Table 4-8: Performance of the secondary ANN

(a) Case 1

Model	Training performance (MSE)	Validation performance (MSE)	Elapsed time (Second)
NNS1 (24-14-8)	0.0432	0.0882	201.7

(b) Case 2

Model	Training performance (MSE)	Validation performance (MSE)	Elapsed time (Second)
NNS1 (24-14-8)	0.0603	0.0872	197.3
NNS2 (24-16-8)	0.0741	0.0932	217.2

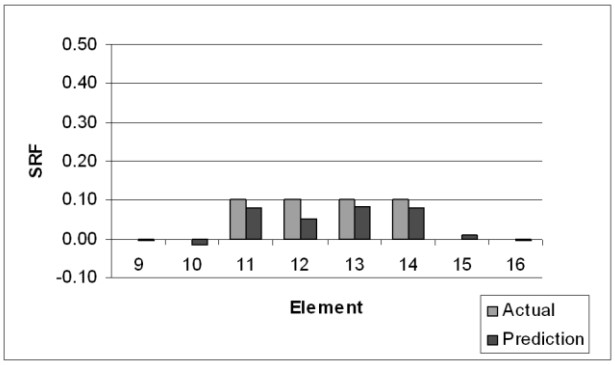

(a) Case 1

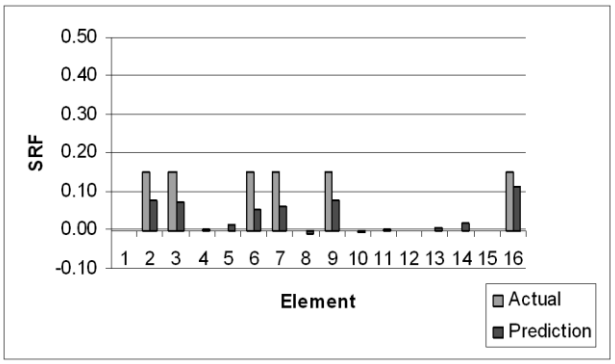

(b) Case 2

Figure 4-14: Identification results

4.5 Sensitivity study

More detailed studies are carried out in this section to investigate the sensitivity of the proposed method to different substructure sizes. At this stage, only the primary ANN is involved. The purpose of this study is to determine the reliability level of FCI of substructures for which a secondary ANN model needs be built for further analyses. Below this level of FCI the substructure is considered not damaged, and no subsequent analysis is needed.

First, an analysis is conducted to define whether the detectability depends on the absolute value of the substructure length or the ratio of the substructure length to the span length of the structure. For this purpose, two simply supported concrete girder models with span length 4.8m and 8m are analysed. 400mm elements are used to model the structure and the modal parameters are obtained using finite element analysis.

The material properties are: $E = 2.8 \times 10^{10} N/mm^2, \rho = 2.45 \times 10^3 kg/m^3, v = 0.2$. Figure 6-15(a)-(b) show the finite element model of the structures.

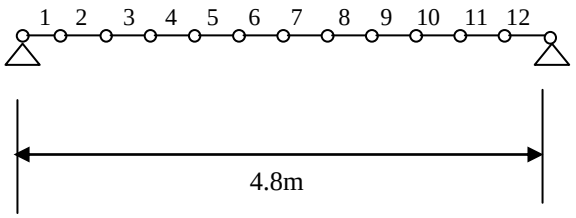

(a) 4.8 m girder

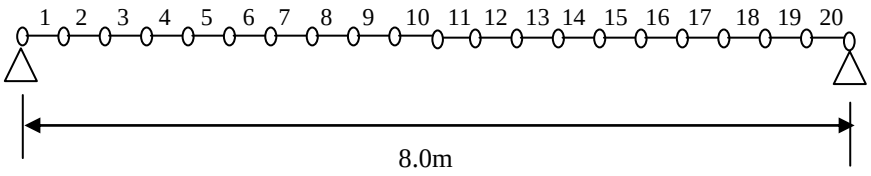

(b) 8.0 m girder

Figure 4-15: Finite element model of the beams

The structure is divided into two substructures, i.e., the ratio of the substructure length to the span length is 0.5. Three damage levels are introduced to element 5 and 6 in substructure 1. The damage levels are -15%, -10% and -5% in terms of SRF. The outputs of the primary ANN for both cases are shown in Figure 6-16(a)-(b).

The output of the primary ANN for both cases shows that the FCI values are higher at substructure 1 than substructure 2, indicating the damaged substructure 1 for all levels is correctly identified. However, the FCI values of the 8m girder is about 30% less than the 4.8m girder. This indicates the detectability depends on the absolute length of the substructure, instead of the length ratio. When the damage is the same, increase the substructure length will dilute the damage effect on the substructure, thus reduce the FCI values. The results also indicate that a FCI value of 0.05 implies a possible damage of 5% in a length of 0.8m (two 400 mm elements) in a substructure of length 4m, whereas the FCI value becomes 0.075 when the substructure is 2.4m long.

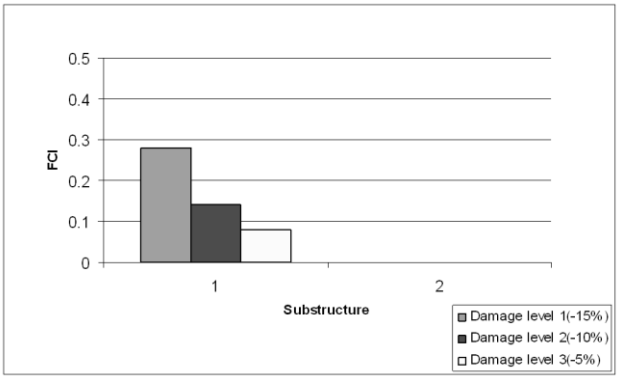

(a) Output for 4.8m span girder

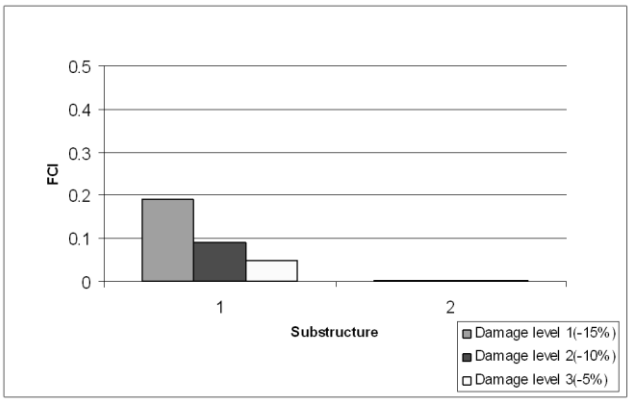

(b) Output for 8m span girder

Figure 4-16: Primary ANN output for 4.8m and 8.0 m girder

In order to investigate the sensitivity of substructure size to damage level, an analysis is performed by varying the substructure size and damage severity. The same girder as above with a 16m span is used in the analysis. Three different substructure sizes are considered, namely, i) 8m, ii) 4m and iii) 2m. Damage is introduced to element 8 (length 0.4 m) with SRF ranging from -5% to -50% at 0.5% intervals. Figure 6-17(a)-(c) show the finite element model together with the element number and substructure size. When the substructure is 8m or 4m long, the simulated damage is in the first substructure. When it is 2m long, the damage is in the second substructure. Figure 6-18(a)-(c) show the output of the primary ANN.

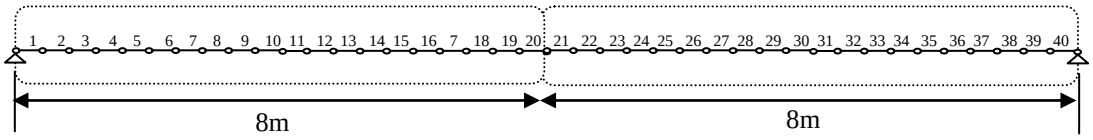

a) 8m substructure

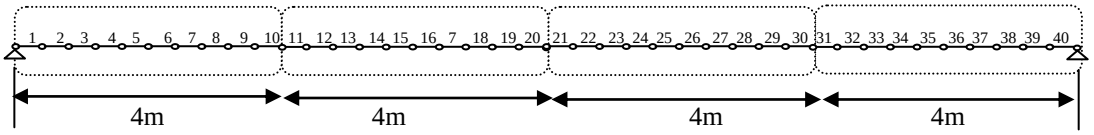

b) 4m substructure

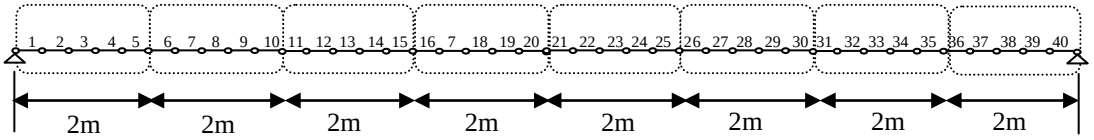

c) 2m substructure

Figure 4-17: Segmentation of the girder

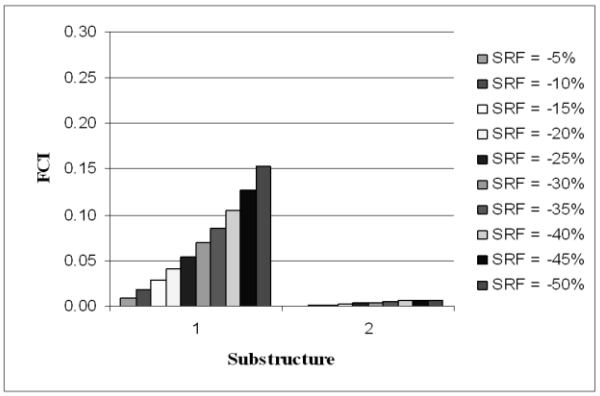

(a) Output of 8m substructure

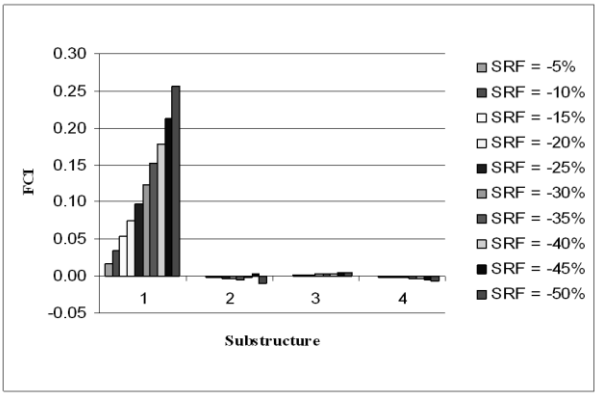

(b) Output of 4m substructure

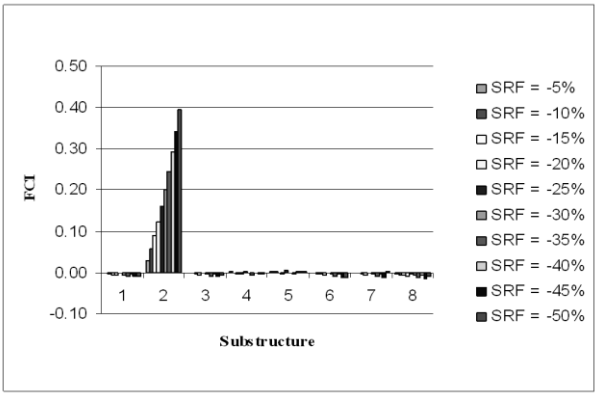

(c) Output of 2m substructure

Figure 4-18: Primary ANN output for 8m, 4m and 2m substructure

As indicated, the higher FCI values occurred at the damaged substructure, indicating that the damaged substructures are correctly predicted. It is observed the FCI values increase with damage level and reduce with the substructure size. However, some minor false identification occurs in the undamaged substructure for all the three cases. But this false FCI value is always smaller than the FCI values of the damaged substructure.

The effect of boundary conditions and structure type on the relationship between substructure size and damage detectability is also investigated. Other than simply supported girder as demonstrated earlier, another cases considered are i) flexible support, ii) continuous support, and iii) slab structure. For the flexible support case the pin supports in the previous example are replaced with three parallel spring elements of Young's Modulus $1.9\times10^{9}\,N/mm^{2}$ to simulate the bearing stiffness of bridge structures. For the continuous support case, an extra pin support is placed at the middle of the girder span. For the slab, the support is considered as simply supported and the slab width is 800mm. The same damage levels as in the previous analysis are used and the same damage detection process is applied. Figure 6-19 summarizes the numerical results obtained. The solid line is the relationship for the simply supported and continuous beam, and slab structure, while the dashed line is for the flexible support case. The area below and above those lines represent detectable and undetectable damage level respectively and the corresponding substructure size. The numerical results indicate that the relation between the substructure size and the detectable damage level is independent of the structure type and the structure indeterminacy because the results from the continuous beam and slab are similar to those obtained above. However, the flexible boundary conditions affect the relationship between the substructure size and the detectable damage level. The reason that a smaller substructure is needed to detect same level of damage in the flexible support case is because the spring elements are also damageable. Including spring elements in the substructure increases the number of variables in the analysis, which is equivalent to increase the number of elements in the substructure. If the spring is not considered as a variable in the analysis, the results will then be the same as the case with pin supports.

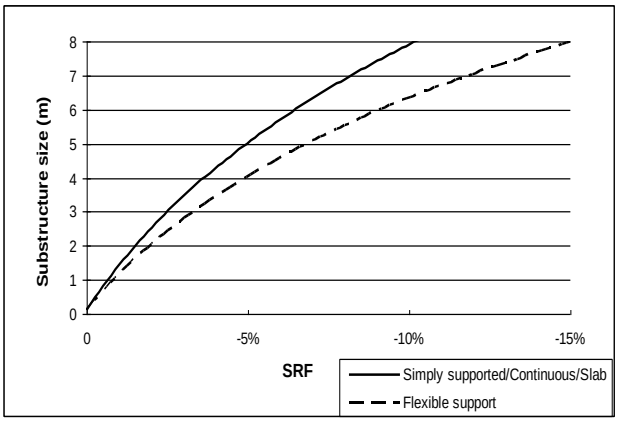

Figure 4-19: Primary ANN output for different structure condition

Based on the above results, the detectability levels with respect to the ratio of damaged element size to substructure size can be calculated. Figure 6-20(a) illustrates the result for simply supported and continuous beam and slab, while Figure 6-20 (b) illustrates the results for beam with flexible supports.

The vertical lines indicate the detectability limit of different ratio between damaged element size (l_{el}) to substructure size (L_{sub}).The area at the right side of the lines represent the detectable damage level. This analysis indicates that for both cases, if all the elements in a substructure suffer damage, even a small damage can be detected with a large substructure. This is because the ratio l_{el}/L_{sub} significantly affects the vibration frequencies of the substructure.

The numerical results indicate that damage detectability depends on the substructure size, damage level and the size of the damaged elements in a substructure. It is independent of the structure type and boundary conditions. However, it should be noted that this observation is based on beam-like structures. Further analyses are needed for other structure types such as shell and plate structures.

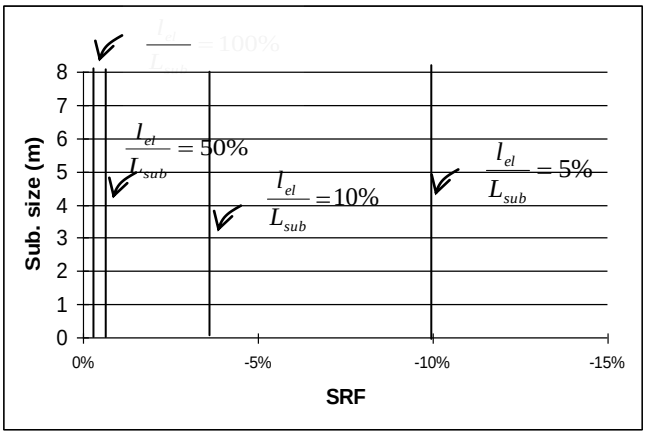

(a) Simply supported beam, continuous beam and slab

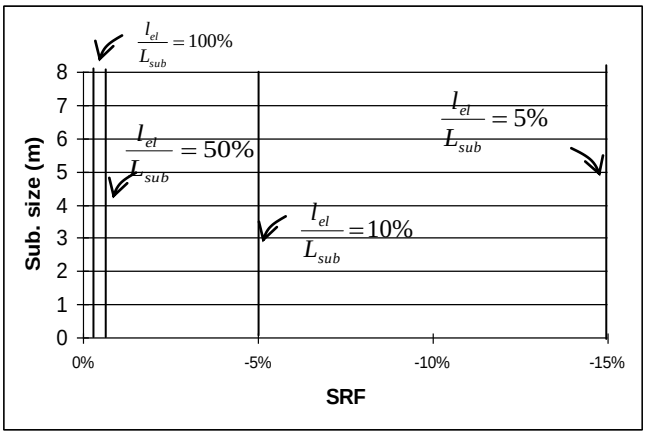

(b) Simply-supported beam with flexible supports

Figure 4-20: Detectability of different ratios of damaged element size to substructure size

4.6 Summary

This chapter presented a new approach for applying ANN for damage identification. A substructuring technique is employed together with a multi-stage ANN to detect local damage in structures. A comparison with the conventional technique demonstrated the efficiency and reliability of the proposed approach. This study also demonstrated that using a one-stage ANN model for damage detection of large structures requires excessive computational time and a large amount of computer memory. The proposed approach is feasible in reducing the size of the required ANN models, and as a result the computational effort can be reduced substantially. The results show that by dividing the full structure into substructures and analysing each substructure independently, local damage can be better identified. The proposed approach can also be used to identify multiple damages in multiple substructures,

thus overcoming the difficulties present in the multiple stage method proposed by Ko et al. (2002), which requires expensive computation when multiple damage locations exist in the structure. In comparison with the work by Yun and Bahng (2000) and Mehrjoo et al. (2007), which requires other means such as visual inspection to approximately locate the damage before applying ANN, the proposed approach identifies damages in structures directly from the modal parameters of the structure.

CHAPTER 5

MULTI-STAGE SUBSTRUCTURING TECHNIQUE FOR DAMAGE DETECTION USING STATISTICAL ARTIFICIAL NEURAL NETWORK

5.1 Introduction

The multi-stage substructuring technique proposed in the previous chapter is shown to be feasible in detecting damage in structures with large number of degrees of freedom. However, as mentioned earlier, the uncertainties in finite element model and measurement data will reduce the capability of ANN to detect damage, thus it is necessary to consider the uncertainties in damage detection. In previous studies involving the application of substructure technique using ANN model (Mehrjoo et al. 2007; Qu et al. 2004; Yun and Bahng 2000), only numerical data which are noise free are used as examples. The application of the method to experimental data, which is inevitably contaminated with noise, cannot be found in the open literature yet. The finite element model of the tested structure in experiments or real structures also often consists of modeling errors as discussed in Chapter 5; this makes the application of the method to detect structure damages even more difficult. In this chapter the existence of uncertainties is considered and the reliability of the proposed substructure method with ANN model under the influence of uncertainties is analysed.

The purpose of this study is to investigate the sensitivity of multi-stage substructuring method under the influence of uncertainties. Statistical ANN model as explained in Chapter 5 is used to determine the damage detectability under the influence of uncertainties in terms of the probability of damage existence (PDE).

In this chapter, an analysis is performed to investigate the damage detectability of structures with different levels of noises in measured vibration data and errors in finite element model. A numerical example and an experimental example are used to demonstrate the method.

5.2 Methodology

As mentioned earlier, the detectibility level is measured by PDE of substructure. As demonstrated in the previous chapter, the damage detectability decreases with the increase of the substructure size. Since the substructure size at the primary level of the multi-stage ANN model is the largest, the damage detectability very much depends on the sensitivity of the primary level ANN model. As the outputs of the primary ANN model are frequencies of each substructure, the PDEs are calculated from statistical distributions of FCI values. The Rossenblueth's PEM as explained in Chapter 5 are used to obtain the statistics of FCI values. The upper and lower limits of FCI values are calculated based on the upper and lower limits of frequencies predicted by ANN models in the primary stage. Based on Equation (6-1) to (6-5), the upper and lower limits of FCI values for the j^{th} substructure are calculated as below:

$$FCI_{j++} = 1 - \left(\frac{F_j{}'_{++}}{F_{j++}} \right)^2 \tag{5-1}$$

$$FCI_{j+-} = 1 - \left(\frac{F_j{}'_{+-}}{F_{j+-}} \right)^2 \tag{5-2}$$

$$FCI_{j-+} = 1 - \left(\frac{F_j{}'_{-+}}{F_{j-+}} \right)^2 \tag{5-3}$$

$$FCI_{j--} = 1 - \left(\frac{F_j{}'_{--}}{F_{j--}} \right)^2 \tag{5-4}$$

$F_j{}'_{++} \ldots F_j{}'_{--}$ and $F_{j++} \ldots F_{j--}$ are calculated as below:

$$F_{j++} = \frac{1}{k} \sum_{i=1}^{k} f_{j_{i++}} \tag{5-5}$$

$$F_{j+-} = \frac{1}{k} \sum_{i=1}^{k} f_{j_{i+-}} \tag{5-6}$$

$$F_{j-+} = \frac{1}{k} \sum_{i=1}^{k} {}_{j_{i-+}} \tag{5-7}$$

$$F_{j--} = \frac{1}{k} \sum_{i=1}^{k} f_{j_{i--}} \tag{5-8}$$

$$F_j{}'_{++} = \frac{1}{k}\sum_{i=1}^{k} f_{ji}{}'_{++} \tag{5-9}$$

$$F_{j+-}{}' = \frac{1}{k}\sum_{i=1}^{k} f_{ji}{}'_{+-} \tag{5-10}$$

$$F_{j-+}{}' = \frac{1}{k}\sum_{i=1}^{k} f_{ji}{}'_{-+} \tag{5-11}$$

$$F_{j--}{}' = \frac{1}{k}\sum_{i=1}^{k} f_{ji}{}'_{--} \tag{5-12}$$

where $f_{ji}{}'_{++}\ldots\ f_{ji}{}'$-- and $f_{ji\ ++}\ldots f_{ji}$ -- are the upper and lower limit of normalized damaged and undamaged frequency of the j^{th} substructure and i is the number of modes (i = 1, 2, …k). They are calculated as below:

$$f_{ji++} = \frac{\hat{f}_{ji\ ++} - f_{ji_{\min}++}}{f_{ji_{\max}++} - f_{ji_{\min}++}} \tag{5-13}$$

$$f_{ji+-} = \frac{\hat{f}_{ji\ +-} - f_{ji_{\min}+-}}{f_{ji_{\max}+-} - f_{ji_{\min}+-}} \tag{5-14}$$

$$f_{ji-+} = \frac{\hat{f}_{ji\ -+} - f_{ji_{\min}-+}}{f_{ji_{\max}-+} - f_{ji_{\min}-+}} \tag{5-15}$$

$$f_{ji--} = \frac{\hat{f}_{ji\ --} - f_{ji_{\min}--}}{f_{ji_{\max}--} - f_{ji_{\min}--}} \tag{5-16}$$

$$f_{ji}{}'_{++} = \frac{\hat{f}_{ji}{}'_{++} - f_{ji_{\min}++}}{f_{ji_{\max}++} - f_{ji_{\min}++}} \tag{5-17}$$

$$f_{ji}{}'_{+-} = \frac{\hat{f}_{ji}{}'_{+-} - f_{ji_{\min}+-}}{f_{ji_{\max}+-} - f_{ji_{\min}+-}} \tag{5-18}$$

$$f_{ji}{}'_{-+} = \frac{\hat{f}_{ji}{}'_{-+} - f_{ji_{\min}-+}}{f_{ji_{\max}-+} - f_{ji_{\min}-+}} \tag{5-19}$$

$$f_{ji}{}'_{--} = \frac{\hat{f}_{ji_p}{}'_{--} - f_{ji_{\min}--}}{f_{ji_{\max}--} - f_{ji_{\min}--}} \tag{5-20}$$

Here $\hat{f}_{ji++} \ldots \hat{f}_{ji\,--}$ and $\hat{f}_{ji}{}'_{++} \ldots \hat{f}_{ji}{}'_{--}$ are the upper and lower limits of the predicted damaged and undamaged i^{th} modal frequency of the j^{th} substructure. $f_{ji_{\min}}$ and $f_{ji_{\max}}$ are the minimum and maximum of the i^{th} modal frequency of the j^{th} substructure used to train the corresponding ANN model. The upper and lower limits of the modal frequencies are obtained through statistical ANN model (primary) by applying mean plus one standard deviation and mean minus one standard deviation of each random variable in training and testing the ANN model. The training functions of the primary ANN models involved are listed in Table 7-1. Table 7-2 listed the testing variables for the corresponding primary ANN models and their corresponding outputs.

Table 5-1: Training functions for primary ANN model

Model *n*	**Training function**
1	$f_j{}^n{}_{++} = fn(\lambda_i{}^0 + \sigma_{\lambda_i}, \phi_i{}^0 + \sigma_{\phi_i})$
2	$f_j{}^n{}_{--} = fn(\lambda_i{}^0 - \sigma_{\lambda_i}, \phi_i{}^0 - \sigma_{\phi_i})$
3	$f_j{}^n{}_{+-} = fn(\lambda_i{}^0 + \sigma_{\lambda_i}, \phi_i{}^0 - \sigma_{\phi_i})$
4	$f_j{}^n{}_{-+} = fn(\lambda_i{}^0 - \sigma_{\lambda_i}, \phi_i{}^0 + \sigma_{\phi_i})$

Here $f_j{}^n{}_{++}, f_j{}^n{}_{--}, f_j{}^n{}_{+-}, f_j{}^n{}_{-+}$ are the target outputs of the primary ANN models trained with different combinations of mean plus one standard deviation and mean minus one standard deviation of frequencies and mode shapes for the j^{th} segment. σ_{λ_i} and σ_{ϕ_i} are the standard deviation of the i^{th} frequency and mode shape. n is the ANN model number.

Table 5-2: Input and output variables for testing

Testing variable	
Input	**Output**
$\hat{\lambda}_i^{\,0} + \sigma_{\lambda i}, \hat{\phi}_i^{\,0} + \sigma_{\phi_i}$	$\hat{f}_j^{\,n}{}_{++}$
$\hat{\lambda}_i^{\,0} - \sigma_{\lambda i}, \hat{\phi}_i^{\,0} - \sigma_{\phi_i}$	$\hat{f}_j^{\,n}{}_{--}$
$\hat{\lambda}_i^{\,0} + \sigma_{\lambda i}, \hat{\phi}_i^{\,0} - \sigma_{\phi_i}$	$\hat{f}_j^{\,n}{}_{+-}$
$\hat{\lambda}_i^{\,0} - \sigma_{\lambda i}, \hat{\phi}_i^{\,0} + \sigma_{\phi_i}$	$\hat{f}_j^{\,n}{}_{-+}$

Here $\hat{\lambda}_i$ and $\hat{\phi}_i$ are the i^{th} frequencies and mode shapes for testing respectively. $\hat{f}_j^{\,n}{}_{++}, \hat{f}_j^{\,n}{}_{--}, \hat{f}_j^{\,n}{}_{+-}, \hat{f}_j^{\,n}{}_{-+}$ are the predicted frequencies of the n^{th} primary ANN model for the j^{th} substructure. Superscript '0' represents the corresponding mean value. The means $E(FCI)$ and standard deviations $\sigma(FCI)$ are calculated as below:

$$E(FCI) = \frac{1}{16}(FCI^{1}_{j_{++}} + FCI^{1}_{j_{+-}} + FCI^{1}_{j_{-+}} + FCI^{1}_{j_{--}} + \ldots + FCI^{4}_{j_{++}} + FCI^{4}_{j_{+-}} + FCI^{4}_{j_{-+}} + FCI^{4}_{j_{--}}) \quad (5\text{-}21)$$

$$\sigma(FCI) = \left[E(FCI^2) - (E(FCI))^2\right]^{\frac{1}{2}} \quad (5\text{-}22)$$

The PDEs are calculated from statistical distributions of FCI values. For example, for substructure *j*, the lower bound is $L_{FCI_j} = E(FCI_j) - 1.645\sigma(FCI_j)$ if the confidence level is set to 95%, the healthy substructure falls in the range of $[E(FCI_j) - 1.645\sigma(FCI_j), \infty]$ with $E(FCI_j)$ and $\sigma(FCI_j)$ are the mean and standard deviation of FCI values respectively. The PDEs are calculated with Equation (5-14) with the L_{FCI_j} terms substituted for L_{α_j} and $x_{FCI'}$ is the mean value of FCI. The PDE of substructure *j* is calculated as below.

$$P_d^j = 1 - prob(L_{FCI_j} \le x_{FCI'} \le \infty)$$
$$= prob(-\infty \le x_{FCI'} \le L_{FCI_j}) \quad (5\text{-}23)$$

As in Chapter 5, the PDE ranges between 0 and 1, where if PDE of a substructure close to 1, then most likely the substructure is damaged; and on the other hand, if the PDE is close to 0, the substructure is less likely to be damaged. For secondary ANN, the same calculation as explained in section 5.2.4 is used.

5.3 The effect of uncertainties on damage detectability with the multi-stage ANN method

In order to investigate the damage detectibility of the multi-stage ANN method under the influence of uncertainties, an analysis is conducted to detect structural damages with different levels of uncertainties. The same substructure sizes, structure types, boundary conditions and damage severities as in the sensitivity study in the previous chapter (section 6.5) are used. The substructure sizes are: i) 8m; ii) 4m and iii) 2m in length (refer to figure 6-16). Four different structure types and boundary conditions are: i) girder with simple support condition; ii) girder with flexible supports; iii) girder with continuous supports; and iv) simply-supported slab structure. Single damage is applied to element 8 with intensity ranging from -5% to -50% with a 5% interval in terms of SRF, resulting in ten levels of damage severities. Three levels of uncertainties are assumed in terms of C.O.V. for frequencies and mode shapes respectively, they are: i) 0.5% and 5%; ii) 1% and 10%; and iii) 2% and 20%. In this analysis, the uncertainties are applied to testing data only; while the training data are assumed as noise free.

Since the uncertainties are only applied to the testing data, only one multi-stage ANN model is involved in determining the PDEs. Based on Rossenblueth's PEM, this ANN model is tested with mean plus one standard deviation and mean minus one standard deviation of each random variable in testing data to obtain the two upper limits (FCI_{++}, FCI_{-+}) and two lower limits (FCI_{--}, FCI_{+-}) of FCI of each substructure. This is followed by the calculation of the mean and standard deviation of FCI using the same procedure as outlined in 5.2.4. Those upper and lower limits, and mean and

standard deviation of FCI for different substructure size are obtained in the primary ANN.

First an analysis is performed based on a simply supported girder. The same ANN model for simply supported girder in section 6.5 is used. As mentioned above, the ANN is tested with the ten levels of damage severities and the three levels of uncertainties. The simulated damage cases are in the first substructure when the substructure size is 8m and 4m. When the structure size is 2m, the damage is in the second substructure. The PDE of each structure corresponding to the different levels of uncertainties are illustrated in Figure 7-1(a)-(c) to 7-3(a)-(c).

Figure 7-1(a)-(c) show the PDEs of substructures when the testing data are smeared with 0.5% noise in frequencies and 5% noise in mode shapes. It is observed that the damaged substructure is always associated with a higher PDE value than the undamaged substructure, indicating that the damaged substructure is detected with high confidence and the undamaged substructures are less likely to be falsely detected. It is also observed that the confidence level increases with the damage level and decreases with the substructure size. For example, when the substructure is 8m long, only damages with 30% or more reduction in stiffness are confidently detected with PDE more than 50%. When the substructure size is reduced to 4m long, the detectability level is increased where damages with 15% or more reduction in stiffness are confidently detected with a PDE value larger than 60%. When the substructure is 2m long, damages at all levels considered in this study are confidently detected.

The same trend is also observed when the testing data is smeared with 1% noise in frequencies and 10% noise in mode shapes, as shown in Figure 7-2(a)-(c), and 2% noise in frequencies and 20% noise in mode shapes as shown in Figure 7-3(a)-(c). However, with the increase in the uncertainty level, the PDE values at the corresponding damage level and the same substructure size decreases, indicating the damage is detected with less confidence. For example, when the testing data is smeared with 1% noise in frequencies and 10% noise in mode shapes, for 8m long substructure, only damage with 50% are confidently identified (above 50% confident

level) while for higher noise (2% noise in frequencies and 20% noise in mode shapes) with the same substructure size.all the damages considered are not detected.

From this result, it is clear that damage detectability of the proposed approach is influenced by the level of uncertainties.

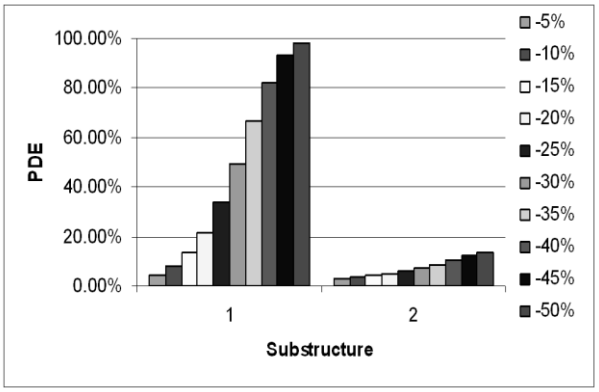

(a) 8m substructure

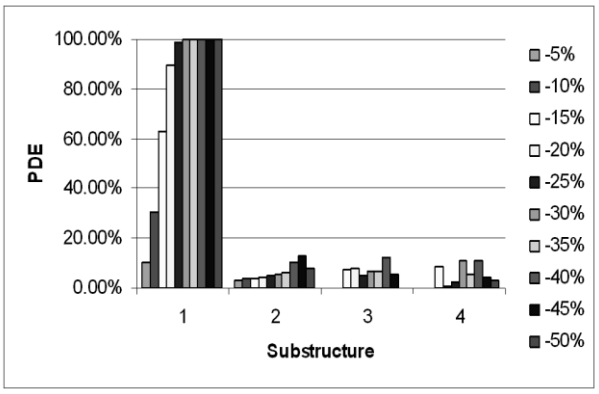

(b) 4m substructure

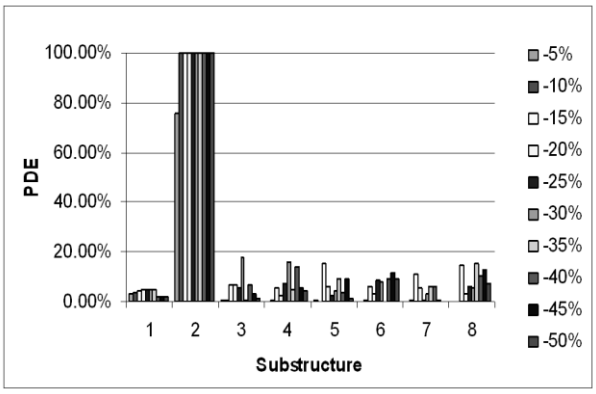

(c) 2m substructure

Figure 5-1: PDE of simply supported girder with 0.5% noise in frequencies and 5% noise in mode shapes

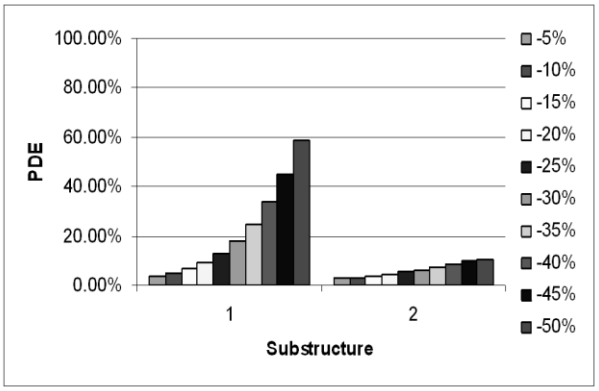

(a) 8m substructure

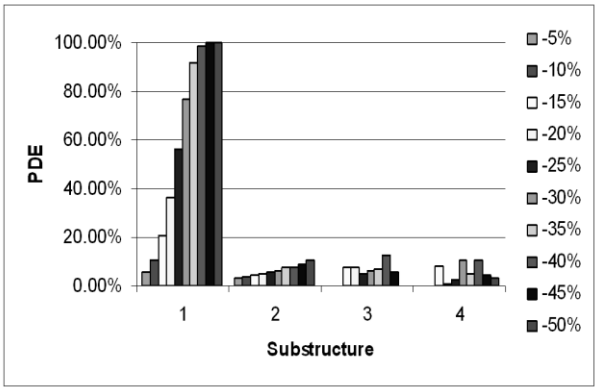

(b) 4m substructure

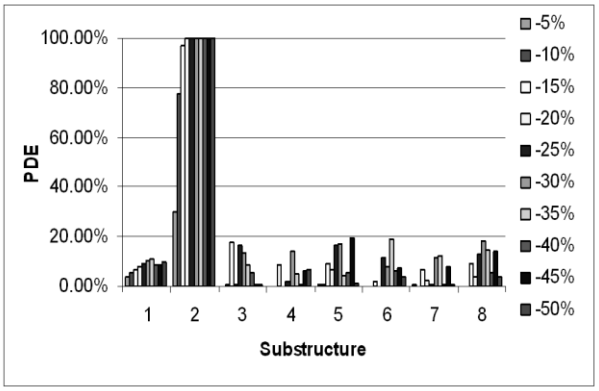

(c) 2m substructure

Figure 5-2: PDE of simply supported girder with 1% noise in frequencies and 10% noise in mode shapes

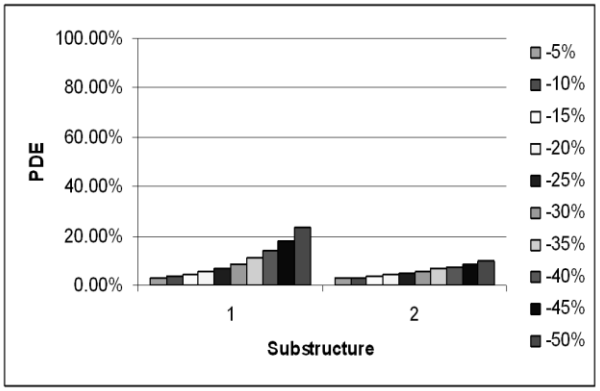

(a) 8m substructure

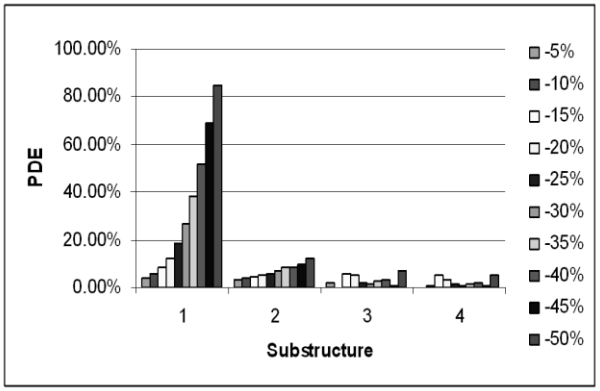

(b) 4m substructure

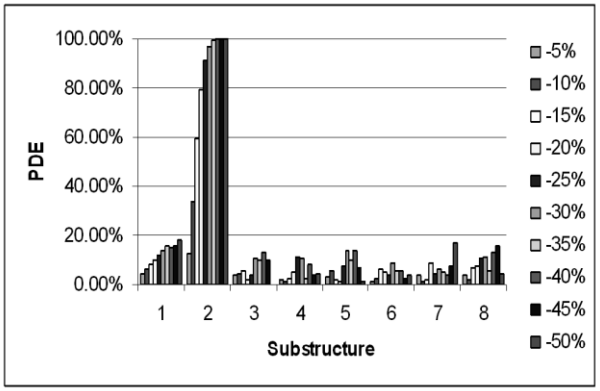

(c) 2m substructure

Figure 5-3: PDE of simply supported girder with 2% noise in frequencies and 20% noise in mode shapes

Figure 7.4(a) summarizes the damage detectable level of the simply-supported girder corresponding to the three uncertainty levels considered in this study. The damaged substructure is considered as detected if the confident level is 50% and above. The solid lines in the graph represent 50% confident level of damage detectability for the three uncertainty levels. The area below and above those lines represent detectable and undetectable damage level respectively and the corresponding substructure size.

From the figure, it is clearly seen that the damage detectable level decreases as the uncertainty level increases. In other words, as expected, the higher is the uncertainty level, the smaller is the substructure in order to confidently detect a same level of damage. For example, at -15% damage in a substructure, if the uncertainty level is 0.5% for frequencies and 5% in mode shapes, a 6m long substructure can be used to identify damage confidently, when the uncertainties increase to 1% in frequencies and 10% in mode shapes, or 2% in frequencies and 20% in mode shapes, substructure sizes equal or less than 4.5m or 2m; respectively, are needed to detect the damage in the substructure with a 15% stiffness reduction confidently.

The damage detectable levels with respect to the ratio of damaged element size to the substructure size under the influence of different levels of uncertainties are illustrated in Figure 7-4(b)-(d). The vertical lines indicate the detectability limit of different ratio between damaged element size (l_{el}) to substructure size (L_{sub}). The area at the right side of the lines represents the detectable damage level. The results show that, at higher uncertainty levels, only severer damage can be detected confidently at the same $\frac{l_{el}}{L_{sub}}$.

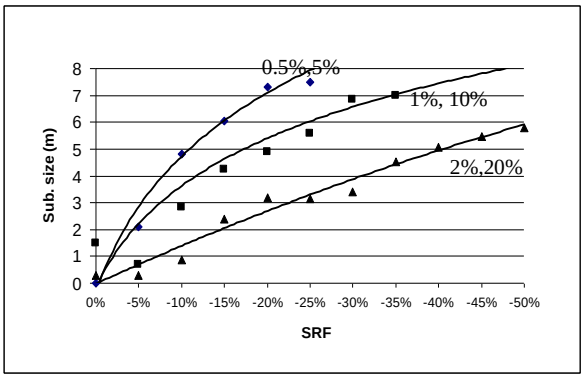

(a) Damage detectable level with respect to different uncertainties

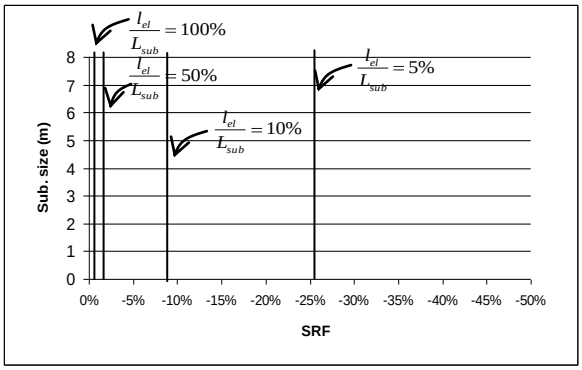

(b) 0.5% noise in frequencies and 5% noise in mode shapes

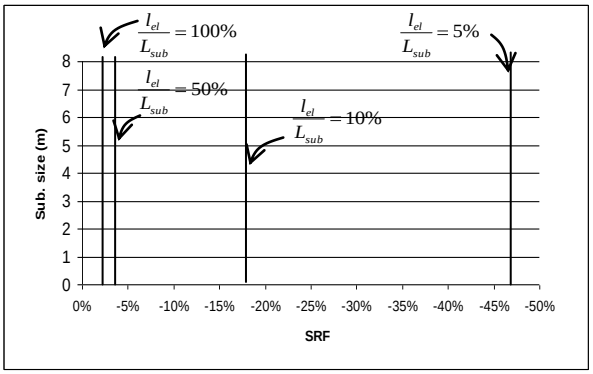

(c) 1% noise in frequencies and 10% noise in mode shapes

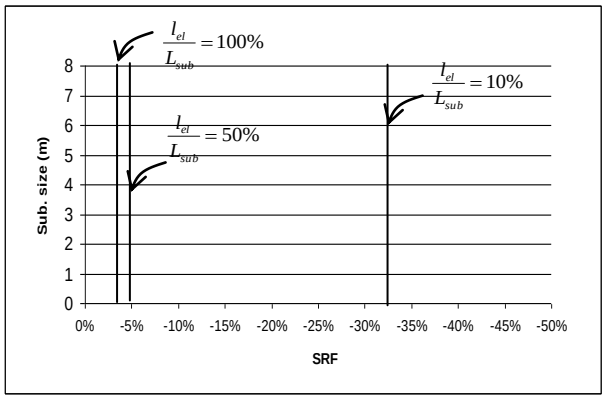

(d) 2% noise in frequencies and 20% noise in mode shapes

Figure 5-4: Results of the simply supported girder

Figure 7-5(a)-(d), Figure 7-6(a)-(d) and Figure 7-7(a)-(d) show the result for the girder with flexible supports, for the continuously supported girder and the slab structure, respectively. These figures show that the detectability levels of the simply supported girder, continuously supported girder and the slab structure are similar, whereas the detectability level for the flexibly supported structure is lower. These observations are similar to those in section 6.5, where the detectibility level is independent of the structure type, but dependent on the boundary condition because flexible boundary conditions increase the number of variables in the analysis, which is equivalent to increase the number of elements in the substructure as discussed in section 6.5. Minor differences among the results for the simply supported girder, the continuously supported girder and the slab structure are due to ANN prediction errors. These results also show that the detectability level is dependent on the uncertainty level.

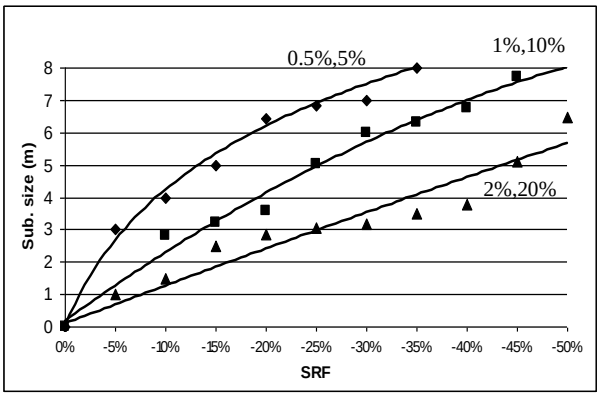

(a) Damage detectable level with respect to different uncertainties

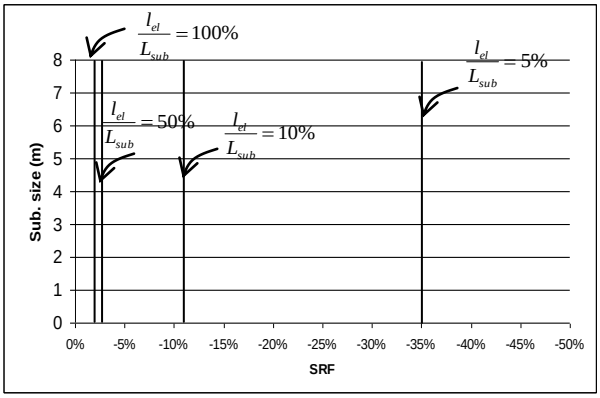

(b) 0.5% noise in frequencies and 5% noise in mode shapes

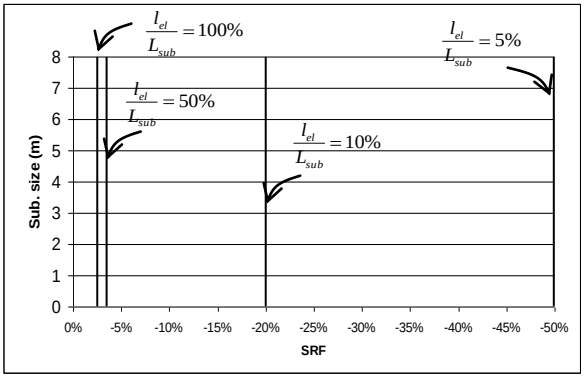

(c) 1% noise in frequencies and 10% noise in mode shapes

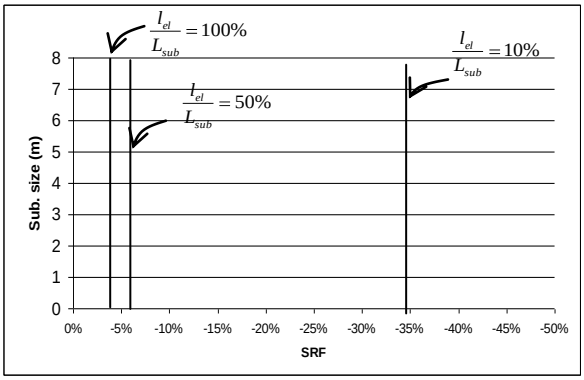

(d) 2% noise in frequenciesand 20% noise in mode shapes

Figure 5-5: Results of the flexibly supported girder

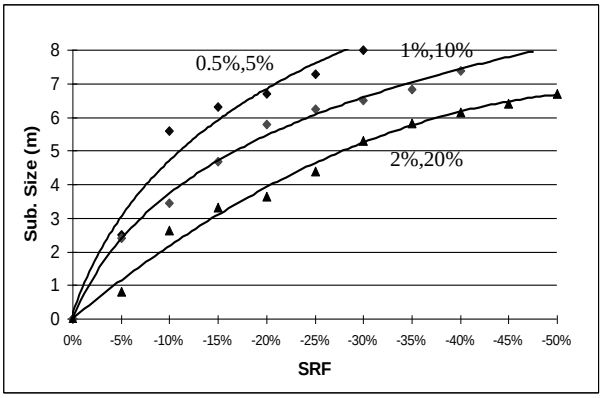

(a) Damage detectable level with respect to different uncertainties

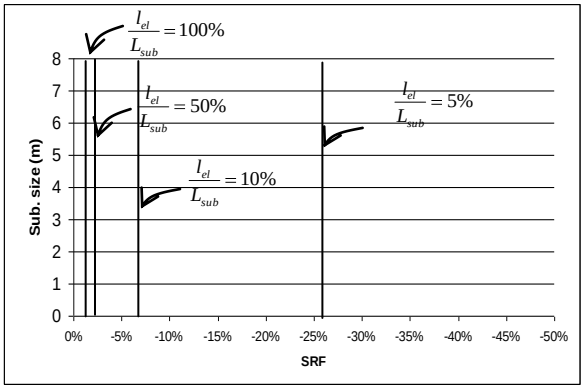

(b) 0.5% noise in frequencies and 5% noise in mode shapes

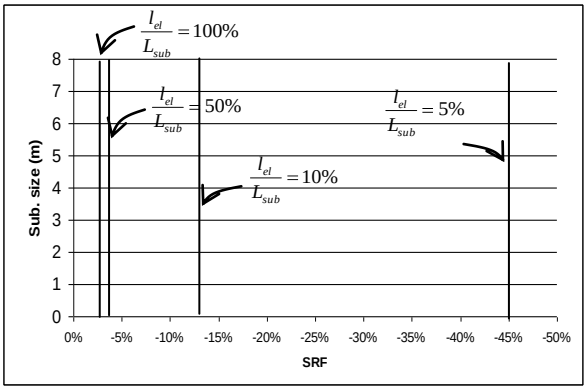

(c) 1% noise in frequencies and 10% noise in mode shapes

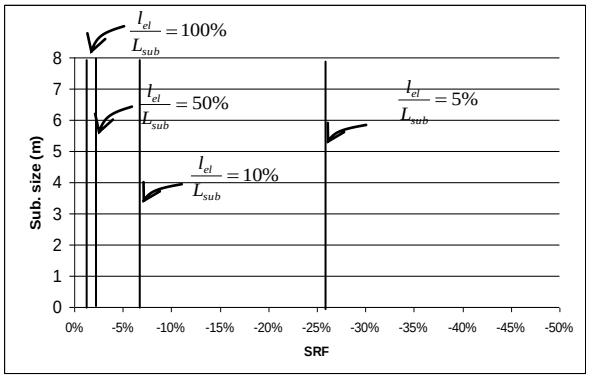

(d) 2% noise in frequencies and 20% noise in mode shapes

Figure 5-6: Results of the continuously supported girder

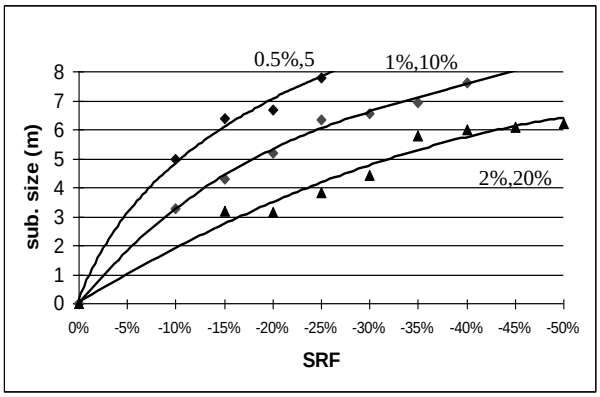

(a) Damage detectable level with respect to different uncertainties

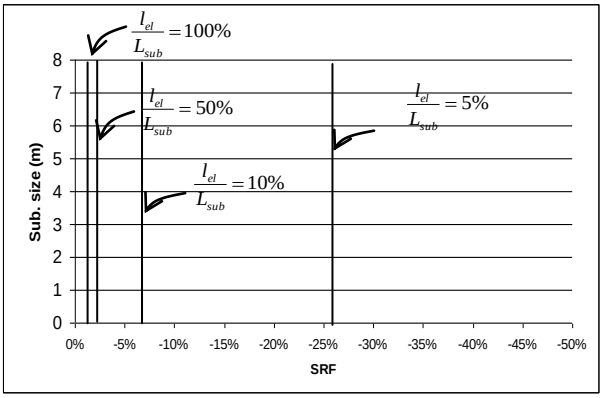

(b) 0.5% noise in frequencies and 5% noise in mode shapes

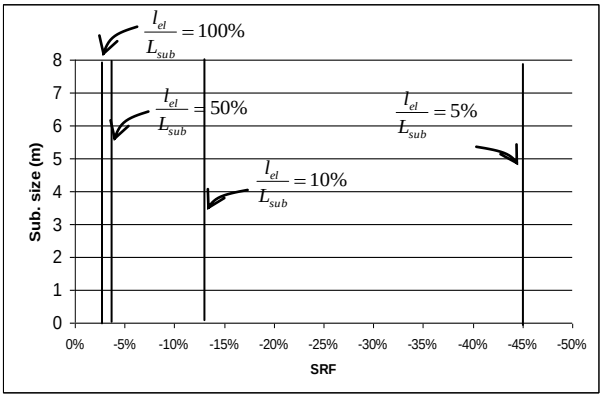

(c) 1% noise in frequencies and 10% noise in mode shapes

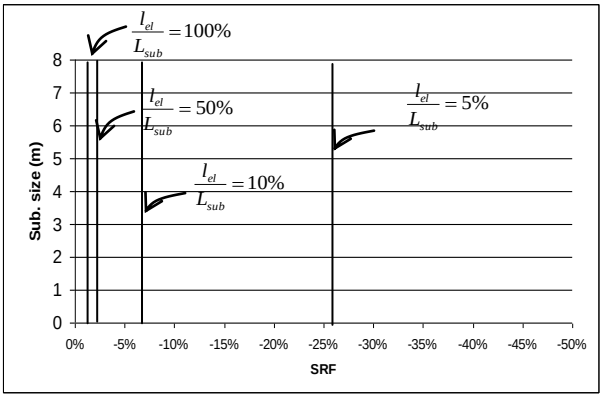

(d) 2% noise in frequencies and 20% noise in mode shapes

Figure 5-7: Results of the slab structure

5.4 Numerical example

The same slab structure as in section 6.3 is utilized as the numerical example in this section. The same substructure size and multi-stage ANN model as in section 6.3.2 are also adopted here. All the four simulated damage cases are used as testing data. By assuming the uncertainty levels in the testing data are 1% for frequencies and 10% for mode shapes, the PDEs in the primary and secondary ANN model are obtained using the probability method where the ANN models (Table 6.5(a)-(c)) are tested with testing data that is smeared with the specified random noise. The PDEs in the primary ANN model are based on the FCI value of each substructure, while in the secondary ANN model the PDEs are calculated based on the *E* value of every element in the damaged substructure. The calculated PDEs in the primary stage are given in Table 7-1. Figure 7-8(a)-(d) show the PDEs of elements obtained in the secondary stage.

Table 5-3: PDE (%) of substructure (numerical)

	Sub. 1	**Sub. 2**	**Sub.3**	**Sub. 4**
Scenario 1	**53.6**	3.2	0.79	0.24
Scenario 2	**98.9**	7.0	0.31	0.01
Scenario 3	**100.0**	**100.0**	26.61	0.00
Scenario 4	**100.0**	**100.0**	**100.0**	**100.0**

From Table 7-1, it is seen that the highest PDE values occur at substructure 1 for scenario 1 and 2, for scenario 3 the highest PDEs are at substructure 1 and 2 and at every substructure for scenario 4, while the PDEs at others substructures are low. These results indicate that the damaged substructures are correctly identified with high confidence in the primary ANN level. Figure 7-8(a)-(d) show the PDEs obtained in the secondary ANN model for the four simulated damage scenarios. It can be seen that the highest PDEs occur at the damaged elements for every scenario while the PDEs of other undamaged elements are low, indicating that the damages are confidently detected and the undamaged elements are less likely to be falsely detected. In comparison with the deterministic method in Chapter 6 (refer to Figure 6-10), it is noticed that by using the statistical method, more reliable results are obtained with less false identification. This may be due to the reasons that the

uncertainties in the frequencies due to error duplication and in mode shapes due to the effect of damage in other substructures are accounted for using the statistical method. This leads to a more reliable damage detection result than the deterministic approach. However, as shown, rather high PDEs in some undamaged elements such as element 20 in scenario 4 are still predicted, however, the values are substantially smaller than the PDEs of the true damaged elements. This is because of the nonlinear effect discussed previously.

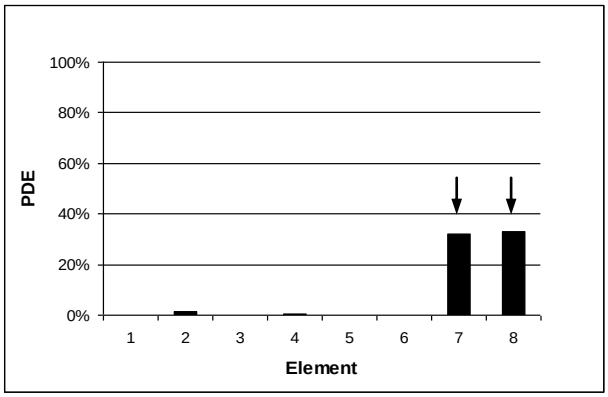

(a) Scenario 1

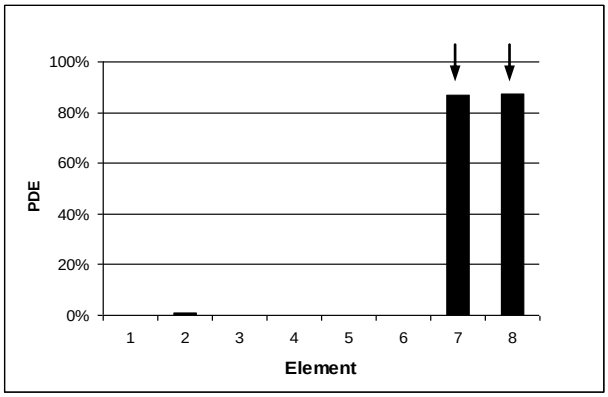

(b) Scenario 2

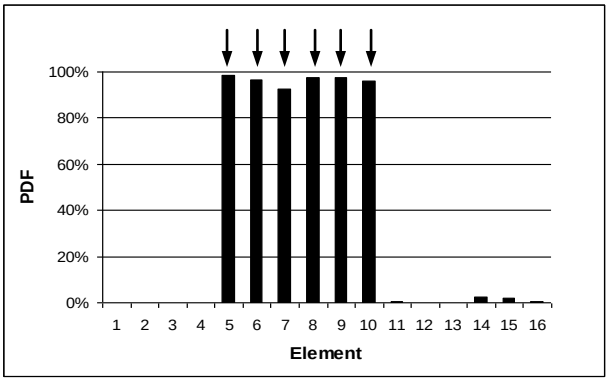

(c) Scenario 3

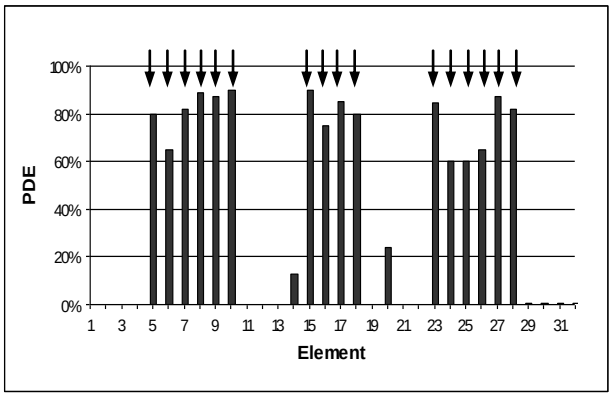

↓ Actual damage location

(d) Scenario 4

Figure 5-8: PDE of element for scenario 1 to scenario 4

5.5 Experimental example

To further demonstrate the applicability of the proposed method, the method is applied to detect the damages of the laboratory tested concrete slab described in Chapter 3. All the ten damage levels are used as the testing data in ANN model to predict damage. As the existence of modeling error and measurement error are inevitable, it is assumed that the uncertainties in the finite element model and the testing data are both 2% in frequencies and 15% in mode shapes. Based on Rossebleuth's PEM, four multi-stage ANN models are used. Each of the ANN models is trained and tested with the combination of the mean plus one standard deviation and mean minus one standard deviation of the considered errors in the training and testing data.

The slab is divided into 4 substructures and each substructure consists of 4 segments as shown in Figure 7-9. 1700 training data are generated based on OA17.16.2.3 to train the primary ANN models. Two stages of primary ANN model are considered to identify the damaged substructure. The same ANN structure as in Figure 6-8 is used.

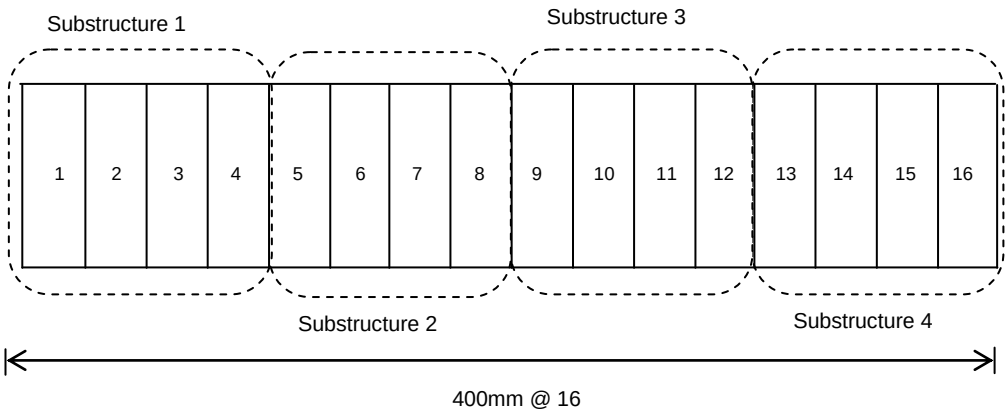

Figure 5-9: Segmentation of the slab

Three ANN models are involved in the primary ANN stage which are NNP1 (14-17-4), NNP2(8-14-4) and NNP3(8-14-4). These ANN models are trained and validated using 1700 and 400 data generated using OA17.16.2.3.3. The PDEs of every substructure for every damage level are given in Table 7-4. By comparing the PDEs of the substructures at every level in the table against the experimental results, it can be seen that the PDE values obtained are consistent with the observed damage

patterns in the experiment. The gradual increments of PDE values of substructure 1 and 2 from level 1 to level 5 are consistent with the crack propagation at the left span of the slab with the increase of load. The increase of PDE values of substructure 3 within those damage levels is due to the crack propagation at the middle support. The high PDEs of every substructure from level 7 to level 10 indicates that these substructures are very likely damaged, which also agrees with the damage observed in the experiment.

Table 5-4: PDE (%) of substructure (experimental)

	Sub. 1	**Sub. 2**	**Sub.3**	**Sub. 4**
Level 1	0.14	14.11	13.45	3.65
Level 2	42.99	38.70	28.97	1.22
Level 3	**67.26**	**56.84**	31.62	0.14
Level 4	**75.31**	**56.50**	39.49	0.02
Level 5	**81.09**	**62.91**	49.59	0.06
Level 6	**78.85**	**57.46**	**68.11**	40.68
Level 7	**85.16**	**57.85**	**98.20**	**68.20**
Level 8	**95.22**	**82.96**	**96.65**	**70.96**
Level 9	**98.24**	**93.11**	**98.82**	**81.30**
Level 10	**100.0**	**99.73**	**99.05**	**81.01**

Based on the results of the primary ANN model, only secondary ANN models involving substructure 1 and 2 are built to detect damage at level 3 to 5, namely NNS1 and NNS2. These ANN models are trained and validated using 900 and 270 training and validation data which are generated using OA9.8.2.3. The outputs of those NNS1 and NNS2 are *E* values for segment 1 to 4 and *E* values for segment 5 to 8 respectively. These ANN models are tested with experimental data from level 3 to level 5, for the purpose of comparison, levels 1 and 2 which are identified as undamaged are also included in the testing data.

For damage at level 6, three ANN models are built to detect damage in substructure 1 to substructure 3 (NNS1, NNS2 and NNS3). These ANN models are trained and validated using 1200 and 400 data that generated using OA24.12.2.3. Only

experimental data for damage level 6 is used as the testing data. For level 7 to 10; ANN models for all substructures are built using the same data as in the primary ANN model.

Figure 7-10(a)-(j) show the results of the ten damage levels obtained from the secondary ANN models in terms of PDE. Figure 7-10(a)-(e) show the PDEs of segment 1 to 8 for level 1 to 5. Figure 7-10(f) shows the PDEs of segment 1 to 12 of substructure 1 to 3 for level 6, while PDEs of corresponding segments for levels 7 to 10 (segments 1 to 16) are shown in Figure 7-10(g)-(j).

It is seen the identified damages are close to the observed damage in the experiment, indicated by high PDE values occur at the damage locations. The low PDEs predicted at level 1 and level 2 at segment 1 to segment 8 indicate that there is no significant damage detected. This agrees with the observations in the experiment for levels 1 and 2 when 6kN and 12kN loads were applied to the left span. At level 3, the highest PDE values are obtained at segments 4 and 5 which are at the middle of the left span. The PDE at other segments remains low. This is also the observed damage location when 18kN load was applied at the left span. The results for levels 4, 5 and 6 show that the PDE values for segments 4 and 5 are remained almost at the same value as in the level 3, while the PDE value for segment 8 which is at the middle support is high. Again, these results agree with the observations in the experiment, when the load at the left span remained at 18kN, but the crack intensity increased at the middle support when the load at the right span increased from 3kN to 12kN.

The trend of the predicted PDEs for levels 7 to 10 also agree with the crack propagation observed in the experiment, where the PDE values are observed high at the middle of left and right span and at the middle support. Those PDE values are also increased with the increment of loads at the left and right span. However, several inaccurate estimations still occur, such as, in damage level 7 and level 8, the PDE of segments 4, 5, 6 and 8 are lower compared to PDE values in level 6. This probably due to numerical errors in ANN predictions

These results demonstrate that, the damage is correctly identified using the proposed method. By comparing the current results with those in Chapter 5 (refer to Figure 5-6) where multi-stage substructuring technique was not used, it is seen that most of the PDEs obtained are higher at every damage level. It should be noted that the PDE values obtained here are expected to be higher because the element size used in the analysis is smaller than that in Chapter 5. However, several inaccurate estimations still occur, such as, in damage level 7 and level 8, the PDE of segment 4, 5, 6 and 8 are lower compared to PDE values in level 6 and the estimated PDEs at the same damage levels in Figure 5-7. This is probably due to numerical errors in ANN predictions. From the results, it can be said that by incorporating the probability method, the multi-stage ANN method can provide better damage identification results.

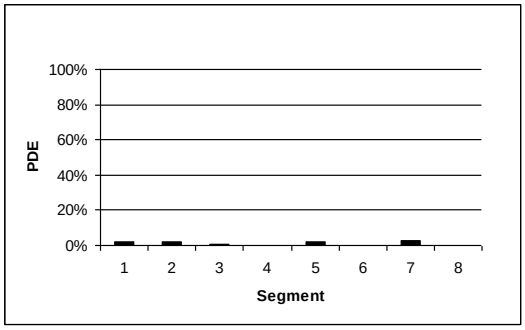

(a) Level 1 (6kN (left)-0kN(right))

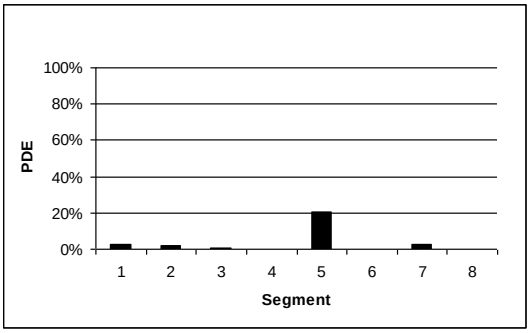

(b) Level 2 (12kN (left)-0kN(right))

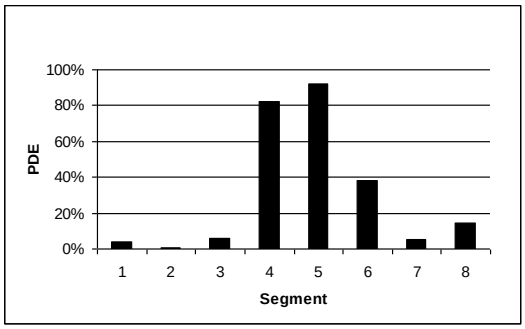

(c) Level 3 (18kN (left)-0kN(right))

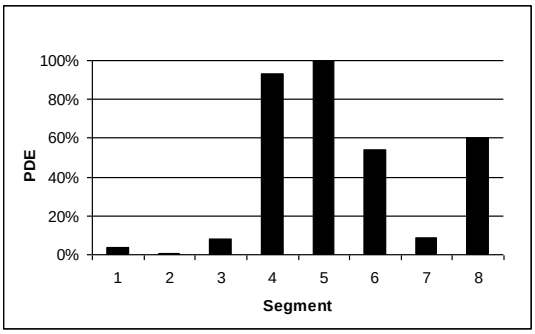

(d) Level 4 (18kN (left)-3kN(right))

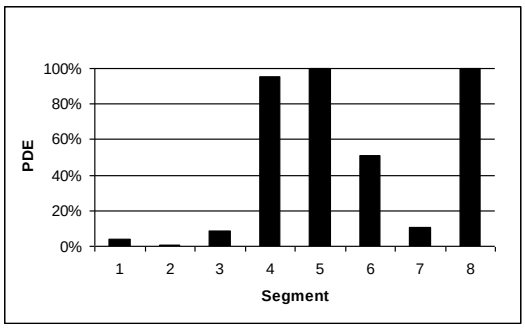

(e) Level 5 (18kN (left)-6kN(right))

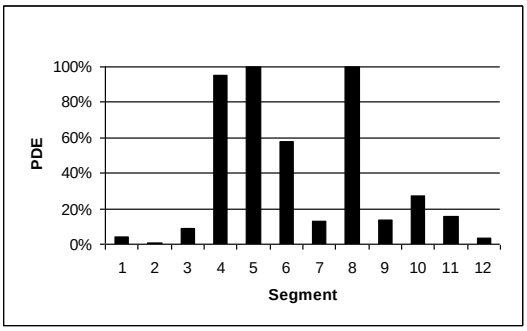

(f) Level 6 (18kN (left)-12kN(right))

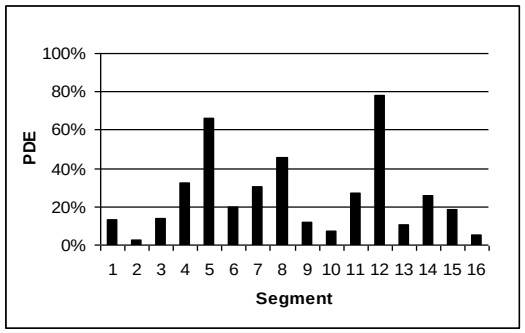

(g) Level 7 (18kN (left)-18kN(right))

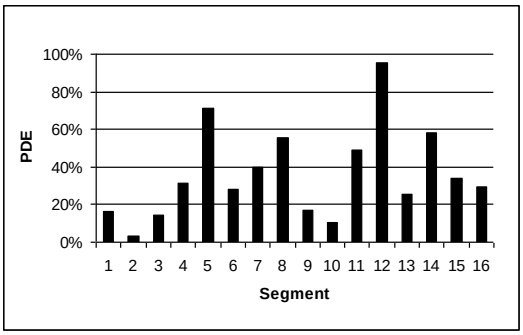

(h) Level 8 (25kN (left)-25kN(right))

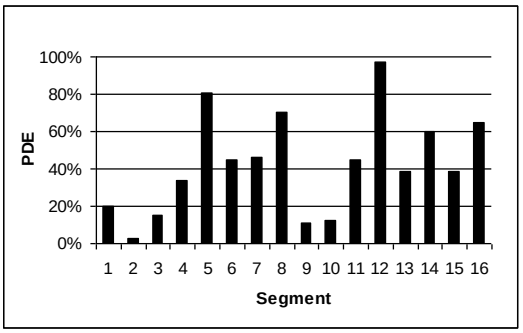

(i) Level 9 (32kN (left)-26kN(right))

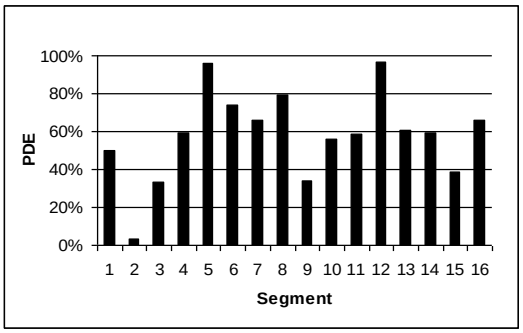

(j) Level 10 (38kN (left)-38kN(right))

Figure 5-10: PDE (%) for every segment of level 1 to level 10

5.6 Summary

This chapter studies the effect of uncertainties on the damage detectability of ANN-based substructuring technique proposed in Chapter 6. The applicability of probability method to consider uncertainties in finite element model and in measurement noise is also demonstrated through the statistical ANN approach described in Chapter 5. The results clearly showed that the damage detectability of the proposed method is dependent on the uncertainty level and substructure size. The damage detectability level decreases with the increase in uncertainty level and substructure size. The damage identification results from the statistical ANN model showed that by using the probability method, better results can be obtained because the method not only accounts for the uncertainty effect from the finite element modeling error and measurement noise, but also accounts for the uncertainties in frequencies due to duplication error in multi-stage ANN model and uncertainties in mode shapes due to the nonlinear effect of damage in other substructures. This observation agrees with the suggestion by Trendafilova et al. (1998) and the result in Yuen and Katafygiotis (2006) that damage identification using the substructure method should be treated in terms of probability of damage rather than deterministic determination of damage levels.

CHAPTER 6

CONCLUSIONS AND RECOMMENDATIONS

6.1 Summary and findings

This study began with a review of vibration-based damage detection methods, emphasising ANN methods. Advantages and disadvantages of various methods have been compared and discussed. Due to several advantages, ANN has been extensively researched and widely accepted in the field of damage detection. However, its practical application is still limited owing to i) uncertainties in finite element model simulation that is usually used to train an ANN model and noises in measured data that is used to identify structural damage; and ii) enormous computational time and required computer memory when the number of structural degree of freedom is large.

In this study the applicability of ANN in damage detection using frequencies and mode shapes as the diagnosis parameters has been investigated. A backpropagation ANN together with Levenberg Maquartd algorithm was applied to correlate modal parameters with structural parameters. The applicability of ANN in damage detection based on modal parameters has been demonstrated, and several techniques to deal with the existing problems have been proposed and demonstrated.

Chapter 4 demonstrated that an ANN can effectively in detect damage from modal parameters. Single and multiple damage cases were considered using numerical examples. The influence of different combinations of input parameters and number of modes to ANN performance was also investigated. Using the frequency alone, mode shapes alone and the combination of both parameters led to the conclusion that the combination of frequencies and mode shapes as the input variables provides more reliable results. The parametric study of ANN performance under different number of modes indicated that it is more reliable when more modes are used as the input parameters.

An attempt to apply the deterministic ANN to identify damage using experimental data yielded poor results due to the existence of uncertainties in finite element modeling and measured data.

The results using numerical and experimental examples have demonstrated that;

i) The ANN can reliably identify structural damages when uncertainties in finite element model and measured data are considered using probabilistic method.
ii) Structural damage can be more confidently identified by using the developed probabilistic ANN model than the deterministic ANN model.
iii) Statistical ANN is more reliable in identifying damage if the difference between uncertainty level in training and testing data is small.

Numerical results and parametric study demonstrate that:

i) The proposed method is capable of identifying damaged and undamaged substructures and detecting local damages and their severities.
ii) Computational effort can be reduced using the proposed method especially when involving multiple damage locations.
iii) The reliability of the method is dependant on the substructure size, damage level and the size of damaged elements in a substructure but independent of the structure type.

The effects of uncertainties on damage detectability of the proposed multi-stage substructuring method have been studied in Chapter 7. It is found that:

i) The uncertainties reduce the detectability of the proposed technique in identifying damaged substructures.
ii) The probability method provides more reliable results in detecting damage with the proposed multi-stage substructuring method.

6.2 Contributions

This study has three contributions to existing literature. They are as follows:

i) As mentioned in the literature review, the success of ANN in damage detection is limited to numerical examples and small controlled experiments only. Its application to experimental data in uncontrolled condition was less successful due to the uncertainties in finite element modeling and measured data. Adding to the existing literature, the present study introduced a new method that combines the probability technique and ANN to consider these uncertainties in damage detection.

ii) This study adds to the limited current research in the use of substructure technique with ANN by introducing a multi-stage ANN method to detect damage in substructures. The proposed method reduces the training time and high computer memory requirement. Therefore, it makes the application of ANN in detecting damage in large civil structure possible.

iii) This study adds to the growing research on ANN-based damage detection by providing a guideline in selection of efficient substructure size to identify the damaged substructure. Additionally, by applying the probability method to the multi-stage ANN substructure technique, the effects of uncertainties on the selection of substructure size have also been studied and a guideline in selecting the substructure size under various uncertainty levels are proposed.

6.3 Recommendations

Based on the literature review and the present study, several recommendations for future work are drawn below:

i) This study did not compare the effect of different methods in preparing the training data. Since ANN performance is very much dependant on training sample, a comparison study on the ANN performance under different methods for training sample selection is recommended.

ii) It has been realized that the number of measurement points and locations have a great influence on the accuracy of damage detection results. A detailed study regarding the influence of different number of measurement points and locations to ANN-based damage detection performance should be done.

iii) The application of ANN-based damage detection method to a real structure is limited. It is recommended that a real structure should be used as an example in the future work.

REFERENCES

Abdo, M. A., and Hori, M. (2002). "A numerical study of structural damage detection using changes in the rotation of mode shapes." Journal of Sound and Vibration, 251(2), 227-239.

Adeli, H. (2001). "Neural networks in civil engineering: 1989-2000." Journal of Computer -Aided Civil and Infrastructure Engineering, 16, 126-142.

Adeli, H. (2006). "Dynamic fuzzy wavelet neural network model for structural system identification." Journal of Structural Engineering 132(1), 102-111.

Adeli, H., and Yeh, C. (1989). "Perceptron learning in engineering design." Microcomputers in Civil Engineering, 4(4), 247-256.

Allemang, R. J. (2002). "The modal assurance criterion (MAC): twenty years of use and abuse. ." Proceeding of 20th International Modal Analysis Conference, Bethel, CT, 397-405.

Armon, D., Ben-Haim, Y., and Braun, S. (1994). "Crack detection in beams by rankordering of eigenfrequency shifts." Mechanical Systems and Signal Processing 8(1), 81-91.

Ash, T. (1989). "Dynamic node creation in backpropagation networks." Connection science, 1(4), 365-375.

Ayyub, B. M., and Gupta, M. M. (1997). *Uncertainty analysis in engineering and sciences: Fuzzy logic, statistics and neural network approach*, Kluwer Academic.

Ayyub, B. M., and McCuen, R. H. (2003). *Probability, statistics and reliability for engineers and scientist*, Chapman and Hall/CRC Press, Florida.

Azroff, M. E. (1994). *Neural time series forecasting of financial markets*, John Wiley & Sons, New York.

Balmes, E. (1996). "Structural Dynamics Toolbox: For Use with MATLAB."

Banan, H. T., and Hjelmstad, K. D. (1994). "Parameter Estimation of Structures from Static Response. I: Numerical Simulation Studies." Journal of Structural Engineering, 120(11), 3243-3258.

Banan, M. R., and Hjelmstad, K. D. (1994a). "Parameter Estimation of Structures from Static Response. II: Numerical Simulation Studies." Journal of Structural Engineering, 120(11), 3259-3283.

Banks, H. T., Inman, D. J., Leo, D. J., and Wang, Y. (1996). "An experimentally validated damage detection theory in smart structures." Journal of Sound and Vibration, 191(5), 859-880.

Barai, S. V., and Pandey, A. K. (1995). "Vibration signature analysis using Artificial Neural Network." Journal of Computing in Civil Engineering, 9(4), 259-265.

Besterfield, D. H., Besterfield-Michna, C., Besterfield, G., and Besterfield-Sacre, M. (1995). *Total quality management*, Prentice Hall, Englewood Cliffs, NJ.

Bhagat, P. (1990). "An introduction to neural nets." Chemical Engineering Progress, 55-60.

Bishop, C. M. (1995). *Neural network for pattern recognition*, Oxford University Press, Oxford.

Cao, T. T., and Zimmerman, D. C. (1997). "Application of load-dependat Ritz vectors in structural damage detection." Proceeding of 15th International Modal Analysis Conference, Orlando, FL.

Cao, T. T., and Zimmerman, D. C. (1999). "Procedure to Extract Ritz Vectors from Dynamic Testing Data." Journal of Structural Engineering, 125(12), 1393-1400.

Carden, P. E., and Fanning, P. (2004). "Vibration based condition monitoring: A review." Structural Health Monitoring, 3(4), 355-377.

Casas, J. R., and Aparicio, A. C. (1994). "Structural Damage Identification from Dynamic-Test Data." Journal of Structural Engineering, 12(8), 2437-2450.

Cawley, P., and Adams, R. D. (1979). "The location of defects in structures from measurements of natural frequencies." Journal of Strain Analysis, 14(2), 49-57.

Ceravolo, R., and De Stefano, A. (1995). "Damage location in structures through a connectivistic use of FEM modal analyses." The International Journal of Analytical and Experimental Modal Analysis, 10(3), 178-186.

Ceravolo, R., De Stefano, A., and Sabia, D. (1995). "Hierarchical use of neural techniques in structural damage recognition." Smart Materials and Structures, 4, 270-280.

Chang, C. C., Chang, T. Y. P., and Xu, Y. G. (2000). "Structural damage detection using an iterative neural network." Journal of Intelligence Material Systems and Structure, 11(1), 32-42.

Chang, C. C., Chang, T. Y. P., and Xu, Y. G. (2002). "Selection of training samples for model updating using neural networks." Journal of Sound and Vibration, 245(5), 867-883.

Chen, J. C., and Garba, J. A. (1988). "On-orbit damage assessment for large space structures " AIAA Journal, 26(9), 1119-1126.

Choy, F. K., Liang, R., and Xu, P. (1995). "Fault identification of beams on elastic foundation " Computers and Geotechnics 17(2), 157-176.

Doeblíng, S. W. (1996). "Minimum-Rank Optimal Update of elemental stiffness parameters for structural damage identification." AIAA Journal, 31(12), 2615-2621.

Doebling, S. W., Farrar, C. R., and Cornwell, P. (1997). "DIAMOND: A graphical interface toolbox for comparative modal analysis and damage identification." Proceeding of 6th International Conference on Recent Advance in Structural Dynamics, Southampton, 399-412.

Doebling, S. W., Farrar, C. R., and Prime, M. B. (1998). "A summary review of vibration-based damage identification methods." The Shock and Vibration Digest, 30(2), 91-105.

Doeblíng, S. W., Farrar, C. R., Prime, M. B., and Shevitz, D. W. (1996). "Damage identification and health monitoring of structural and mechanical systems from changes in their vibration characteristics: A literature review." Technical Report LA-13070-MS, Los Alamos National Laboratory, Los Alamos, MA.

Elkordy, M. F., Chang, K. C., and Lee, G. C. (1992). "Neural networks in dynamic analysis of bridges." Proceeding of 8th Annual Conference of Computing in Civil Engineering, Texas, USA.

Elkordy, M. F., Chang, K. C., and Lee, G. C. (1993). "Neural network trained by analytically simulated damage states." Journal of Computing in Civil Engineering, 7(2), 130-145.

Elkordy, M. F., Chang, K. C., and Lee, G. C. (1994). "A structural damage neural network monitoring system." Microcomputers in Civil Engineering, 9(2), 83-96.

Engineers Australia. (2005). "Australian Infrastructure Report Card ", http://www.infrastructurereportcard.org.au/

Evans, D. H. (1967). "An application of numerical integration techniques to statistical tolerancing. ." Technometrics, 9(3), 441-456.

Fang, X., Luo, H., and Tang, J. (2005). "Structural damage detection using neural network with learning rate improvement." Computers and Structures, 83(25-26), 2150-2161.

Farrar, C. R., and Doebling, S. W. (1997). "An Overview of Modal-Based Damage Identification Methods." Proceeding of DAMAS Conference, , Sheffield, U.K., .

Farrar, C. R., and Doeblíng, S. W. (1998). "Comparative study of damage identification algorithms applied to a bridge: II. Numerical study." Smart Materials and Structures, 7, 720-731.

Farrar, C. R., Doeblíng, S. W., and Nix, D. A. (2001). "Vibration-based structural damage identification." Philosophical Transactions: Mathematical, Physical & Engineering Sciences, 359, 131-149.

Fausett, L. (1994). *Fundamentals of neural networks*, Prentice Hall, New York.

Feng, Q. M., and Bahng, E. Y. (1999). "Damage assessment of jacketed RC columns using vibration tests." Journal of Structural Engineering, 125(3), 265-271.

Ferregut, C., Osegueda, A., and Ortiz, J. (1995). "Artificial neural networks for structural damage detection and classification." Proceeding of SPIE Smart Structures Conference, San Diego, USA.

Finnoff, W., Hergert, F., and Zimmerman, H. S. (1993). "Improving model selection by nonconvergent methods." Neural Networks, 6(6), 771-783.

Friswell, M. I., and Mottershead, J. E. (2001). "Inverse methods in structural health monitoring." Key Engineering Material, 204-205, 201-210.

Friswell, M. I., and Pandey, A. K. (1997). "Is damage location using vibration measurements practical?" Proceeding of EUROMECH 365 International Workshop: DAMAS 97, Sheffield, UK.

Fritzen, C. P., Jennewein, D., and Keifer, T. (1998). "Damage detection based on model updating methods." Mechanical Systems and Signal Processing, 12(1), 163-186.

Fujino, Y., and Abe, M. (2001). "Structural health monitoring in civil infrastructures and R&D of SHM of bridge at University of Tokyo." Proceeding of 3rd International Workshop Structural Health Monitoring: The Demands and Challenges, Stanford, CA, USA, 61-79.

Funahashi, K. (1989). "On the approximate realization of continuous mappings by neural networks." Neural Networks, 2(3), 183-192.

Gately, E. (1996). *Neural Networks for Financial Forecasting.*, John Wiley and Sons, New York.

Geman, S., Bienenstock, E., and Doursat, R. (1992). "Neural networks and the bias/variance dilemma." Neural Computation, 4(1), 1-58.

Guyonnet, D., Come, B., Perrochet, P., and Parriaux, A. (1999). "Comparing two methods for addressing uncertainty in risk assessments." Journal of Environmental Engineering, 125(6), 660-666.

Hagan, M. T., Demuth, H. B., and Beale, M. (1995). *Neural network design*, PWS Publishing Company.

Hagan, M. T., and Menhaj, M. (1994). "Training feedforward networks with the Maquardt algorithm." IEEE Transaction on Neural Networks, 5(6), 989-993.

Harr, M. E. (1989). "Probabilistic estimates for multivariate analysis." Applied Mathematical Modelling, 13(5), 313-318.

Hassibi, B., and Stork, D. G. (1993). "Second order derivatives for network pruning: Optimal brain surgeon." Proceeding of Advances in neural information processing systems 5, San Mateo, CA.

Hassiotis, S., and Jeong, G. D. (1995). "Identification of stiffness reduction using natural frequencies." Journal of Engineering Mechanics, 121(10), 1106-1113.

Haykin, S. (1994). *Neural networks: A comprehensive foundation*, Macmillan Publishing, New York.

Hedayat, A. S., Sloane, N. J. A., and Stufken, J. (1999). *Orthogonal arrays - Theory and Applications*, Springer Verlag, New York.

Helton, J. C., and Davis, F. J. (2003). "Latin hypercube sampling and the propagation of uncertainty in analyses of complex system." Reliability Engineering and System Safety, 81, 23-69.

Hjelmstad, K. D., and Shin, J. (1997). "Damage Detection and Assessment of Structures from Static Response." Journal of Engineering Mechanics, 123(6), 568-576.

Ho, Y. K., and Ewins, D. J. (2000). "On structural damage identification with mode shapes." Proceeding of COST F3 Conference on System Identification and Structural Health Monitoring, Madrid, Spain, 677-686.

Hornik, K., Stinchcombe, M., and White, H. (1989). "Multilayer feedforward networks are universal approximator." Neural Networks, 2(5), 359-366.

Hung, S., Huang, C. S., Wen, C. M., and Hsu, Y. C. (2003). "Nonparametric identification of a building structure from experimental data wavelet neural network." Computer-aided and Infrastructure Engineering, 18(5), 356-368.

Hung, S., and Kao, C. Y. (2002). "Structural damage detection using the optimal weights of the approximating neural networks." Earthquake Engineering and Structural Dynamics, 31, 217-234.

Hurty, W. C. (1964). "Dynamic Analysis of structural systems using component modes." AIAA Journal, 3(4), 678-684.

Islam, A. S., and Craig, K. C. (1994). "damage detection in composite structures using piezoelectric materials." Smart Materials and Structures, 3(3), 318-328.

James, G. H., Zimmerman, D. C., Farrar, C. R., and Doeblíng, S. W. (1997). "Current horizon for structural damage detection course." Proceeding of SEM short course held at the 15th Int. Modal Analysis Conference, Orlando, Florida.

Jiang, X., and Adeli, H. (2005). "Dynamic wavelet neural network for nonlinear identification of highrise buildings." Computer-aided and Infrastructure Engineering, 20(5), 316-330.

Jung, H., C., and Ghaboussi, J. (1999). "Genetic algorithm in structural damage detection " Computers & Structures, 79(14), 1335-1353.

Kaastra, I., and Boyd, M. (1996). "Designing a neural network for forcasting financial and economic time series." Neurocomputing, 10(3), 215-236.

Kabe, A. M. (1985). "Stiiffness matrix adjustment using mode data." AIAA Journal, 23(9), 1431-1436.

Kao, C. Y., and Hung, S. (2003). "Detection of structural damage via free vibration responses generated by approximating artificial neural network." Computers & Structures, 81, 2631-2644.

Kermanshahi, B. (1999). *Design and application of neural networks*, Shokodo, Tokyo.

Kim, Y. Y., and Kapania, K. R. (2006). "Neural networks for inverse problems using principal component analysis and orthogonal arrays." AIAA Journal, 44(7), 1628-1634.

Kirkegaard, P., and Rytter, A. (1994). "Use of neural networks for damage assessment in a steel mast." Proceeding of 12th International Modal Analysis Conference, Orlando, USA.

Ko, J. M., Sun, Z. G., and Ni, Y. Q. (2002). "Multi-stage identification scheme for detecting damage in cable-stayed Kap Shui Mun bridge." Engineering Structures, 24(7), 857-868.

Koh, C. G., Hong, B., and Liaw, C. Y. (2003). "Substructural and progressive structural identification method." Engineering Structures, 25(12), 1551-1563.

Krogh, A., and Hertz, J. A. (1995). "A simple weight decay can improve generalization." Proceeding of Advances in Neural Information Processing System 4, San Mateo, CA.

Kudva, J. N., Munir, N., and Tan, P. W. (1992). "Damage detection in smart structures using neural networks and finite-element analysis." Journal of Smart Materials and Structures, 1, 108-112.

Lam, H. F., Yuen, K. V., and Beck, J. (2006). "Structural health monitoring via measured Ritz vectors utilizing artificial neural network." Computer-Aided and Infrastructure Engineering, 21(4), 232-241.

Lee, J., Kim, J. D., Yun, C. B., Yi, J. H., and Shim, J. M. (2002a). "Health-monitoring method for bridge under ordinary traffic loadings." Journal of Sound and Vibration, 257(2), 247-264.

Lee, J. J., Lee, J. W., Yi, J. H., Yun, C. B., and Jung, Y. J. (2005). "Neural network-based damage detection for bridges considering errors in baseline finite elements models." Journal of Sound and Vibration, 280(3-5), 555-578.

Lee, J. J., and Yun, C. B. (2006). "Damage diagnosis of steel girder bridges using ambient vibration data." Engineering Structures, 28(6), 912-925.

Lee, J. W., Kim, J. D., Yun, C. B., Yi, J. H., and Shim, J. M. (2002b). "Health-monitoring method for bridges under ordinary traffic loading." Journal of Sound and Vibration, 257(2), 247-264.

Lee, U., and Shin, J. (2002). "A frequency response function-based structural damage identification method." Computers & Structures, 80(2), 117-132.

Levin, R. I., and Lieven, N. A. J. (1998). "Dynamic finite element model updating using neural networks." Journal of Sound and Vibration, 210(5), 593-607.

Liang, Y. C., and Feng, D. P. (2001). "Identification of restoring forces in non-linear vibration systems using fuzzy adaptive neural network." Journal of Sound and Vibration, 242(1), 47-58.

Lim, T. W., and Ewins, D. J. (1996). "Structural damage detection using real-time modal parameter identification algorithm." AIAA Journal, 34(11), 2370-2376.

Lim, T. W., and Kashangaki, T. A. L. (1994). "Structural damage detection of space truss structure using best achievable eigenvectors." AIAA Journal, 32(5), 1049-1057.

Luo, H., and Hanagud, S. (1997). "Dynamic learning rate neural network training and composite structural damage detection." AIAA Journal, 39(9), 1522-1527.

Maren, A. J., Jones, D., and Franklin, S. (1990). "Configuring and optimizing the back-propagation network." Handbook of neural computing applications, A. Maren, C. Harston, and R. Pap, eds., Academic press, San Diego, CA.

Marwala, T. (2000). "Damage identification using committee of neural network." Journal of Engineering Mechanics, 126(1), 43-50.

Marwala, T., and Hunt, H. E. M. (1999). "Fault identification using finite element models and neural networks." Mechanical Systems and Signal Processing, 13(3), 475-490.

Masri, S. F., Nakamura, M., Chassiakos, A. G., and Caughey, T. K. (1996). "Neural network approach to detection of changes in structural parameters." Journal of Engineering Mechanics, 122(4), 350-360.

Masri, S. F., Smyth, A. W., Chassiakos, A. G., Caughey, T. K., and Hunter, N. F. (2000). "Application of neural networks for detection of changes in nonlinear systems." Journal of Engineering Mechanics, 126(7), 666-676.

Matsouka, K. (1992). "Noise injection into inputs in back-propagation learning." IEEE Transaction of System, Man and Cybernatics, 22(3), 436-440.

Mehrjoo, M., Khaji, N., Moharrami, H., and Bahreininejad, A. (2007). "Damage detection of truss bridges using artificial neural networks." Expert System with Application, Article in press.

Mendrok, K., and Uhl, T. (2005). "Comparison of different Ritz vectors extraction." Key engineering material, 293-294, 143-150.

Messina, A., Williams, E. J., and Contursi, T. (1998). "Structural damage detection by a sensitivity and statistical-based method." Journal of Sound and Vibration, 216(5), 794-808.

Morassi, A., and Rovere, N. (1997). "Localizing a Notch in a Steel Frame from Frequency Measurements." Journal of Engineering Mechanics, 123(5), 422-432.

Nakamura, M., Masri, S. F., Chassiakos, A. G., and Caughey, T. K. (1998). "A method for non-parametric damage detection through the use of neural networks." Earthquake Engineering & Structural Dynamics, 27(9), 997-1010.

Narkis, Y. (1994). "Identification of crack location in vibrating simply supported beams." Journal of Sound and Vibration, 174(4), 549-558.

Ni, Y. Q., Wang, B. S., and Ko, J. M. (2002). "Construction inputs vectors to neural networks for structural damage identification." Journal of Smart Materials and Structures, 11(6), 825-833.

Ni, Y. Q., Zhou, X. T., Ko, J. M., and Wang, B. S. (2000). "Vibration-based damage localization in Ting Kau Bridge using Probabilistic Neural Network." Proceeding of Advances in Structural Dynamics, Hong Kong, 1069-1076.

Oh, B. H., and Jung, B. S. (1998). "Structural damage assessment with combined data of static and modal tests." Journal of Structural Engineering, 124(8), 956-965.

Oreta, W. C., and Tanabe, T. (1994). "Element identification of member properties of framed structures." Journal of Structural Engineering ASCE, 120(7), 1961-1976.

Ortiz, J., Ferregut, C., and Osegueda, A. (1997). "Damage detection from vibration measurements using neural network technology." ARTIFICIAL NEURAL NETWORKS FOR CIVIL ENGINEERS: Fundamentals and Application, N. Kartam, I. Flood, and J. Garrett, J. H., eds., ASCE, New York.

Palacz, M., and Krawczuk, M. (2002). "Vibration parameters for damage detection in structures." Journal of Sound and Vibration, 245(5), 999-1010.

Pandey, A. K., Biswas, M., and Samman, M. M. (1991). "Damage detection from changes in curvature mode shapes." Journal of Sound and Vibration, 145(2), 321-332.

Pandey, P. C., and Barai, S. V. (1995). "Multilayer perceptron in damage detection of bridge structures." Computers & Structures, 54(4), 597-608.

Papadopoulos, L., and Garcia, E. (1998). "Structural damage identification: a probabilistic approach." AIAA Journal, 39(11), 2137-2145.

Povich, C., and Lim, T. W. (1994). "An artificial neural network approach to structural damage detection using frequency response function." Proceeding of AIAA Adaptive Structures Forum, Washington, DC.

Prechelt, L. (1995). "Automatic early stopping using cross validation: quantifying the criteria." Neural Networks, 11(4), 761-767.

Qu, F., Zou, D., and Wang, X. (2004). "Substructural damage detection using neural networks and ICA." Advances in Neural Networks, Springer Berlin/Heidelberg.

Rhim, J., and Lee, S. W. (1995). "A neural network approach for damage detection and identification of structures." Computational Mechanics, 16(6), 437-443.

Rizos, P. F., Aspragathos, N., and Dimarogonas, A. D. (1990). "Identification of crack location and magnitude in a cantilever beam from the vibration modes " Journal of Sound and Vibration, 138(3), 381-388.

Rosenblueth, E. (1975). "Point estimates for probability moments." Proc. National Acedemy of Science, 72(10), 3812-3814.

Rumelhart, D. E., Hinton, G. E., and Williams, R. J. (1986). "Learning internal representation by error propogation." Parallel Distributed Processing, D. E. Rumelhart, G. E. Hinton, and R. J. Williams, eds., MIT Press, Cambridge, 318-62.

Rumelhart, D. E., and McCleland, J. L. (1986). *Paralel distribution processing*, M.I.T. Press.

Rytter, A. (1993). "Vibration based inspection of civil engineering structures," Phd Dissertation, Aalborg University, Denmark.

Sahin, M., and Shenoi, R. A. (2003). "Quantification and localisation of damage in beam-like structures by using artificial neural networks with experimental validation." Engineering Structures, 25(14), 1785-1802.

Sahoo, B., and Maity, D. (2007). "Damage assessment of structures using hybrid neuro-genetic algorithm." Applied Soft Computing, 7(1), 89-104.

Salawu, O. S. (1997a). "Detection of structural damage through changes in frequency: a review." Engineering Structures, 19(9), 718-723.

Salawu, O. S. (1997b). "An integrity index method for structural assessment of engineering structures using modal testing." Insight, 39(1), 33-37.

Salawu, O. S., and Williams, R. J. (1995). "Bridge assessment using forced-vibration testing." Journal of Structural Engineering, 19(9), 718-723.

Sampaio, R. P. C., Maia, N. M. M., and Silva, J. M. M. (1999). "Damage detection using frequency-response-function curvature method." Journal of Sound and Vibration, 226(5), 1029-1042.

Sanayei, M., and Onipede, O. (1991). "Damage assessment of structures using static test data " AIAA Journal, 29(7), 1174-1179.

Sanayei, M., and Saletnik, M. J. (1996a). "Parameter estimation of structures from static strain measurements, Part 1: Formulation." Journal of Structural Engineering, 122(5), 555-562.

Sanayei, M., and Saletnik, M. J. (1996b). "Parameter estimation of structures from static strain measurements, Part 2: Error sensitivity analysis." Journal of Structural Engineering, 122(5), 563-572.

Shahin, M. A., Maier, H. R., and Jaksa, M. B. (2003). "Settlement prediction of shallow foundations on granular soils using B-spline Neurofuzzy model." Journal of Computer and Geotechnics, 30(8), 431-440.

Shepherd, A. J. (1997). *Second-order methods for neural networks*, Springer-Verlag, New Jersey.

Shi, Z. Y., Law, S. S., and Zhang, L. M. (2000). "Damage localization by direct using incomplete mode shapes." Journal of Engineering Mechanics, 126(6), 656-660.

Shi, Z. Y., Law, S. S., and Zhang, L. M. (2002). "Improved damage quantification from element modal strain energy change." Journal of Engineering Mechanics, 128(5), 512-529.

Shih, Y. (1994). *Neuralyst user guide*, Cheshire Engineering Cooperation, Pasadena.

Sloane, N. J. A. (2007). "A Library of Orthogonal Arrays."

Smith, S. W., and Beattie, C. A. (1991). "Model correlation and damage location for large space structures:secant method developement and evaluation." NASA Report NASA-CR-188102.

Sohn, H., and Law, K. H. (1999). "Application of Ritz Vectors to damage detection for a grid-type bridge model." Proceeding of 17th International Modal Analysis Conference, Kissimmee, FL.

Sohn, H., and Law, K. H. (2000). "Application of load-dependent Ritz vectors to Bayesian probabilistic damage detection
" Probabilistic Engineering Mechanics, 15(2), 139-153.

Sohn, H., and Law, K. H. (2001). "Extraction of Ritz vectors from vibration test data." Mechanical Systems and Signal Processing, 15(1), 213-226.

Spillman, W., Huston, D., Fuhr, P., and Lord, J. (1993). "Neural network damage detection in bridge element." Smart Sensing, Processing, and Instrumentation, 1918, 288-295.

Stein, M. (1987). "Large sample properties of simulations using Latin Hypercube Sampling." Technometrics, 29(2), 143-151.

Stidger, R. (2006). "America's Bridges: Deterioration Inches Downward." Better Roads.

Stubb, N., and Osegueda, A. (1990a). "Global non-destructive damage evaluation in solids " International Journal of Analytical and Experimental Modal Analysis, 5(2), 67-79.

Stubb, N., and Osegueda, A. (1990b). "Global damage detection in solids - Experimental verification " International Journal of Analytical and Experimental Modal Analysis, 5(2), 81-97.

Suh, M. W., Shim, M. B., and Kim, M. Y. (2000). "Crack identification using hybrid neuro-genetic technique." Journal of Sound and Vibration, 234(4), 617-635.

Surendra, P. S., Popovics, J. S., Subramaniam, K. V., and Aldea, C. M. (2000). "New Directions in Concrete Health Monitoring Technology
" Journal of Engineering Mechanics, 127(7), 754-760.

Szewczyk, Z. P., and Hajela, P. (1992). "Damage detection in structures based on Feature-sensitive neural network." Journal of Computing in Civil Engineering, 8(2), 163-178.

Szewczyk, Z. P., and Hajela, P. (1994). "Damage detection in structures based damage detection in structures." Journal of Computing in Civil Engineering, 8(2), 163-178.

Tang, B. (1993). "Orthogonal array-based latin hypercubes." Journal of the American Statistical Association, 88(424), 1392-1397.

Trendafilova, I., Heylen, W., and P., S. (1998). "Damage localization in structures. A pattern recognition perspective." Proceeding of International seminar on modal analysis, Santa Barbara.

Tsou, P., and Shen, M. H. H. (1994). "Structural damage detection and identification using neural networks." AIAA Journal, 32(1).

Wahab, M. M., and De Roeck, G. (1999). "Damage detection in bridges using modal curvature: application to a real damage scenario." Journal of Sound and Vibration, 226(2), 217-235.

Wang, X., Hu, N., Fukunaga, H., and Yao, Z. H. (2001). "Structural damage identification using static test data and changes in frequencies " Engineering Structures, 23(6), 610-621.

Wang, Z., Lin, R. M., and Lim, M. K. (1997). "Structural damage detection using measured FRF data." Computer Methods in Applied Mechanics and Engineering, 147(1-2), 187-197.

Wen, C. M. (2007). "Unsupervised fuzzy neural networks for damage detection of structures." Structural Control and Health Monitoring, 14(1), 144-161.

Worden, K. (1997). "Structural fault detection using novelty measure." Journal of Sound and Vibration, 201(1), 85-101.

Worden, K., Ball, A. D., and Tomlinson, G. R. (1993). "Fault location in a framework structure using neural networks." Smart Materials and Structures, 2(3), 189-200.

Wu, X., Ghaboussi, J., and Garrett, J. H. (1992). "Use of neural networks in detection of structural damage." Computers & Structures, 42(4), 649-659.

Xia, P., and Brownjohn, J. M. W. (2004). "Bridge structural condition assessment using systematically validated finite-element model." Journal of Bridge Engineering, 9(5), 418-423.

Xia, Y., and Hao, H. (2003). "Statistical damage identification of structures with frequency changes." Journal of Sound and Vibration, 263, 853-870.

Xia, Y., Hao, H., Brownjohn, J. M. W., and Xia, P. (2002). "Damage identification of structures with uncertain frequency and mode shape data." Earthquake Engineering and Structural Dynamics, 31(5), 1053-1066.

Xia, Y., Hao, H., Zanardo, G., and Deeks, A. (2006). "Long term vibration vibration monitoring of an RC slab: Temperature and humidity effect." Engineering Structures, 28(3).

Xu, B., Wu, Z., Chen, G., and Yokoyama, K. (2004). "Direct identification of structural parameters from dynamic responses with neural networks." Engineering Applications of Artificial Intelligence, 4(8), 931-943.

Xu, H., and Humar, J. (2006). "Damage detection in a girder bridge by artificial neural network technique." Computer-aided and Infrastructure Engineering, 21(6), 450-464.

Xu, Y. G., Liu, G. R., Wu, X. M., and Huang, X. M. (2000). "Adaptive multilayer perceptron networks for detection of cracks in anisotropic laminated plates." International Journal of Solids and Structures, 38(32-33), 5625-5645.

Yam, L. H., Yan, Y. J., and Jiang, J. S. (2003). "Vibration-based damage detection for composite structures using wavelet transform and neural network identification." Composite Structures, 60(4), 403-412.

Yeung, W. T., and Smith, J. W. (2005). "Damage detection in bridges using neural networks for pattern recognition of vibration signatures." Engineering Structures, 27(5), 685-698.

Yu, L., Cheng, L., Yam, L. H., and Jiang, X. (2007). "Experimental validation of vibration-based damage detection for static laminated composit shells partially filled with fluid." Composite Structures, 79(2), 288-299.

Yuen, K. V., and Katafygiotis, L. S. (2006). "Substructure identification and health monitoring using noisy response measurement only." Computer-Aided and Infrastructure Engineering, 21(4), 280-291.

Yuen, K. V., and Lam, H. F. (2006). "On the complexity of artificial neural networks for smart structures monitoring." Engineering Structures, 28(7).

Yun, C.-B., and Bahng, E. Y. (2000). "Substructural identification using neural networks." Computers & Structures, 77(1), 41-52.

Yun, C. B., Yi, H. K., and Bahng, E. Y. (2001). "Joint damage assessment of framed structures using a neural networks technique." Engineering Structures, 23(15), 425-435.

Zang, C., and Imregun, M. (2001a). "Structural damage detection using artificial neural network and measured FRF data reduced via principal component projection." Journal of Sound and Vibration, 242(5), 813-827.

Zang, C., and Imregun, M. (2001b). "Combined neural network and reduced FRF techniques for slight damage detection using measured response data." Archive of Applied Mechanics, 71(8), 525-536.

Zapico, J. L., Worden, K., and Molina, F. J. (2001). "Vibration-based damage assessment in steel frames using neural networks." Journal of Smart Materials and Structures, 10(3), 553-559.

Zhang, Q., and Benveniste, A. (1992). "Wavelet networks." IEEE Trans. Neural Network, 3(6), 889-898.

Zhao, J., Ivan, J. N., and DeWolf, J. T. (1998). "Structural damage detection using artificial neural network." Journal of Infrastructure Systems, 4(3), 93-101.

Zhao, J., and Nowak, A. S. (1988). "Integration formulas to evaluate functions of random variables." Structural Safety, 5(4), 267-284.

Zhu, H., Sima, Y., and Tang, J. (2002). "Damage identification in structures using modified backpropagation neural networks." Acta Mechanica Solida Siniva, 15(4), 358-370.

Zimmerman, D. C., and Kaouk, M. (1994). "Structural damage detection using a Minimum Rank Theory." Journal of Sound and Vibration, 116(2), 222-231.

Zimmerman, D. C., and Kauok, M. (1992). "Eigenstructure assignment approach for structural damage detection " AIAA Journal, 30(7), 1848-1855.

Zimmerman, D. C., and Widengren, M. (1990). "Correcting finite element models using a symmetric eigenstructure assignment technique." AIAA Journal, 28(9), 1670-1676.

Zou, R., Lung, W., and Guo, H. (2002). "Neural network embedded Monte Carlo approach for water quality modeling under input information uncertainty." Journal of Computing in Civil Engineering, 16(2), 135-142.